Deanship of Graduate Studies
Al-Quds University

Synthesis and Characterization of Mono and Dinuclear Coordination Compounds of Nickel and Copper with 2,2'-Bipyrazine and 2,2'-Dipyridylamine Ligands

Khaled Adel Nael Abusharkh

M.Sc. Thesis

Jerusalem –Palestine

1439/2017

Synthesis and Characterization of Mono and Dinuclear Coordination Compounds of Nickel and Copper with 2,2'-Bipyrazine and 2,2'-Dipyridylamine Ligands

Prepared by:

Khaled Adel Nael Abusharkh

B.Sc. Chemistry. Al-Quds University/ Palestine

Supervisor: Dr. Huseein Alkam
Co supervisor: Late Dr. Khalid kanan

A thesis submitted in partial fulfillment of requirement for the degree of the Master of Applied and Industrial Technology, Al-Quds University

1439/2017

Al-Quds University

Deanship of Graduate Studies

Applied and Industrial Technology Program

Thesis Approval

Synthesis and Characterization of Mono and Dinuclear Coordination Compounds of Nickel and Copper with 2,2'-Bipyrazine and 2,2'-Dipyridylamine Ligands

Prepared by: Khaled Adel Nael Abusharkh
Registration No: 21220063

Supervisor: Dr. Huseein Alkam
Co supervisor: late Dr. Khalid kanan

Master thesis submitted and accepted, Date: 5/ 12/ 2017
The names and signatures of the examining committee members are as follows:

1- Head of Committee/ Dr. Huseein Alkam Signature .....

2- Internal Examiner/ Dr. Mohammad Abul-Haj Signature .....

3- External Examiner/ Dr. Hijazi Abu Ali Signature 19/12/2017

Jerusalem-Palestine

1439/2017

Dedication

This thesis (study) is dedicated to my late teacher Dr. Khalid kanan, whose death was a great loss for Chemistry Faculty /Department, and Al –Quds University. My special and great thanks to his efforts and help, God bless his soul. To all of those who encouraged me and helped me; to my Mom and Dad, my wife, my son Adel, my brothers, sisters my precious family, and my dearest friends, my supervisor Dr. Huseein Alkam, all members in my department, to Palestinian martyrs and prisoners, to my beloved University; Al-Quds University, to my beloved homeland; Palestine.

Khaled Adel Abusharkh

Declaration

I certify that this thesis submitted for the degree of master is the result of my own research, except where otherwise acknowledged , and that this thesis (or any part of the same) has not been submitted for a higher degree to any other university or institute.

Signed ……

Name: Khaled Adel Nael Abusharkh

Date: 5/12/2017

Acknowledgements

I express my endless thanks and gratitude to Almighty God, Allah, for providing me with great patience in accomplishing my thesis. I am very pleased to express my gratitude to all people who assisted me to go forward in my studies, and to all people who offered me help and support. Special appreciation goes to my supervisor, the most perfect man who has taught me a lot since my bachelor's to my master's degrees Dr. Huseein Alkam, for his special help and recommendations on my experiments and analysis. Sincere thanks are given to late Dr. Khalid kanan for encouraging and providing me with important research requirements. Special thanks are given to Professor Pablo J. Sanz from University of Zaragoza – Spain, for his efforts in solving the X-ray structures. My thanks also go to Dr. Mohammad Abul-Haj, for his encouragements and constant support to me. I am also very grateful to all my colleagues in the chemistry department at Al Quds University for their support. I would like also to express my sincere gratitude to Mrs. Maryam Faroun in the Nanotechnology centre at Al-Quds University and Dr. Muhanad Qrei in the Centre of Chemical and Biological Analysis at Al-Quds University and Beit Jala Pharmaceutical Company (BJP), especially my friend, Mr. maher Aljamal for their kind efforts. Finally, it is of my honor to express my thanks to my family who supported and encouraged me during this period.

Abstract:

The crystal structure of $[Cu(bpz)(OH)(ClO_4)(H_2O)]_2.H_2O$ **(1)**, $[Cu(dipyam)]_2(ClO_4)_2$ **(2)** and $[Ni(bpz)_3](ClO_4)_2 .H_2O$ **(3)** have been synthesized and characterized by Single Crystal X-ray diffraction analysis (SCXRD), FTIR, UV-Vis spectroscopy and Thermal analysis by Differential Scanning Calorimetry (DSC). The 2,2'- bipyrazine ligand (bpz) has been synthesized and characterized by FTIR, UV-Vis spectroscopy and Single Crystal X-ray diffraction (SCXRD).

The crystal of a new binuclear **(1)** are triclinic, with a = 7.9796(5), b = 8.0290(5), c = 10.5550(7) Å, α = 77.7120(1)°, β = 79.9150(1)°, γ = 84.7840(1)°, Z=1 and V= 649.526 $A°^3$.The structure consists of discrete centrosymmetric di-μ-hydroxo-copper(II) dimer with 2,2'-bipyrazine as outer ligand and coordinated ClO_4^- anions and H_2O solvent molecule. Intramolecular copper-copper distances is 2.824 Å and Cu–O–Cu angle 94.40° exhibiting ferromagnetic interaction with smallest Cu–O–Cu angle and shortest Cu….Cu distance reported so far. The coordination geometry around each copper ion is distorted elongated tetragonal octahedral with the bridging hydroxo groups and two nitrogen atoms of the 2,2'-bipyrazine ligand comprising the basal plane, and the apical site occupied by two oxygen atom of the ClO_4^- and H_2O groups. The packing structure shows the rings of the polypyrizyl ligands are interact through π ---- π interactions. The DSC curve shows endothermic peaks at 272.45 °C owing to melting point.

The compound **(2),** (dipyam = 2,2′-dipyridylamine) has been synthesized and the crystal structure determined by a single X-ray diffraction study, FTIR, UV-Vis spectroscopy ,and thermal analysis (DSC). The Cu(II) center is four-coordinated by the nitrogen donors of the pyridine rings of the ligand, 2,2′-dipyridylamine, by trans-trans mode. A distorted tetrahedral coordination geometry around copper ion. The crystal type monoclinic, with Space group $C_{2/c}$ and the unit cell dimensions a = 9.416 (3), b = 12.955 (4), c = 19.748 (6) Å, α = 90.00°, β = 103.47 °, γ = 90.00°, Z= 4 and V= 2339.5 (11)$A°^3$. The perchlorate anions link the complex cations to form a chain structure through C-H···O close contacts and N-H···O hydrogen bonds. The DSC curve shows endothermic peak at 308.65 °C related to melting point.

The novel mononuclear Ni(II) complex **(3)**, where (bpz =2,2'-bipyrazine). X-ray structural analyses shows that the coordination geometry around the Ni(II) center is a

trigonal distorted octahedral, and the crystal type monoclinic, with Space group P 21/c and the unit cell dimensions a = 17.2943(11), b = 9.8622(6), c = 17.9612(11) Å, α = 90.00°, β = 107.7010(1)°, γ = 90.00°, Z= 4 and V= 2918.4(3) (11)A°^{3}. A careful inspection of the packing pattern in the lattice of complex **(3)** reveals the occurrence of C–H----π, C–H···N–C hydrogen bonds interactions. The packing structure also shows that the rings of the polypyrizyl ligands are interact through π----π interactions in two sets between bpz ligands in complex **(3)** with parallel displaced form interaction. The DSC curve shows endothermic peak at 334.15 °C related to melting point.

Contents

Chapter One

Chapter two

Chapter Three

Chapter Four

Chapter Five

List of Schemes

List of Figures

List of Tables

List of appendices

Abbreviations

bpz	2,2'-Bipyrazine
dipyam	2,2′-Dipyridylamine
SCXRD	Single Crystal X-ray Diffraction
FT-IR	Fourier Transforms Infrared Spectroscopy
DSC	Differential Scanning Calorimetry
UV-Vis	Ultraviolet-visible Spectrophotometry
CCDC	Cambridge Crystallographic Data Centre
MLCT	Metal-to-Ligand Charge Transfer
PCET	Proton-Coupled Electron Transfer

Chapter One

1.1 Introduction:

Nitrogen-containing heterocycles with their tendency of acting as ligands for metal ions have played a major role in the development of the supramolecular chemistry.[1-7] In some case heterocycles provide the directionality, if the coordination occurs in endocyclic donor sites, that way facilitating the construction a particular molecular architecture, and providing some degree of predictability of the composition of the product. A lot of the heterocyclic ring systems have functional groups suitable for hydrogen bonding interactions. This feature then permits the unique opportunity to combine hydrogen bonding motifs for the generation of supramolecular architectures with the concept of useing the coordinative bond.

Experience showed that metal binding to ring atoms of nucleobases frequently leads to rather 'soft' structures and that marked deviations from expectations can be anticipated for a number of reasons: (i) External ring angles (Scheme 1). They may strongly deviate from the ideal case, e.g. from 120° in six-membered ring systems.

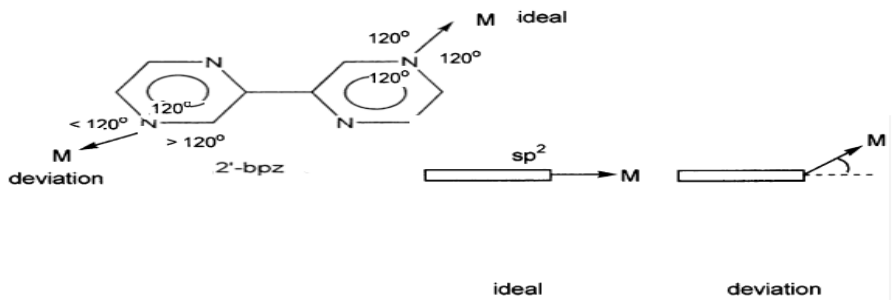

Scheme 1.1: The ideal and the deviation angle in six-membered ring system in nitrogen bases.

Even H-bond formation between substituent of the heterocyclic ring and other ligands at the metal may be sufficient to cause marked deviations. (ii) Metal out-of-plane. In heteroaromatic systems the metal may be substantially out-of-plane, hence deviation from the 'ideal' sp^2 hybridazation may be large. (iii) Torsional angles within C–C coupled heterocycles. With flexible heterocycles such as 2,2'-bipyrazine, any torsion between the

two halves of the molecule may have a strong influence on the resulting architecture. (iv) Metal geometry. Deviations of 'ideal' angular values of square-planar, tetrahedral or octahedral metal ions can be substantial[8,9,10].

The structure of 2,2'-bipyrazine shows that the ligand adopts a planar structure with the two pyrazine rings related to each other by an inversion centre. As a result the ligand adopts an arrangement such that the two central nitrogen atoms are placed *anti* to each other as observed in the structure of 2,2'-bipyridyl[11]. The 2,2'-bipyrazine molecules are stacked with a ring centroid to plane separation of 3.36 Å representing a significant π–π interaction.

An impressive amount of work has been devoted to magneto-structural studies of 2,2'-bipyrazine (bpz) due to structural feature of bpz is its flexibility: rotation of two pyrazine rings with respect to each other enables many possibilities to bind metals. (Scheme 1.2)

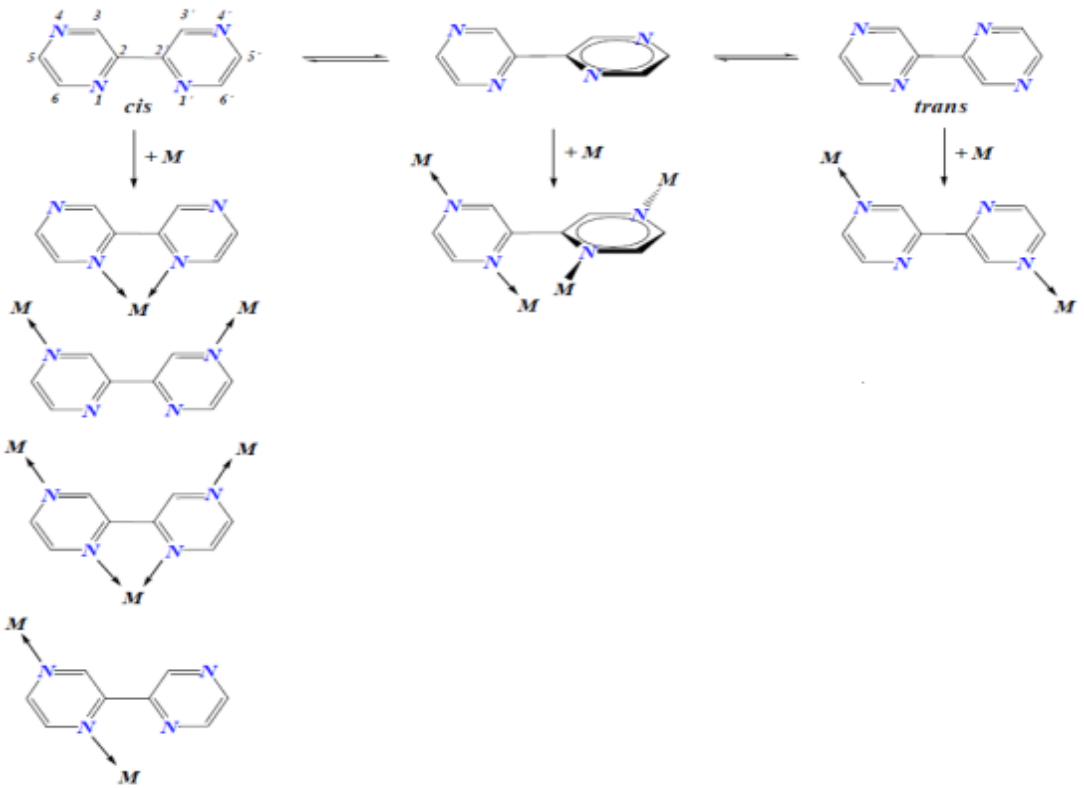

Scheme 1.2: Conformations of bpz (top) and principal metal binding modes (below) adopted from[13].

Polypyridyl transition metal complexes are attracting considerable interest due to peculiar electrochemical, spectroelectrochemical, magnetic, optical, and medicinal properties. Some studies have recently found the efficiency of polypyridyl complexes as an electrochemical probe for nucleic acid sensing, particularly for CT-DNA[{14,15}], fluorescent probes for nuclear and protein components[{16}], DNA photocleavage agents [{17}].

Polynuclear metal complexes containing photophysically active center are particularly interesting from the point of view of photoinduced electron transfer and energy transfer processes. The presence of a metal complex attached to the photoactive center via a bridging ligand provides additional pathways for the deactivation of the excited states, in these systems, the geometry inter metallic separation distance, and electronic properties of the bridging ligands are relevant factors to be considered, in addition to the photochemical and photophysical characteristics of the metal ions[{18}].

The magnetic properties of copper(II) complexes have been an attractive area of research. This is due to the fact that copper(II) (d^9) has a single unpaired electron and therefore can be used as a model system for probing the nature of magnetic exchange interactions between single unpaired electrons on two or more metal centres, and in particular, how this interaction is mediated by the ligands that bridge the metal centers[{19}], on the other hand, copper is an essential element to biological function, while the exchangeable portion of copper in blood plasma occurs mainly as a result of mixed-ligand formation involving copper-nitrogen interaction. Further more the unique spectral features of the blue-copper proteins have stimulated investigation involving low molecular mass copper(II) chelates that have nitrogen atom in the immediate vicinity of copper(II) in coordination unites of tetragonal or lower ligand filed symmetry and may mimic the characteristic properties of these proteins[{20}].

Nickel is an essential trace metal involved in many biological process. Nickel complexes have been receiving much attention, due to biological applicability such as antiepileptic[{138}], anticonvulsant[{139}], antibacterial[{140}], antifungal[{140}], antimicrobial[{141}], and anticancer/antiproliferative activities[{142, 143}], and can inhibit DNA repair mechanism due to interfering with enzymes or proteins synthesis involved in DNA replication or DNA repair[{144}].

The Polypyridyl Ni(II) complexes show good affinity in DNA binding to exert biological effects. DNA is a target molecule for cancer therapy, therefore, the experimental and theoretical investigations of interaction of DNA with suitable molecules is very important to the design of pharmaceutical molecules [145, 146].

The Organonickel(II) complexes are widely used in organometallic catalysis. One of the first benchmarks in that field was the nickel phosphane complexes used in the shell higher olefin process (SHOP). In the last decade the interest in organonickel catalysts has mainly focused on nickel diimine complexes. Highly reactive catalysts for olefin polymerization, nickel diimine complexes which gained a large interest in electrocatalytic applications[22].

1.2 Historical background:

In recent year's synthesis of the coordination compounds with 2,2'-bipyrazine ligand is focused on ruthenium, palladium, platinum and rhenium and studied its coordination behaviour which show a different coordination modes by using different metal ions and different synthesis conditions.

In the last few years great attention has been focused on complexes contains 2,2'-bipyrazine due to extensive applications of photochemistry, photophysics, photocatalysis, electrochemistry, biochemistry and others, especially because of their important applications in DNA binding and solar energy battery material.

1.2.1 Synthesis of 2,2'-bipyrazine:

The synthesis of 2,2'-bipyrazine was started in 1967[{23}] by J. J. Lafferty and F. H. Case, with low percentage yield(7%).

In 1982[{24}] when R. J. Crutchley and A. B. P. Lever reported a new synthtic procedure of 2, 2'-bipyrazine with percentage yield relatively higher than the previously reported.

The single crystal structures of 2,2'-bipyrazine was determined in order to compare the degree of π–π interactions in the "free" ligand and that observed in the complexes [{66}].

1.2.2 Ruthenium complexes:

In 1982[{24}] R. J. Crutchley and A. B. P. Lever started the synthesis of new complexes of 2,2'-bipyrazine ruthenium such as [Ru(bpz)3]Cl2 and $[Ru(bpz)_3](PF_6)$.

The photoanation of the bipyrazyl ligand in $[Ru(bpz)_3](PF_6)$ complex in acetonitrile containing chloride ion, formed cis-$Ru(bpz)_2(CH_3CN)Cl^+$, cis-$Ru(bpz)_2Cl_2$, and an unidentified mono(bipyrazyl)ruthenium(II) derivative. The mechanism of this reaction is discussed.

Synthesis of ruthenium complexes was continued in 1983 when D. P. Rillema et al[{25}], described the synthesis and study the properties of $Ru(bpy)_n,(bpyrz)_{3-n}^{+2}$ and $Ru(bpy)_n,(bpyrm)_{3-n}^{2+}$, where n = 0-2 and bpy is 2,2'-bipyridine, bpyrz is 2,2'-bipyrazine, and bpyrm is 2,2'-bipyrimidine. Absorption spectra contained bands in the (250-290 nm) range that are assigned to ligand π→π* transitions and visible bands (360-470 nm) that

are assigned to dπ→π* MLCT (metal-to-ligand charge transfer) transitions. The π→π* absorptions shift to the red as the number of bipyridine ligands is increased in mixed-ligand complexes. Emission spectra maxima were observed from 600 to 700 nm and also shift to the red with substitution for bipyridine. Redox potentials were found to vary in a systematic way.

In 2011, the structural and pH dependence of excited state (PCET) reactions involving reductive quenching of the MLCT excited state of $[Ru^{II}(bpy)_2(bpz)]_2$ by hydroquinones (bpy = 2,2'-bipyridine, bpz = 2,2'- bipyrazine) was studied.

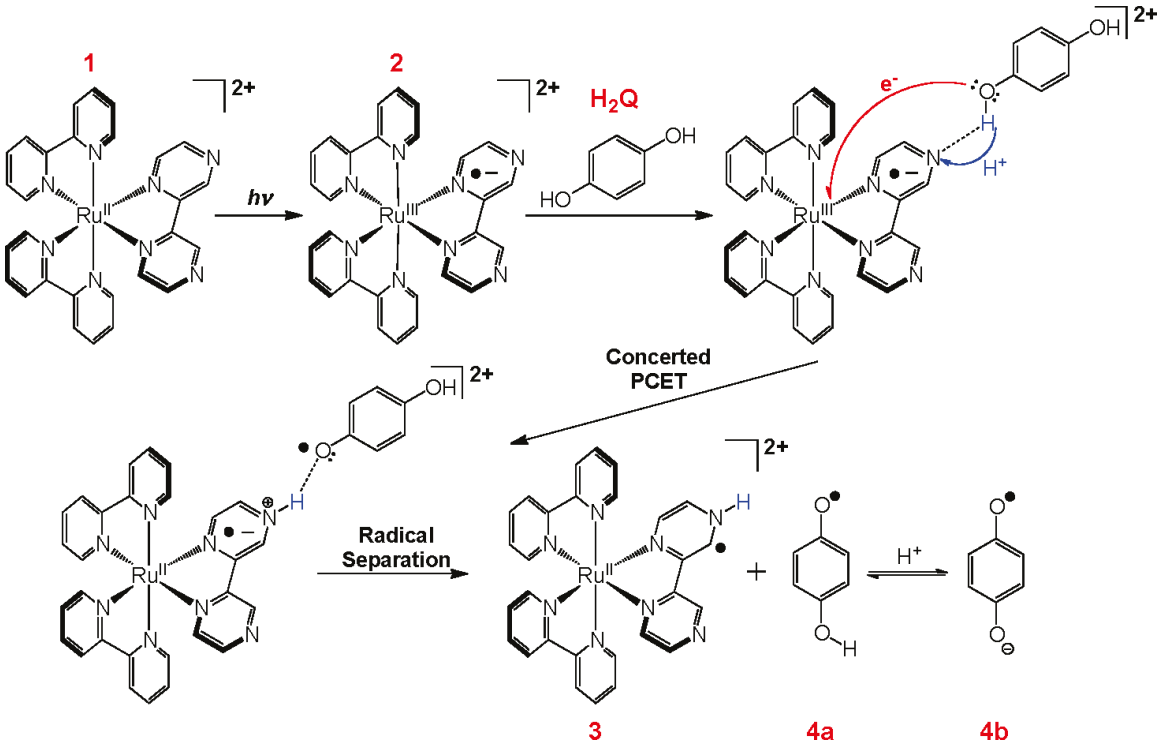

Scheme 1.3: Involves the reductive quenching of 2, the MLCT state (formally RuIII) of $[RuII(bpy)_2(bpz)]_2$ (bpy = 2,2'-bipyridine, bpz = 2,2'-bipyrazine) by hydroquinone (H2Q) adopted from [26].

In 1984 [27] $Ru(bpz)_3^{+2}$ and bpz have been used for the preparation of two types of films, both prepared via oxidative polymerization in acidic solutions. Based on the results described it appears that the films grow uniformly on the GC surface and the film thickness is proportional to the number of positive scans. The bpz film is weakly

conducting and preliminary experiments indicate a resistivity value of ~10^{6} Ω cm for this film.

Ruthenium-2,2'-bipyrazine complexes have many application studied in solar energy and photosensitizers in solar energy conversion[28,29].

T. S. Akasheh and Z. M. Egahmed[30], was synthesis new Mixed-ligand complexes of 2,2'-bipyrazine (bpz), 2,2'-bipyridine (bpy), 2,3-di-(2'-pyridyl)-pyrazine (dpp), 2,3-dihydro-5,6- (2'-pyridyl).pyrazine (dhp), 3,6-di-(2'-pyridyl)-1,2,4,5-tetrazine (dpl) and 2,3-di-(2'-pyridyl)-quinoxaline (dpq) with ruthenium(II), and used $Ru(bpz)_3$ from literature [25], have been studied for evaluation as potential solar energy converters via an estimate of the redox potentials of their 'MLCT excited states, Cyclic voltammetry was used to show that bpz has lower σ-donor and higher π-acceptor abilities than the other ligands[30].

In the next year, T. S. Akasheh et al[31], research group continuous in preparation and characterization of a series of mixed ligands with ruthenium complexes through dihalide replacement in $Ru(bpy)_2Cl_2$, $Ru(bpz)_2Cl_2$and tetrahalide replacement in $HRu(bpy)Cl_4$, (bpy = 2,2'-bipyridine ; bpz = 2,2'-bipyrazine) by one or two bidentate ligands of the diimine type namely, bpd, dbpq and dpp (bpd = 3,3'-bipyridazine ; dbpq = 6,7-dimethyl-2,3-bis-(2'-pyridyl)-quinoxaline ; dpp = 2,3-bis-(2-pyridyl)-pyrazine). The ruthenium dimer $[(bpy)_2Ru(dbpq)Ru(bpy)_2(PF_6)_4.3H_2O$, as well as the tris-complex $[Ru(dbpq)_3](PF_6)_2$. H2O, were also prepared and characterized.

$[Ru(bpz)_2(dpq)]^{2+}$ was used in photosensitize methyl viologen cation radical production in the presence of ethylenediaminetetraacetic acid (EDTA)[32].

Table 1.1: Cyclic voltammetry results in DMF and acetonitrile, adopted from[30].

Compound	Reduction (V)			Oxidation (V)
$[Ru(bpz)_3]^{2+}$	−0.68	−0.80	−1.14	1.98
$[Ru(bpy)_3]^{2+}$	−1.31	−1.50	−1.77	1.27
$[Ru(bpz)_2dpp]^{2+}$	−0.74(60)	−0.96(70)	−1.29(90)	1.94(70)
$[Ru(bpz)_2dhp]^{2+}$	−0.73(60)	−0.94(70)	−1.27(60)	1.91(60)
$[Ru(bpz)_2dpt]^{2+}$	−0.64(60)	−0.83(70)	−1.07(90)	1.76(170)
$[Ru(bpz)_2dpq]^{2+}$	−0.62(70)	−0.87(70)	−1.12(80)	1.90(60)
$[Ru(bpy)_2dhp]^{2+}$	−1.41(80)	−1.83(70)	−2.06(70)	1.46(60)
$[Ru(dhp)_3]^{2+}$	−0.90(100)	−1.10(60)	−1.37(70)	1.65(100)
$[Ru(dpp)_3]^{2+}$	−0.95(80)	−1.12(100)	−1.39(100)	1.68(70)
$[Ru(dpq)_3]^{2+}$	−0.60(60)	−0.76(60)	−1.01(60)	1.70(60)

- Reductions were run in DMF and oxidations in aceronitrile, Values in parentheses are the differences between anodic and cathodic peaks in mV.

In the same year, the excited state properties (emission, lifetimes and redox potentials) are reported and analyzed in the framework of solar energy conversion[33].

T. Iguro et al, in 1994[34] was synthesis ruthenium (II) diimine complex ions in the double complex salts by using cobalt and iron, diimie; (bpz=2,2'-bipyrazine; bpy=2,2'-bipyridine), and the lifetimes of the excited MLCT was studied in the temperature range 77-353 K. The excited MLCT states of $Ru(bpy)^{2+}$ and $Ru(bpz)^{2+}$ undergo electron transfer reaction with $Fe(CN)_6^{-3}$ in the double complex salts $[Ru(bpz)_3]_2[Fe(CN)_6]Cl.\ 14H_2O$ and $[Ru(bpy)_3]_2[Fe(CN)_6]Cl.\ 8H,O$ at 77 and 295 K. The reorganization energy in the crystal is reduced to some extent because of the small number of water molecules in the crystals.

And in the same year[35], a series of mixed-tris complexes of general formula $[ML'L,](ClO_4)_2.H_2O$ [M =Ru or OS; L'= 2,2'-bipyrazine (bpyz) or 2,2'-bipyrimidine (bpym) and L = 2-(phenylazo)pyridine (papy) or 2-(m-tolylazo)pyridine (tapy)] has been prepared and characterized by physicochemical and spectroscopic methods. Using H NMR results, stereochemistry of ML_2 fragment in these tris chelates has been determined. The complexes show a number of MLCT transitions in the visible region; the low intensity spinforbidden transitions are observable in osmium complexes. In MeCN solution, the OsN6 unit displays one metal-centred oxidation and multiple ligand-based

reductions. Relative π-acceptor ability of the ligands is clearly reflected in the electrochemical results.

P. Thanasekaran et al [36], study the photooxidation of organic sulphides with excited $Ru(bpz)_3^{2+}$ (bpz = 2,2'-bipyrazine) results in the formation of sulphoxides and sulphones in aqueous CH_3CN (Scheme 1.4)adopted from [36] and the reaction proceeds via an electron transfer mechanism (Scheme 1.5) adopted from [36].

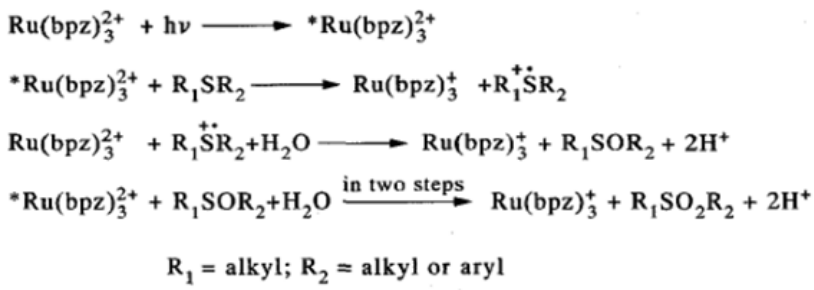

Scheme 1. 4: photooxidation of organic sulphides with excited $Ru(bpz)_3^{2+}$ (bpz = 2,2'-ipyrazine) results in the formation of sulphoxides and sulphones in aqueous CH3CN adopted from [36].

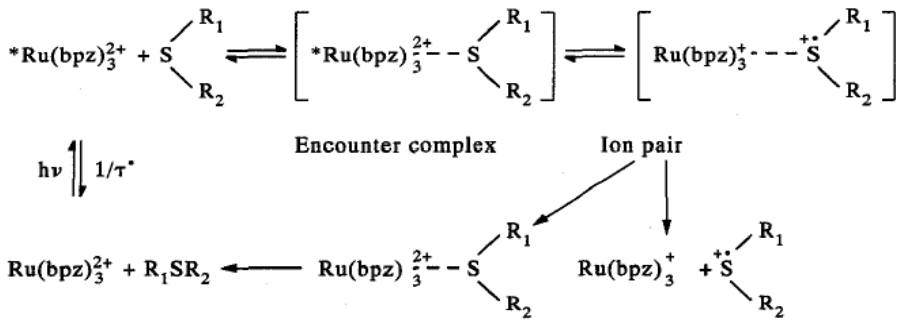

Scheme 1. 5: reaction proceeds via an electron transfer mechanism adopted from [36].

In the period from 2000 to 2004 the research focused on theoretical studies of the $[Ru(bpz)_3]^{+2}$ complex[37,38]. and synthesis, characterization of a new mixed ligand ruthenium complexes $[Ru(deeb)(bpz)_2](PF_6)_2$, $[Ru(deeb)_2(bpz)](PF_6)_2$, and $[Ru(deeb)_2(dpp)](PF_6)_2$, where deeb is 4,4'-(CO2CH2CH3)2-2,2'-bipyridine, bpz is 2,2'-bipyrazine, and dpp is 2,3-bis(2-pyridyl)pyrazine[39]. And dinuclear ruthenium complexes of formulae $[(tpy)(bpy)Ru^{II}(pz)Ru^{III}(edta)]^-$ and $[(CN)4Ru^{II}(bpz)Ru^{III}(edta)]^{-3}$

(where tpy = 2,2':6',2"-terpyridine, bpy = 2,2'-bipyridine, pz = pyrazine, bpz = 2,2'-bipyrazine, edta = ethylenediaminetetraacetate)[40].

In the period from 2012 to 2014 the research focused by O. S. Wenger et al, in studied the Mechanistic Diversity in Proton-Coupled Electron Transfer between Thiophenols and Photoexcited $[Ru(bpz)_3]^{+2}$[41],

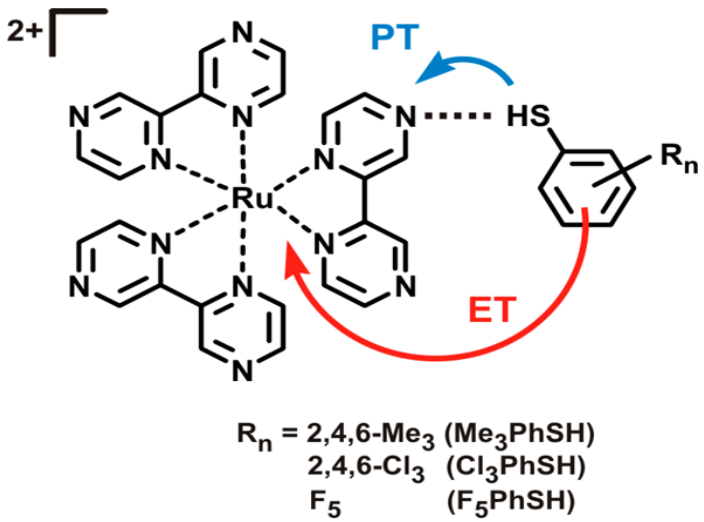

Scheme 1.6: View of the Proton-coupled electron transfer (PCET) between a series of thiophenols and a photoexcited of $[Ru(bpz)_3]^{+2}$ adopted from[41] .

And Proton-Coupled Electron Transfer Originating from Excited States of $[Ru(bpz)_3]^{+2}$[42],

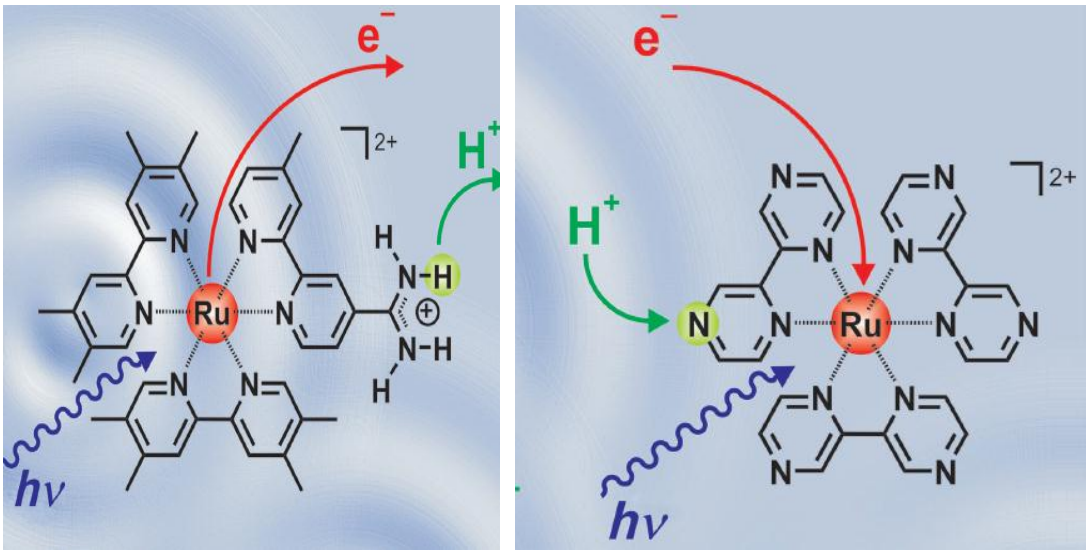

Scheme 1.7: View of the Proton-coupled electron transfer (PCET) reactions originating directly from photoexcited states of [Ru(bpz)3]+2 adopted from [42].

And Long-range proton-coupled electron transfer in phenol–Ru(bpz)$_3^{2+}$ dyads[43],

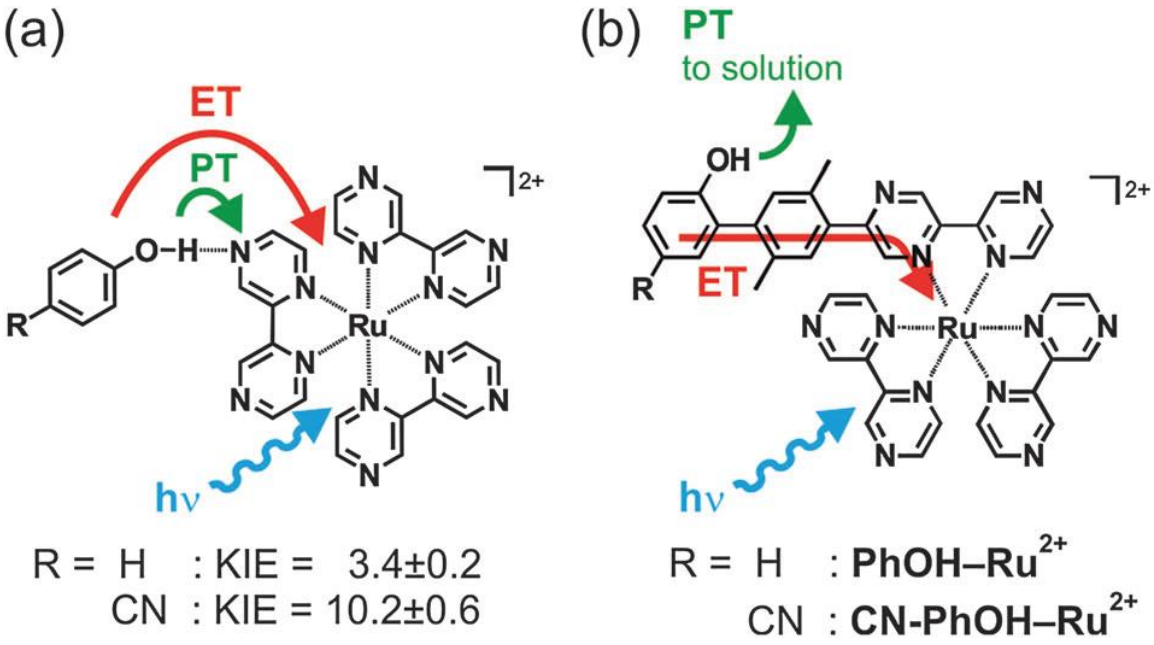

Scheme 1.8: (a) Phenol–Ru(bpz)$_3^{2+}$ reaction pairs which were previously investigated in the context of hydrogen-atom transfer (HAT)-like PCET

(b) Dyads investigated in this work. ET = electron transfer, PT = proton transfer, KIE = H/D kinetic isotope effect adopted[43].

And Kinetic Isotope Effects in Reductive Excited-State Quenching of $Ru(bpz)_3^{2+}$ by Phenols[44].

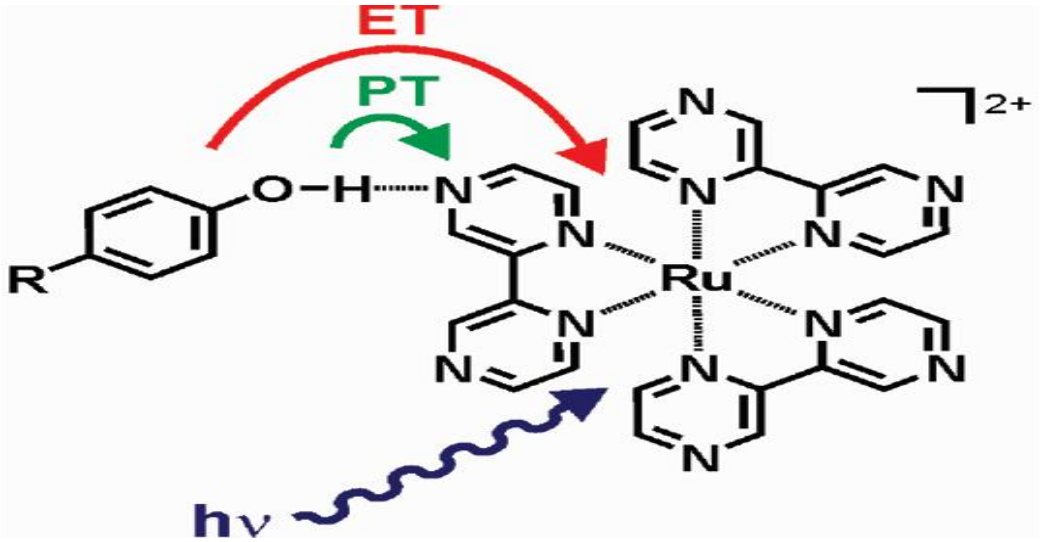

Scheme 1.9: View of the Electron transfer (ET) from phenol molecules to a photoexcited $[Ru(bpz)_3]^{+2}$ was investigated as a function of the para-substituent (R = OCH_3, CH_3, H, Cl, Br, CN) attached to the phenols adopted from[44].

In 2015, D. M. Schultz et al[45], was improved procedure for the preparation of $[Ru(bpz)_3](PF_6)_2$ via a high-yielding synthesis of 2,2'-bipyrazine.

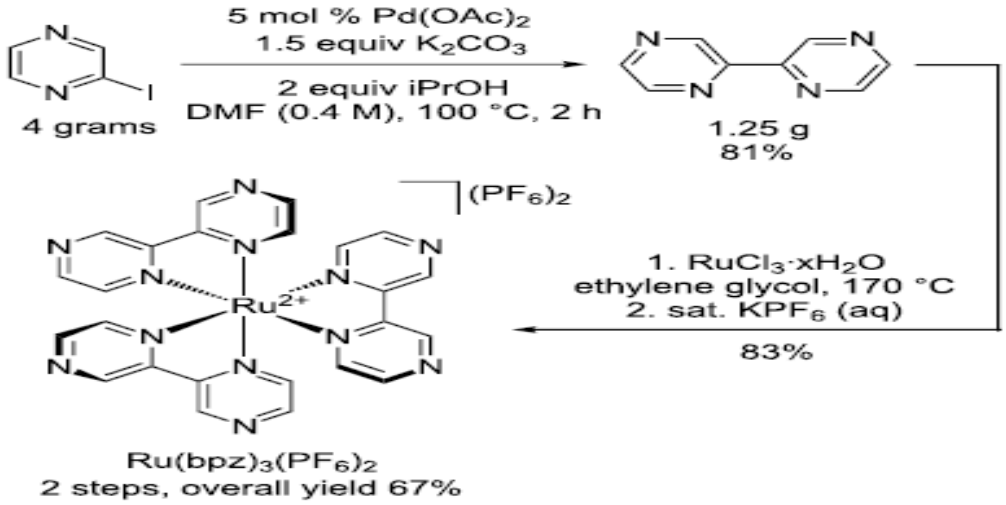

Scheme 1.10: View of the Preparative-scale synthesis of $[Ru(bpz)_3](PF_6)_2$ adopted from [45].

1.2.3 Tungsten and molybdenum complexes:

Preparation of Tungsten and molybdenum with 2,2'-bipyrazine ligand in the literature is not much, most of them are mononuclear, homoleptic complexes.

Its start in 1982 by R. J. Crutchley and A. B. P. Lever when React tungsten and molybdenum with bipyrazyl yields $W(CO)_4bpz$, $Mo(CO)_4bpz$. The electronic, vibrational, and HNMR spectra and electrochemistry of these products were compared with those of their bipyridyl analogues. It is concluded that bipyrazyl is no better a π acceptor than bipyridyl because of weaker σ bonding leaving the metal ion more positively charged [{24}].

In 1986, The Long-wavelength charge transfer absorption energies of $W(CO)_4bpz$, $Mo(CO)_4bpz$ complexes was measured in various solvents and compared with those for corresponding 2,2'-bipyridine complexes[{46}].

And in 1988 synthesis mixed ligand, cis-$Mo(CO)_2(PBu_3)_2$(bdz) which have four isomeric bidiazine(bdz) ligands 3,3'-bipyridazine, 2,2'-bipyrazine, 2,2'- and 4,4'-bipyrimidine, can undergo reversible one-electron oxidation and reduction and show small redox potential differences of less than 1.5 V. The small HOMO-LUMO gap gives rise to long-wavelength metal-to-ligand charge transfer absorptions, an assignment which is supported by ESR studies. Guidelines for the construction of complexes with small charge-transfer absorption energies by CO/PR3 exchange are presented. Although a ligand-centered MO is occupied during reduction, the small g factors of the radical complexes indicate low-lying ligand-field-excited states which are believed to be responsible for the pronounced light-sensitivity of the compounds [{47}].

In 1996[{48}], prepared dinucular molybdenum with diimine ligand one of them 2,2'-bipyrazine in general formula, $Mo_2X_4(diimine)_2$ (X = Cl, Br, I and diimine = 2,2'-bipyridine, 4,4'-dimethyl-2,2'-bipyridine, 2,2'-bipyrazine, 3,3'-bipyridazine, 2,2'-bipyrimidine, 1,10-phenanthroline and 4,7-diphenyl-l,10-phenanthroline) and characterized by a three dimensional X-ray diffraction.

1.2.4 Rhodium and Iridium complexes:

In 1982, W. A. Fordyce and G. A. Crosby [49] prepared new complexes of 2,2'-bipyrazine and other nitrogen-heterocyclic with Rhodium(I) and Iridium(I), 2,2'-bipyrazin react with Rhodium(I) to produce [Rh(cod)(bpz)](PF_6) cod =1,5-cyclooctadien, but doesn't react with Iridium (I). And study the Electronic absorption spectra at room temperature and emission spectra and lifetimes at 77 K, The results from these complexes are compared and contrasted with those from other four-coordinate Rh(I) and Ir(I) d^8 complexes and from six-coordinate d^6 complexes with N-heterocyclic ligands. The rhodium complexes used by A.Furlani et al, 1987[50] as co-catalyst in polymerization reaction of N-benzylpropargylamine gave polymers with molecular weights between about 1000 and 4000. The highest percentage yield of polymerization reaction exist when using rhodium complexes which contains 2,2'-bipyrazine ligand [Rh(cod)(bpz)]PF_6 as co-catalyst.

Table1.2: Polymerization reactions of N-benzylpropargylamine (BPA) in the presence of Rh complexes adopted from[50].

Catalyst	PBPA yield (%)	Molecular weight[a] A	Molecular weight[a] B	Ratio of units I_3^-/monomer	Conductivity (ohm^{-1} cm^{-1})
[Rh(cod)(bipy)] PF_6	17.7		2300	0 0.34 0.68	10^{-14} 10^{-5} 1
[Rh(cod)(bipy)]ClO_4	40.9	3400	1100	0 0.17 0.34 0.68	10^{-13} (A) 10^{-10} (A) 10^{-5} (A), 10^{-6} (B) 4 (A), 2 (B)
[Rh(cod)(bipy)] $B(Ph)_4$	25.3	2800	1400	0 0.17 0.34 0.68	10^{-10} (A), 10^{-13} (B) 10^{-6} (A), 10^{-9} (B) 4 (A), 10^{-6} (B) 2 (B)
[Rh(cod)(dipyam)] PF_6	41.3		1300	0 0.17 0.34 0.68	10^{-13} 10^{-9} 10^{-4} 6
[Rh(cod)(bpz)] PF_6	68.2	3700	1500	0 0.17 0.34 0.68	10^{-12} (A), 10^{-13} (B) 10^{-6} (A), 10^{-10} (B) 10^{-4} (A), 10^{-5} (B)[b] 3 (A), 7 (B)
[Rh(nbd)(bipy)] PF_6	10.2	1500			
[Rh(nbd)(dipyam)] PF_6	25.3		1400	0 0.34 0.68	10^{-13} 10^{-6} 5
[Pt(C≡CCH$_2$NHCH$_2$Ph)$_2$(PPh$_3$)$_2$]	10.2		1500	0 0.17 0.34	10^{-13} 10^{-6} 4

- Fraction A insoluble in CCl_4, fraction B soluble in CCl_4

- B The same value was obtained by dissolving the pellet in THF and reprecipitating with petroleum ether

M. Ladwig and W. Kaim, in 1991[51] was synthesis and study the Electronic structures and the electrochemical properties of $[(C_5Me_5)ClRh(bdz)](X)$ and $(C_5Me_5)Rb(bdz)$; X^- = Cl^-, PF_6^- and bdz = bidiazines (3,3'-bipyridazine, 2,2'-bipyrazine, 2,2'- and 4,4'-bipyrimidine).

1.2.5 Rhenium complexes:

The rhenium transition metal with 2,2'-bipyrazine and other polypyridyl ligand with general formula $[Re(CO)_3(LL)(X)]$, (LL = 2,2-bipyridine, 4,4'-dimethyl-2,2'-bipyridine, 1,10-phenanthroline, 5-chloro-1 ,l0-phenanthroline and 2,2'-bipyrazine) and X= C1,Br, CH_3CN, was synthesis and study the photophysics and photoredox chemistry of the MLCT excited state of rhenium in 1986[52].The absorption spectra of these compounds in the near-UV-Visible region are dominated by intense MLCT transitions depending on the nature of LL and X, these complexes exhibit green/red room-temperature luminescence of weak-to-moderate intensity.

$[Re(CO)_3(LL)(X)]$, is emissive in solution at room temperature and undergoes facile electron-transfer reactions with a variety of electron donor and acceptor molecules. Laser photolysis studies on three aspects of the excited-state photophysics and photoredox chemistry are described in this work: (a) sensitivity of the room-temperature absorption and emission to variation in the nature of the polypyridyl ligand and solvent; (b) excited-state absorption spectral features and (c) reversible and irreversible 'reductive' quenching (using various amines as electron donors) and their relevance to the photocatalytic reduction of CO_2 to CO.

W. Kaim et al, in 1989[53] Synthesis, electrochemistry and emission spectroscopy in fluid solution of $(bdz)Re(CO)_3$ Hal (Hal = Cl or Br) complexes derived from the four isomeric bidiazine (bdz) chelate ligands 3,3′-bipyridazine, 2,2′-bipyrazine, 2,2′- and 4,4′-bipyrimidine from $Re(CO)_3Hal$ by thermal substitution. All the complexes were found to show long-wavelength emission at room temperature in chloroform solution after irradiation into the metal-to-ligand charge transfer (MLCT) band. Spectroscopic data and electrochemical reduction potentials confirm the superior polarizing ability of neutral $Re(CO)_3Hal$ fragments for α-diimine π system, and the electrochemical and

photophysical data can be correlated with the established properties of the free ligands, of their anion radicals, and of other d^6 metal (W^0, Ru^{II}) complexes.

A number of different Re(diimine)$(CO)_3$Cl, [Re(diimine)-$(CO)_3$(py)]$^+$, and [Re(diimine)$(CO)_3$(py-X)]$^+$, where X is a substituent bonded to py and diimine is 2,2′-bipyrazine (bpz) or 5,5′-dimethyl-2,2′-bipyrazine (Me_2bpz), complexes have been synthesized. The photophysical properties and Computational calculation was studied in 2007[54].

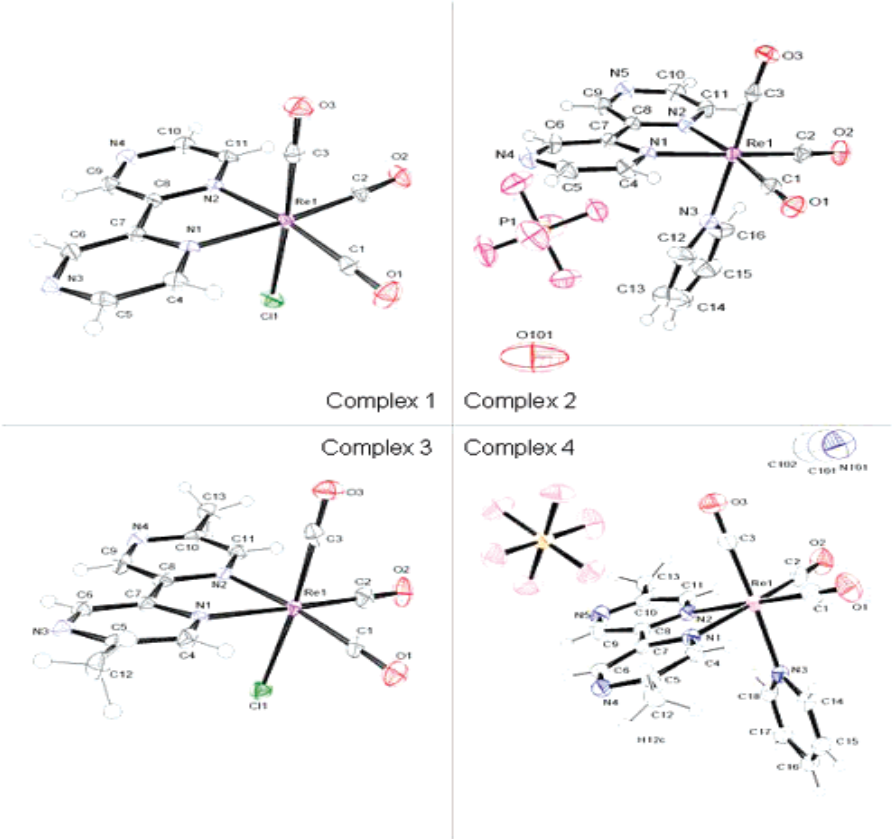

Fig 1.1: View ORTEP figures of Re(bpz)$(CO)_3$Cl (1), [Re(bpz)$(CO)_3$py]PF_6 (2), Re(Me_2bpz)$(CO)_3$Cl (3), [Re(Me_2bpz)$(CO)_3$py]PF_6 (4) , Adopted from [54].

In 2012, C. Bronner and O. S. Wenger, was synthesis Two rhenium(I) tricarbonyl diimine complexes, one of them with a 2,2′-bipyrazine (bpz) and a pyridine (py) ligand in addition to the carbonyls ([Re(bpz) $(CO)_3$(py)]$^+$), and one tricarbonyl complex with a 2,2′-bipyridine (bpy) and a 1,4-pyrazine (pz) ligand ([Re(bpy) $(CO)_3$(pz)]$^+$), and their photochemistry with 4-cyanophenol in acetonitrile solution was explored. Metal-to-

ligand charge transfer (MLCT) excitation occurs toward the protonatable bpz ligand in the $[Re(bpz)(CO)_3(py)]^+$ complex while in the $([Re(bpy)(CO)_3(pz)]^+$ complex the same type of excitation promotes an electron away from the protonatable pz ligand. and to explore how this difference in electronic excited-state structure affects the rates and the reaction mechanism for photoinduced proton-coupled electron transfer (PCET) between 4-cyanophenol and the two rhenium(I) complexes[55].

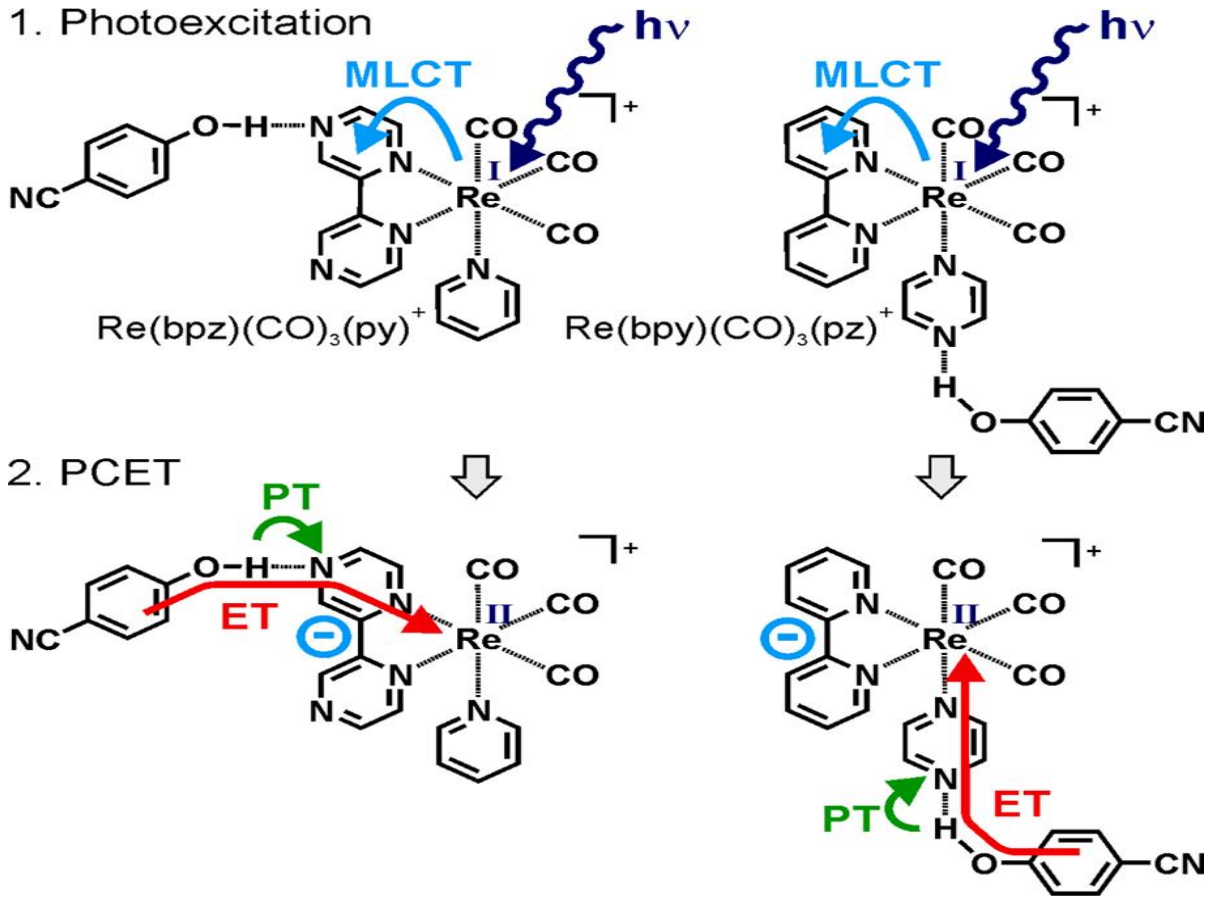

Scheme 1.11: View MLCT Excitation and PCET Chemistry in Two Distinct 4-Cyanophenol/Rhenium Reaction Couples, adopted from [55].

1.2.6 Platinum, Palladium and Silver complexes:

The Platinum- nucleobases complexes have a wide range of research, the preparation of platinum- 2,2′-bipyrazine complexes start in 1989 when V. Christou and G. B. Young, papered $[Pt(CH_2CMe_3)_2(bpz)_2]$ complex by ligand displacement from the diene complex

[Pt(CH_2CMe_3)2(nbd)], (nbd = bicyclo[2.2.1]hepta-2,5diene). And the spectroscopic properties (H^1 and C^{13} NMR, IR and UV-visible) was described [56].

In 1998, lippert group prepared [(en)Pd(bpz)]$(ClO_4)_2$, [(en)Pt(bpz)]$(NO_3)_2$ and a cyclic trimetallic complexes with bridging ligand (2,2′-bipyrazine) [{(en)Pt(bpz)}$_3$] $(NO_3)_6$ with a new coordination modes of 2,2′-bipyrazine ligand[57].

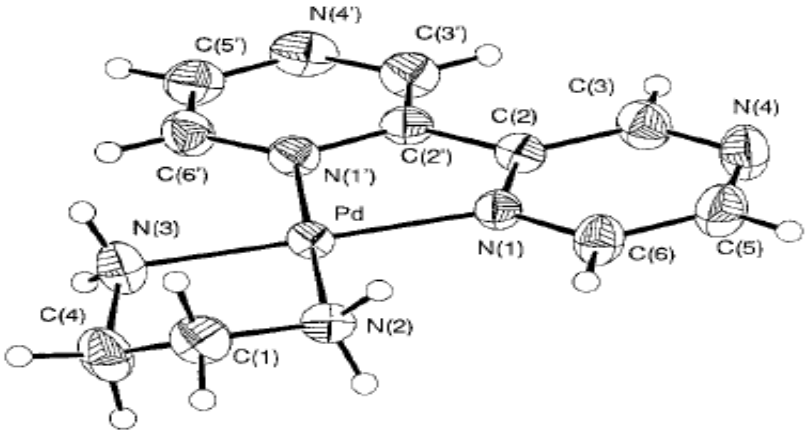

Fig 1.2: View of the [(en)Pd(bpz)]$^{+2}$ cation adopted from [57].

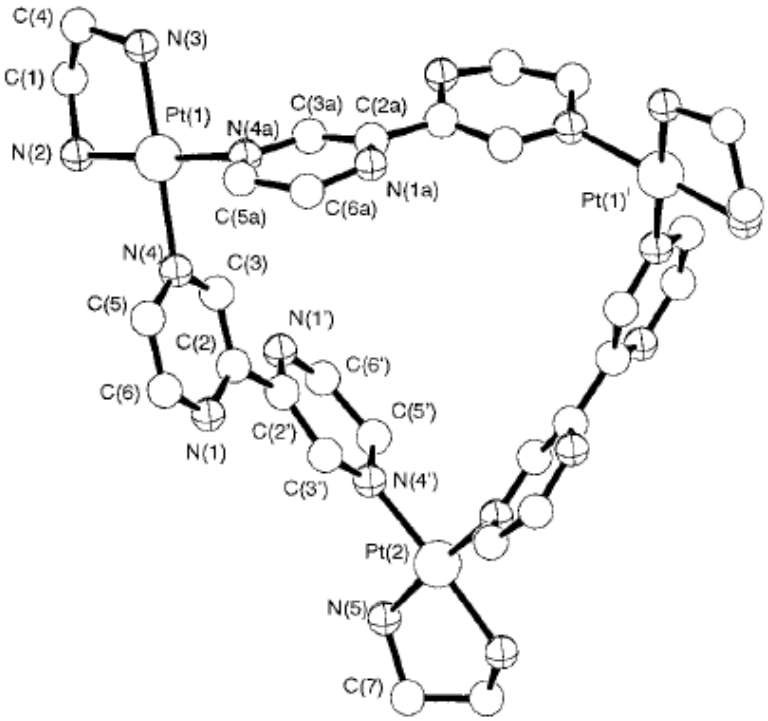

Fig 1.3: View of the a new coordination modes of 2,2′-bipyrazine ligand in [{(en)Pt(bpz)}$_3$] cation adopted from [57].

In the next year, lippert group was described a new molecular triangle, $[\{(en)Pt(bpz)Pd(en)\}_3](NO_3)_4(PF_6)_8$, consisting of three $(en)Pt^{II}$ and three $(en)Pd^{II}$ entities (en = ethylenediamine) and three 2,2' bipyrazine (bpz) ligands that bridge metals through N(4) , N(4') and N(1), N(1') with a new coordination mods [58].

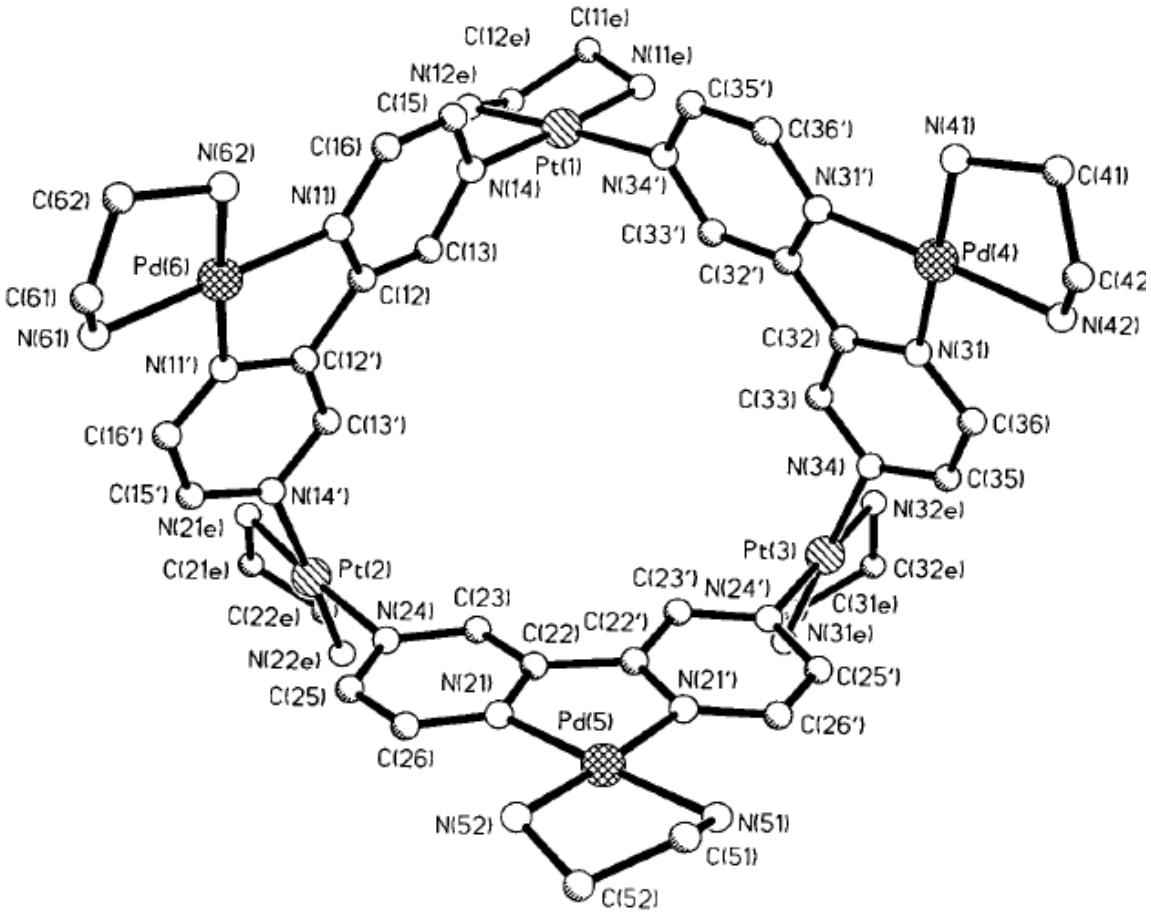

Fig 1.4: View of the a new coordination modes of 2,2′-bipyrazine ligand in $[\{(en)Pt(bpz)Pd(en)\}_3]$ cation adopted from [58].

In 2000[59] a new molecular architecture with a new coordination modes of 2,2′-bipyrazine was prepared by lippert group, Based on metal triangles derived from 2,2′-bipyrazine (bpz) and enM^{II} (M= Pt, Pd), to produce :

$[\{enPt(bpz\text{-}N4,N4')\}_3](NO_3)_2(ClO_4).4H_2O$,

$[\{enPt(bpz\text{-}\ N4,N4')\}_3](NO_3)_2(PF_6)_4.\ 5.25H_2O$, $[enPt(bpz\text{-}N1,N1')](NO_3)_2$,

$[\{enPt(N4,N4'\text{-}bpz\ N1,N1')Pten\}_3](NO_3)_7(PF_6)_5.4H_2O$,

$[\{enPd(N4,N4'\text{-}bpz\text{-}N1,N1')Pden\}_3](NO_3)_4(PF_6)_8.5H_2O$,

$[\{enPt(bpz\text{-}N4,N4')\}_3AgNO_3]_2(NO_3)_8(PF_6)_4.15.5H_2O$,

$[\{enPt(bpz\text{-}N4,N4')\}_3AgNO_3]_3(NO_3)_{12}.AgNO_3.22H_2O$.

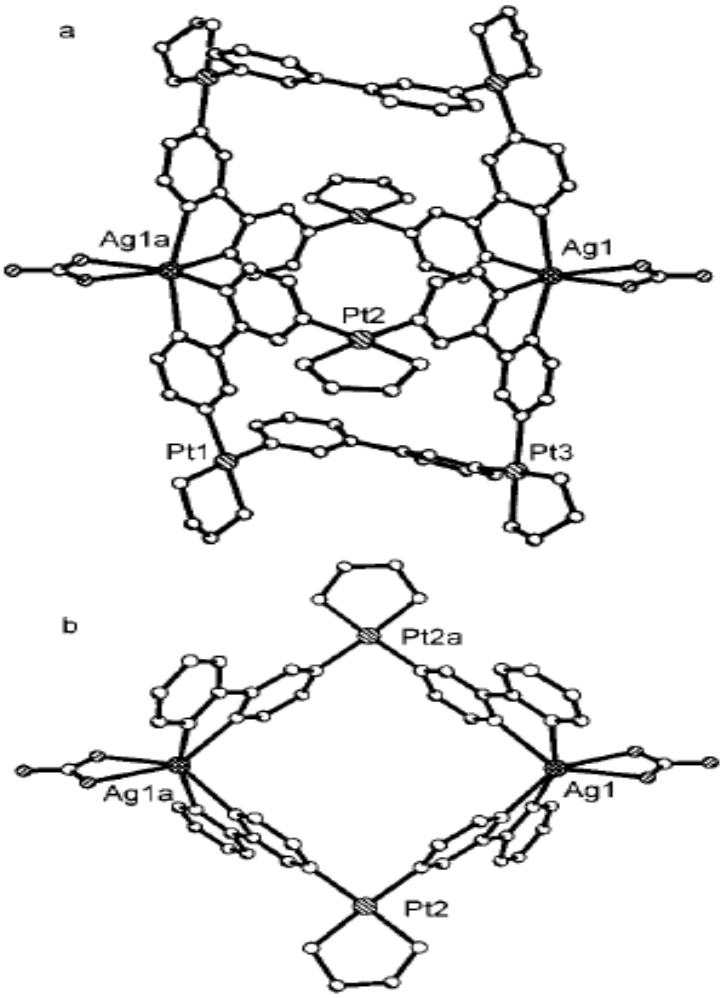

Fig 1.5: View the X-ray crystal structure of (a) cation $[\{enPt(bpzN4,N4')\}_3$-$AgNO_3]_2(NO_3)_8(PF_6)_4.15.5H_2O$ and (b) detail of the central molecular Pt_2Ag_2 square adopted from [59].

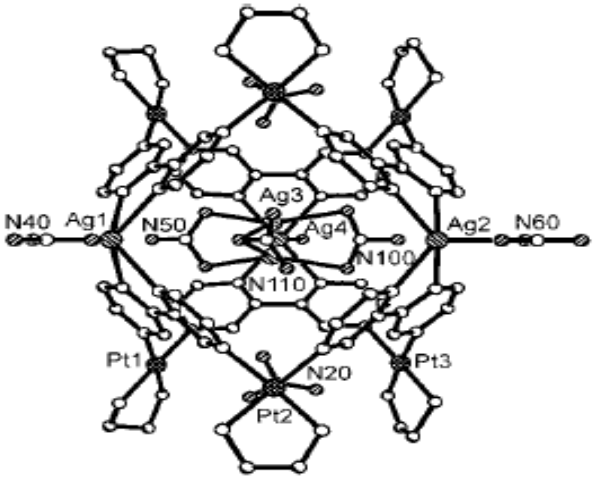

Fig 1.6: View of the Molecular container $[\{enPt(bpz\text{-}N4,N4')\}_3AgNO_3]_3(NO_3)_{12}$ $.AgNO_3.22H_2O$ adopted from [59].

The Triangles $[\{enPd(N4,N4'\text{-}bpz\text{-}N1,N1')Pden\}_3]^{+12}$ used in 2010 as host molecules of Sulfate[60].

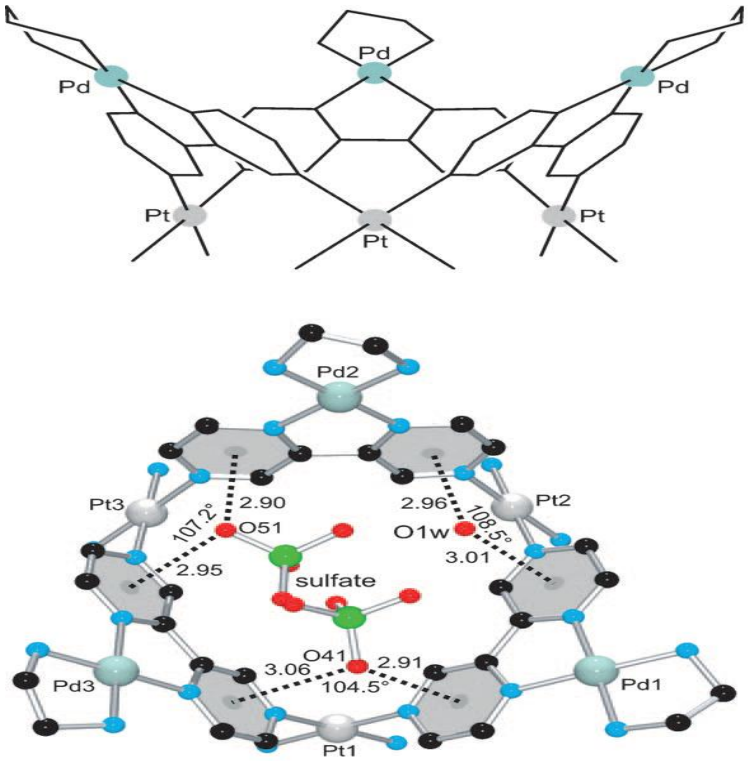

Fig 1.7: Side view (top) view of cation 1 (bottom) without and with $SO_4^{-2} \cdot H_2O$ enclosed. The SO_4^{-2} ion is disordered over two positions, whereas H_2O occupies a single one adopted from [60].

And molecular architecture with 2,2′-bipyrazine and palladium to produce infinite Loop and molecular square. By the potential of $[L_2Pd(2,2'\text{-bpz-}N1,N1')]^{2+}$ [L_2 = en, L = H_2O, 2,2'-bpz = 2,2'-bipyrazine] for use as an angular element in the generation of self-organized systems of variable molecular architecture has been studied. Ag+ forms an infinite loop $[enPd(2,2'\text{-bpz-}N1,N1')Ag]_n(ClO_4)_{3n}$ with $[enPd(2,2'\text{-bpz-}N1,N1')]^{2+}$, in which the metal ions function as cross-linking agents between the organic entities 2,2′-bpz. Complex $[(H_2O)_2Pd(2,2'\text{-bpz-}N1,N1')]^{2+}$, on the other hand, self-assembles as a bis(μ-OH) dinuclear species $[(2,2'\text{-bpz-}N1,N1')Pd(OH)_2Pd(2,2'\text{-bpz-}N1,N1')](NO_3)_2.4\ H_2O$, and in the presence of 4,4′-bipyridine (4,4′-bpy) as a molecular square of $[\{(bpz\text{-}N1,N1')Pd(4,4'\text{-bpy})\}4](NO_3)_8.14.4\ H_2O$ with the heteroaromatic 4,4′-bpy ligands representing the cross-linking entities[61].

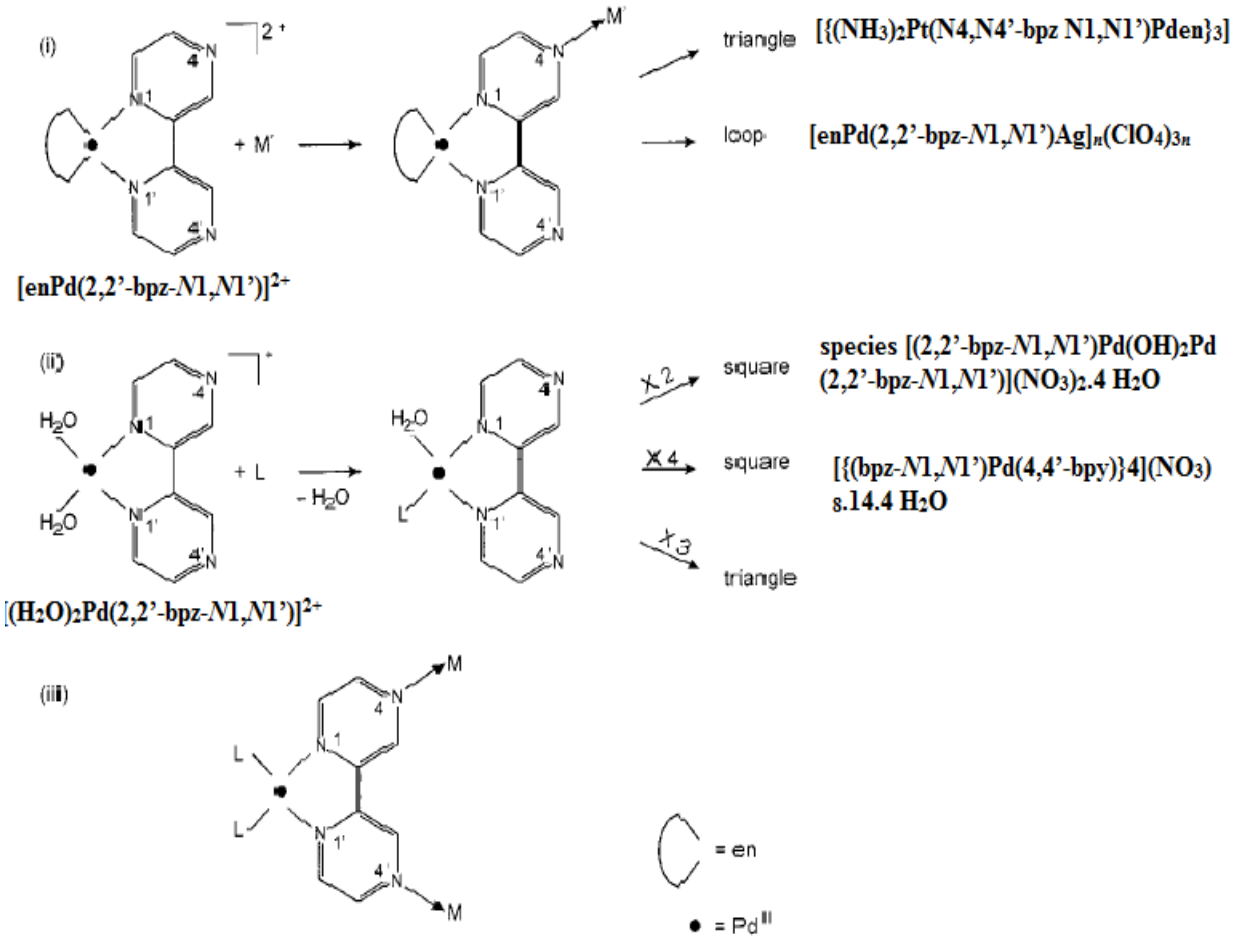

Scheme 1.12: Outlined of $[L_2Pd(2,2'\text{-bpz-N1,N1'})]^{2+}$ cations [L_2 = en, L =H_2O, 2,2'-bpz = 2,2'-bipyrazine] represent useful angular units for the generation of larger cationic aggregates adopted from [61].

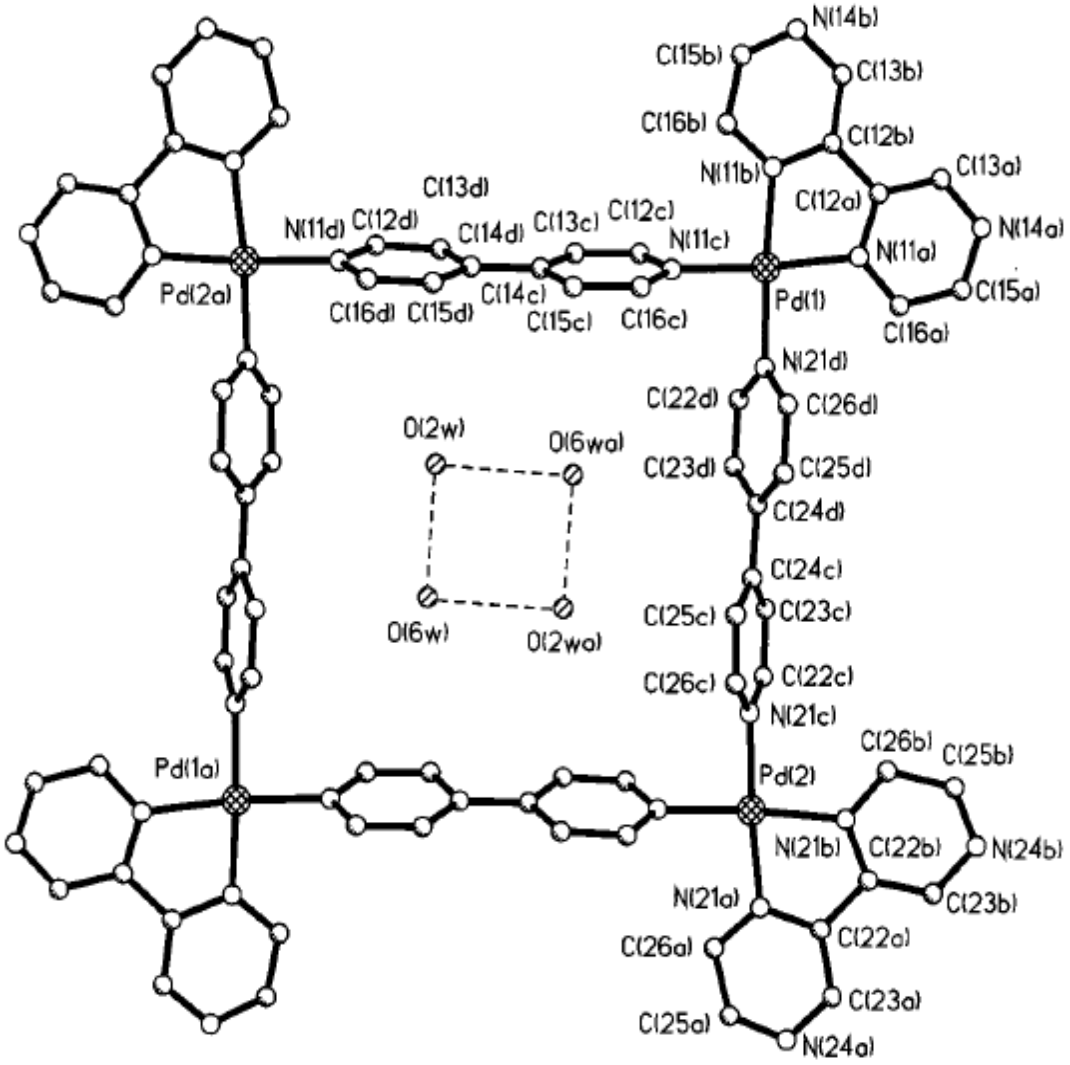

Fig 1.8: View of the tetranuclear cation of $[\{(bpz\text{-}N1,N1')Pd(4,4'\text{-}bpy)\}_4](NO_3)_8.14.4\text{-}H_2O$ with four water molecules inserted adopted from [61].

Lippert group in 2006 prepared a molecular architectures with Pt^{II} and Pyrazine as a building block, start from prepare pyrazine (pz) complexes containing cis-$(NH_3)_2Pt^{II}$, (tmeda)Pt^{II} (tmeda) N,N,N′,N′-tetramethylethylenediamine), and trans-$(NH_3)_2Pt^{II}$ entities, then synthesis a dinuclear complex, a cyclic tetranuclear complex, and a trinuclear mixed-metal complex, And characterized by X-ray crystallography and H^1 NMR spectroscopy. An example of the complexes which prepared in this work is a cyclic tetranuclear complex *cis*-$[\{(NH_3)_2Pt(pz)\}_4](NO_3)_8.3.67H_2O$[62] which is displayed in (Fig 1.9) .

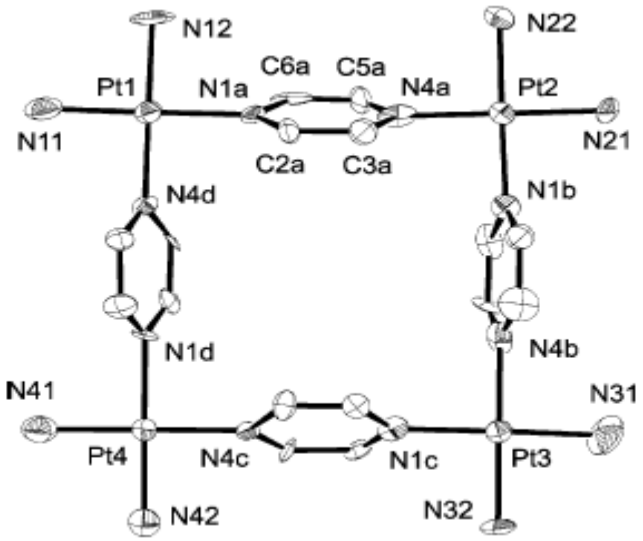

Fig 1.9: View of the cation of open pz box of *cis*-[{$(NH_3)_2Pt(pz)\}_4$]$(NO_3)_8$.3.67H_2O adopted from [62].

M. E. Kelly et al[63], Prepared, characterized and study crystal structures of mononuclear and dinuclear complexes of dibromodimethylplatinum(IV) with chelating bidentate nitrogen donor ligand one of them is 2,2'-bipyrazine, to produces a number of complexes of the types [$PtBr_2Me_2$(N ~ N)], an example of this type of compounds is [$PtBr_2Me_2$(2,2'-bpz)].

A. Galstyan et al[64], studied the X-ray crystal structure of a host–guest [{(en)Pt(2,2'-bpz,*N4*,*N4*')}$_3$]$(NO_3)_2(SO_4)_2 \cdot 13H_2O$ reveals a NO_3^- ion sandwiched between pyrazine moieties and oriented roughly perpendicular to the Pt_3 plane, which is in contrast to the in-plane orientation of NO_3^- when a second anion (ClO_4^-) is taken up by the Pt_3 metallacycle simultaneously.

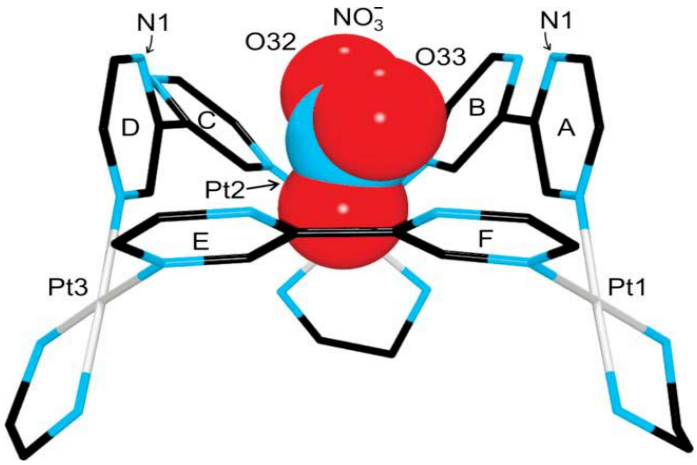

Fig 1.10: View of the NO_3^- sandwiched between pz rings A and D of cation $[\{(en)Pt(2,2'\text{-bpz},N4,N4')\}_3]^{+6}$ adopted from[64].

The reaction of 2,2'-bipyrazine (2,2'-bpz) with cis-$(NH_3)_2Pt^{II}$ in water gives a variety of products, several of which were isolated and characterized by X-ray analysis: *cis*-$[Pt(NH_3)_2(2,2'\text{-bpz-}N4)_2](NO_3)_2\cdot 3H_2O$, $[\{cis\text{-Pt}(NH_3)_2(2,2'\text{-bpz-}N4,N4')\}_3](PF_6)_5NO_3\cdot 7H_2O$, $[\{cis\text{-Pt}(NH_3)_2(2,2'\text{-bpz-}N4, N4')\}_3](BF_4)_2(SiF_6)_2\cdot 15H_2O$, and $[\{cis\text{-Pt}(NH_3)_2(2,2'\text{-bpz-}N4,N4')\}_4](SO_4)_4\cdot 22H_2O$[13].

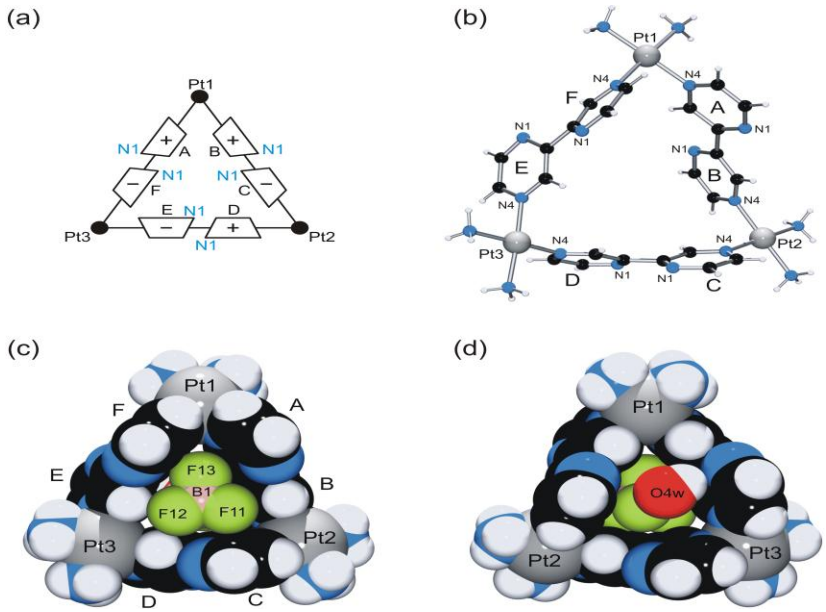

Fig 1.11: View of the(a) Schematic view of cation $[\{cis\text{-Pt}(NH_3)_2(2,2'\text{-bpz-}N4, N4')\}_3](BF_4)_2(SiF_6)_2\cdot 15H_2O$. (b) Molecular cation with atom numbering scheme. (c,d) Space filling representation with a BF_4^-, and H_2O included (upper and lower views, respectively) adopted from[13].

In 2000 start preparation silver-2,2'-bipyrazine complexes when A. J. Blake et al, react 2,2'-bipyrazine with $AgBF_4$ the product of this reaction depend on the crystallization solvent used, to give $\{[Ag(bpyz)](BF_4)\}_\infty$ in a chiral three-dimensional adamantoid coordination network or a two-dimensional sheet incorporating five coordinate Ag(I) ions[65].

And The influence of solvent and anion on the formation of coordination polymers of silver(I) and the multi-modal ligands 2,2'-bipyrazine (bpyz) and pyrazino[2,3-*f*]quinoxaline (pyq) has been studied in the same year. The results of this work a new three-dimensional coordination networks, $\{[Ag(bpyz)]X\}_\infty$ or $\{[Ag(pyq)]X\}_\infty$, Whereas ($X = BF_4^-$ or PF_6^-), two-dimensional sheet, $\{[Ag(bpyz)(MeCN)]BF_4\}_\infty$, and one-dimensional polymer $\{[Ag_2(bpyz)_2(PhCN)][BF_4]_2\}_\infty$[66].

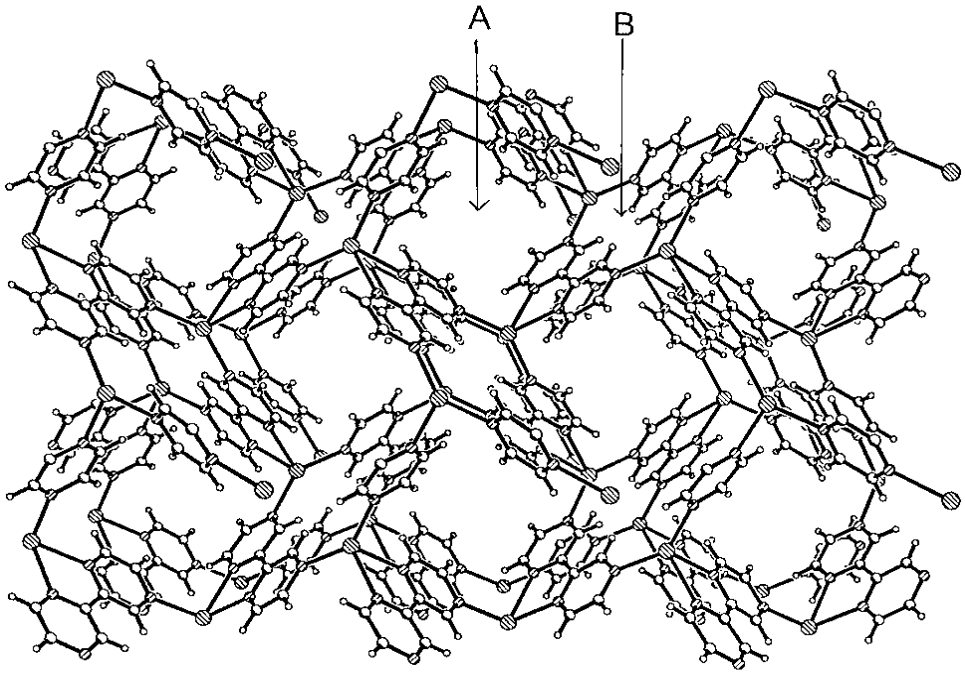

Fig 1.12: View of the two different channels formed (A&B) in $\{[Ag(bpyz)](BF_4)\}_\infty$ adopted from[65].

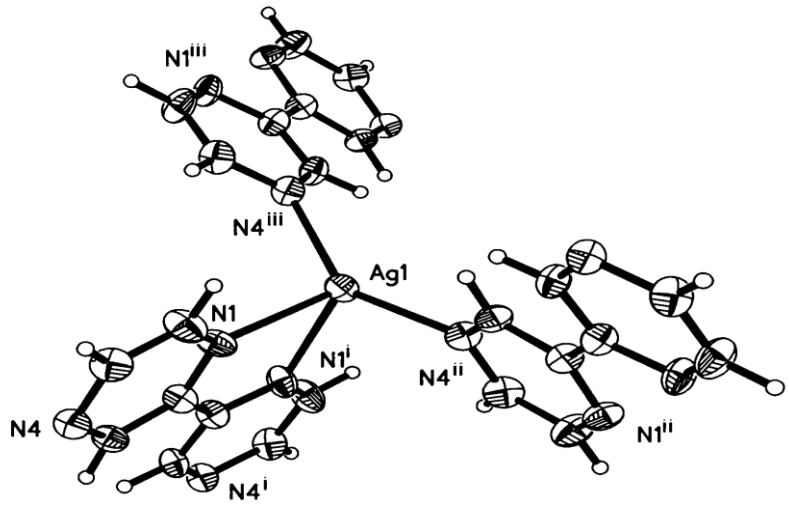

Fig 1.13: View of the silver (I) geometry observed in complex $\{[Ag(bpyz)](PF_6)\}_\infty$ and $\{[Ag(bpyz)](BF_4)\}_\infty$ adopted from[{66}].

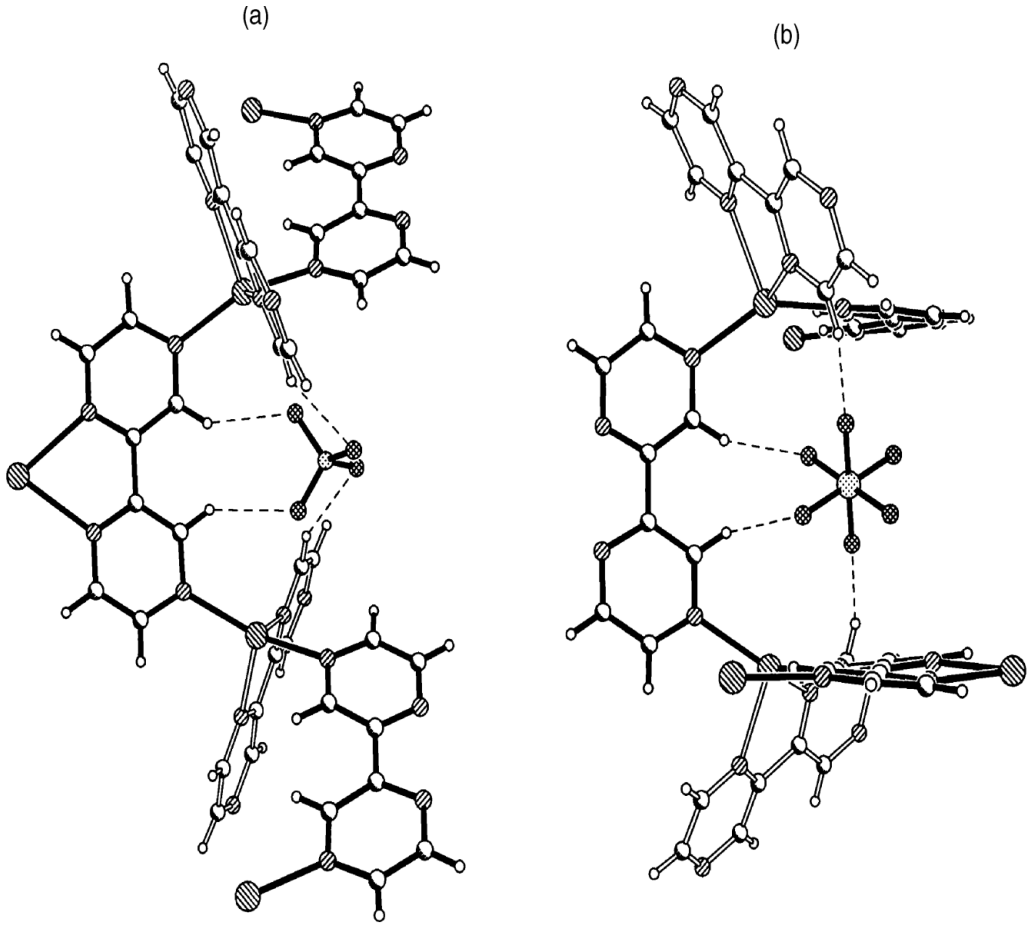

Fig 1.14: Views perpendicular cross section of (a) $\{[Ag(bpyz)](BF_4)\}_\infty$ and (b) $\{[Ag(bpyz)](PF_6)\}_\infty$ indicating how the increased volume of anion results in a decreased pitch, adopted from[{66}] .

The preparation of silver-2,2'-bipyrazine complexes continuous in 2005 when T-T. Yeh et al[67], prepared and characterized a luminescent coordination polymer $[Ag_2(bpyz)(NO_3)_2]_n$, which comprises of silver chains with alternating strong and weak Ag · · ·Ag interactions.

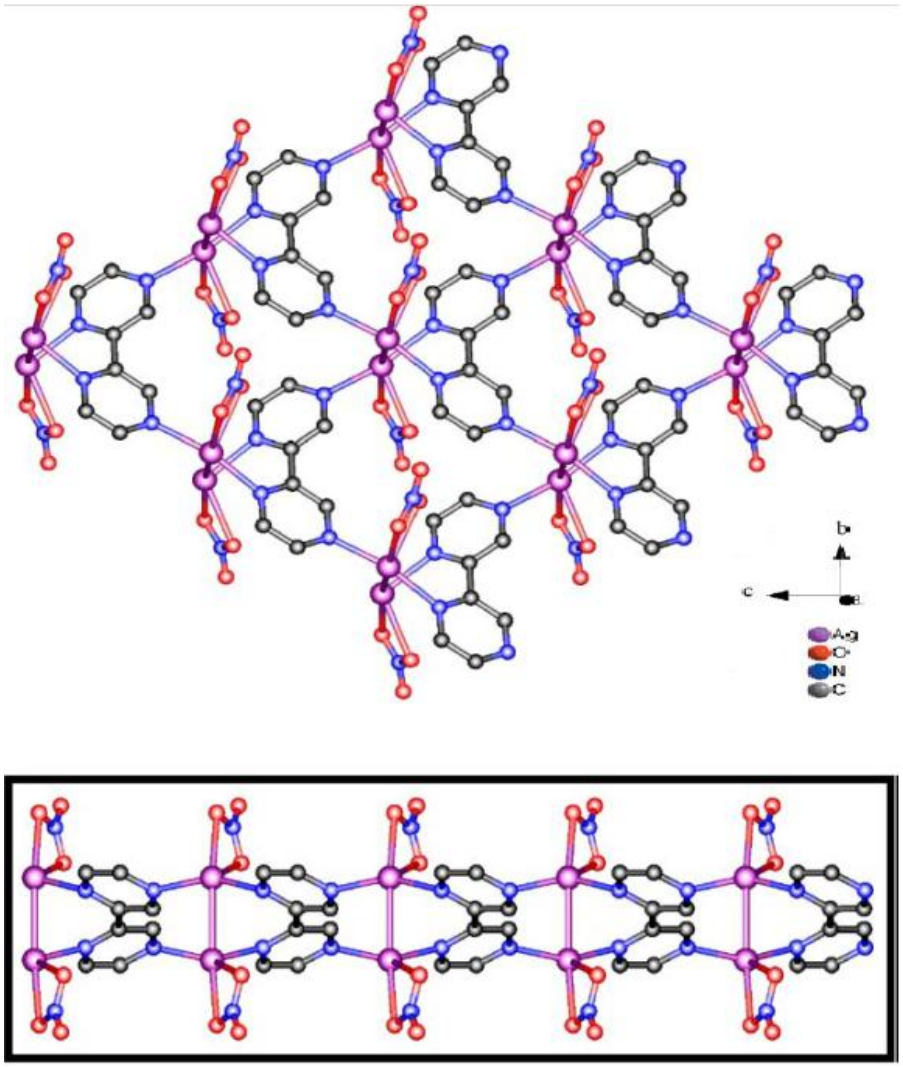

Fig 1.15: Top: 2D layer architecture viewed slightly off the *c*-axis with a (4,4) topology in $[Ag_2(bpyz)(NO_3)_2]_n$ by considering the Ag_2 units as connecting nodes. Bottom: a side-view of the 2D layer along the *a*-axis showing that the coordinated nitrate ions are arranged on both sides of the layer, adapted from[67].

Lippert group[68], prepare a coordination polymer heteronuclear contining silver, constructs derived from triangular 2,2'-bipyrazine complexes of cis-a_2Pt^{II} (with a = NH_3

or a_2= ethylenediamine) with silver(I) to get a [{cis-$(NH_3)_2$Pt(2,2'-bpz)}$_3$]Ag(SiF_6)3(BF_4)·7H_2O. The structures of this compound is dominated by host–guest interactions between the triangular metal vases of [{cis-Pt(NH_3)2(2,2'-bpz-N4,N4')}$_3$]$^{6+}$ and [{cis-Pt(en) (2,2'-bpz-N4,N4')}$_3$]$^{6+}$ and anions, respectively, as well as hydrogen bonding involving anions and water molecules and electrostatics. Preliminary AFM (atomic force microscopy) studies reveal that the +6 cations of [{cis-Pt(NH_3)2(2,2'-bpz-N4,N4')}$_3$]$^{6+}$ have a strong tendency to interact with double-stranded DNA with formation of condensed DNA states.

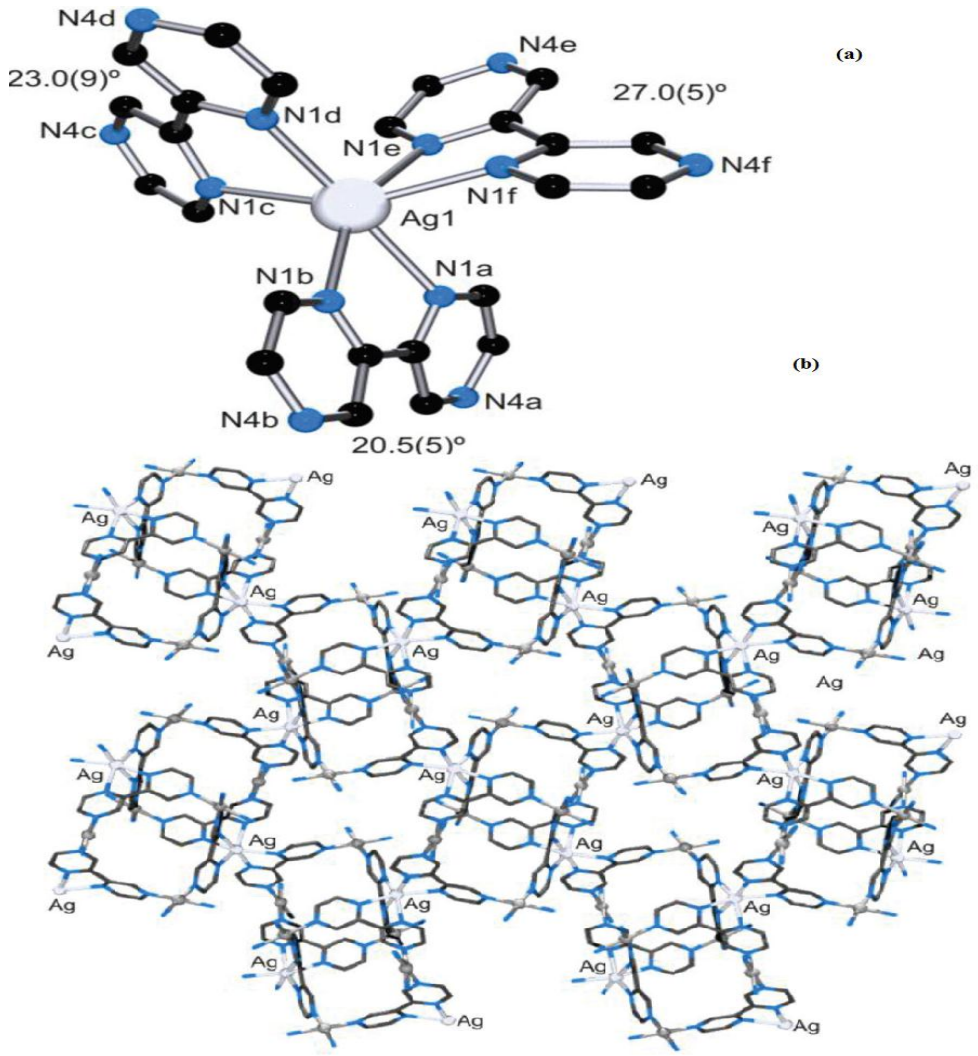

Fig 1.16: (a) View of the coordination sphere of Ag_1 (b) View of the two-dimensional framework of stoichiometry $(Pt_3Ag)_n$ in complex [{cis-$(NH_3)_2$Pt(2,2'-bpz)}$_3$]Ag(SiF_6)3(BF_4)·7H_2O, adopted from[68].

1.2.7 Iron, Cadmium and Mercury complexes:

In the literature has been reported only one crystal structure of iron with 2,2'-Bipyrazine complex, in this work was synthesis and study the crystal structure of the low-spin iron(II) complex $[Fe(bpz)_3](ClO_4)_2 .H_2O$ by a single crystal X-ray diffraction. The iron atom exhibits a FeN6 distorted octahedral geometry and compared to those of other tris-chelated iron(II) complexes with bidentate nitrogen heterocycles[{69}].

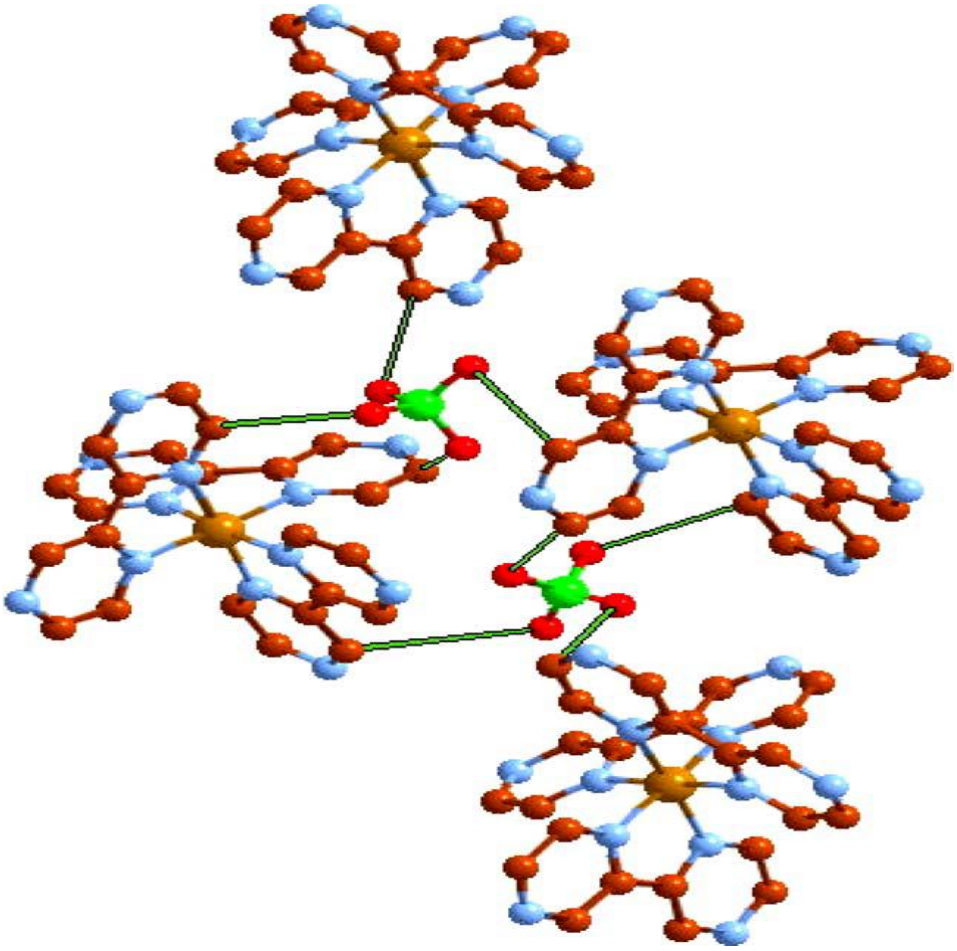

Fig 1.17: Showing of the supramolecular $[Fe(bpz)_3](ClO_4)_2 .H_2O$ and type of interactions C–H(bpz) …... O (ClO_4^-) in $[Fe(bpz)_3](ClO_4)_2 .H_2O$ adopted from[{69}].

Mercury with 2,2'-bipyrazine In the literature has been reported only one work, In 2009 J-Y. Wu et al[{70}], prepared and characterize a Polymeric mercury compounds, $[HgCl_2(bpym)]n$ (bpym = 5,5′-bipyrimidine), $[Hg_2Br_4(bpym)]n$, and $[HgX_2(bpyz)]n$ (bpyz = 2,2′-bipyrazine), which are composed of linear mercury chains were assembled

from HgX_2 (X = Cl, Br). This study showed that face-to-face π-π (aryl-aryl) stacking interaction of coordinated aromatic ligands (bpym and bpyz) is the primary structure directing influence in the formation of linear Hg chains.

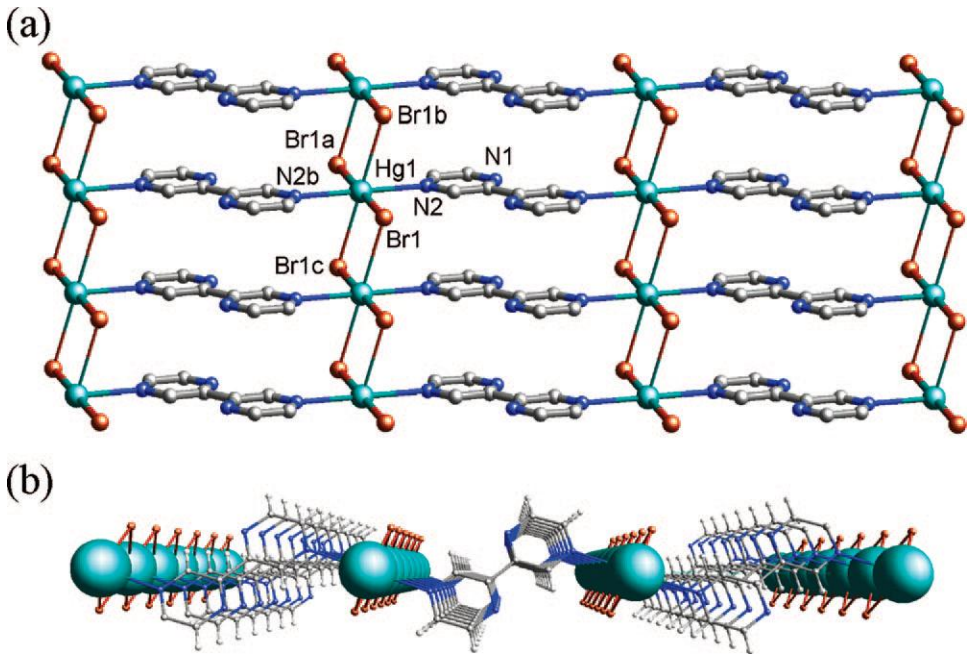

Fig 1.18: (a) 2D layer structure of $[HgB_2(bpyz)]_n$ viewed slightly off the *c*-axis.
(b) Perspective viewed the infinite linear mercury chains along the crystallographic *b* axis adopted from[{70}].

Lippert group[{68}], prepare a coordination polymer heteronuclear contining cadmium transition metal constructs derived from triangular 2,2'-bipyrazine complexes of cis-a_2Pt^{II} (with a = NH_3 or a_2 = ethylenediamine) with cadmium(II) to get a $\{[\{(en)Pt(2,2'\text{-}bpz)\}_3]\ Cd_2(H_2O)_7\}(SO_4)_5 \cdot \{[Cd\text{-}\ (H_2O)_6](SO_4)\}\cdot 15H_2O$. The structures of this compound is dominated by host–guest interactions between the triangular metal vases of $[\{cis\text{-}Pt(NH_3)2(2,2'\text{-}bpz\text{-}N4,N4')\}_3]^{6+}$ and $[\{cis\text{-}Pt(en)\ (2,2'\text{-}bpz\text{-}N4,N4')\}_3]^{6+}$ and anions, respectively, as well as hydrogen bonding involving anions and water molecules and electrostatics. Preliminary AFM (atomic force microscopy) studies reveal that the +6 cations of $[\{cis\text{-}Pt(NH_3)2(2,2'\text{-}bpz\text{-}N4,N4')\}_3]^{6+}$ have a strong tendency to interact with double-stranded DNA with formation of condensed DNA states.

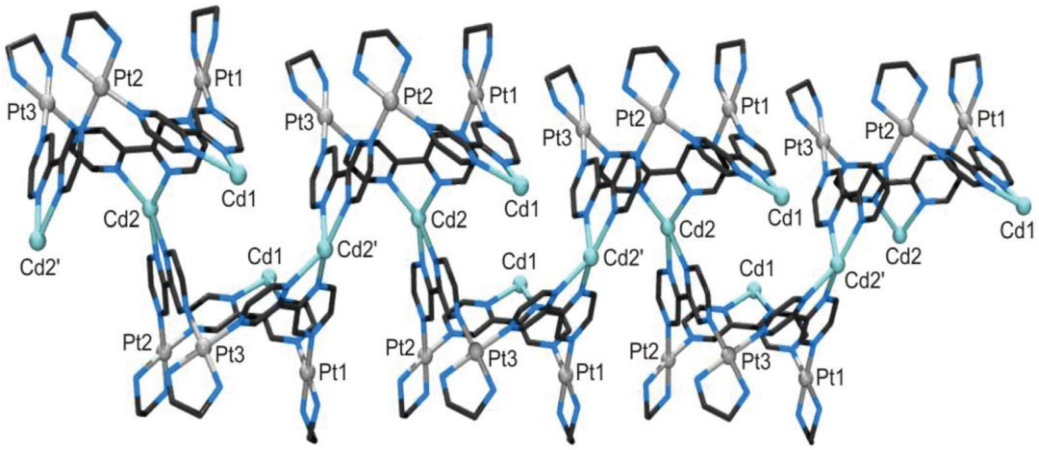

Fig 1.19: View of the polymeric structure of complex{[{(en)Pt(2,2'-bpz)}$_3$] $Cd_2(H_2O)_7$}$(SO_4)_5$ ·{[Cd- $(H_2O)_6$](SO_4)}·15H_2O adopted from[68].

1.2.8 Copper complexes:

Preparation of copper-2,2′-bipyrazine complexes start in 2002 when J. Mathieu et al[71], designed heterotopic ligands (bipyrazine-bipyridine) then reacts with 1 equiv. of Cu^I the dimetallic complex $[Cu_2(L4)_2][PF_6]_2$ is formed in a cooperative process. In this coordination compound the two strands are oriented in opposite directions as illustrated by the X-ray structure of $[Cu_2(L4)_2][PF_6]_2$ in (Fig 1.20) .

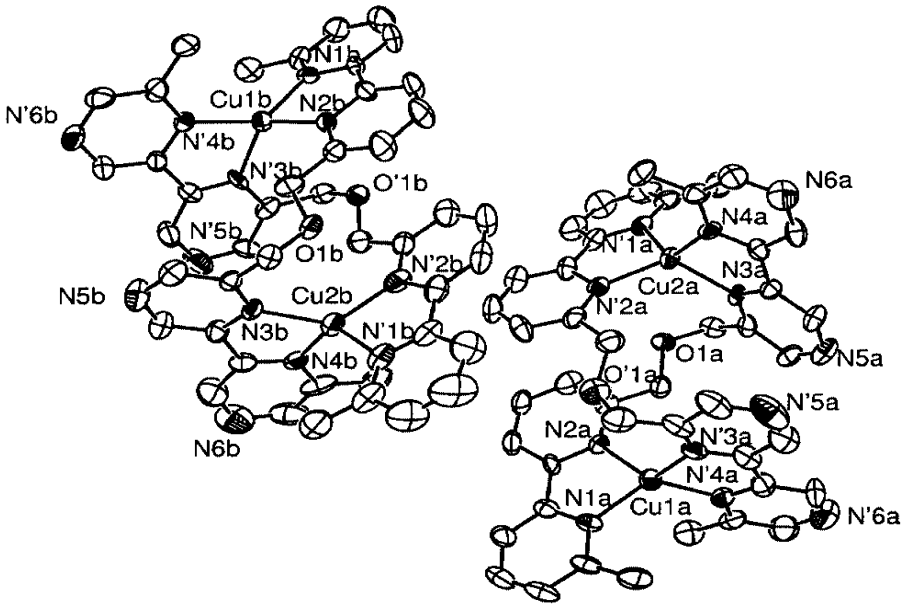

Fig 1.20: Structure (ORTEP view) of the two helicates in the asymmetric unit; the hexafluorophosphate anions and hydrogen atoms have been omitted for clarity, adopted from[71].

A number of new 2,2'-biimidazole, 2,2'-bipyrazine containing copper(II) complexes have been prepared and the crystal structure of some of them have been determined by single crystal X-ray diffraction, and the magnetic properties have been studied, The copper atom has a distorted square pyramidal geometry in this family of complexes for Example $[Cu(bpz)(C_5O_5)(H_2O)]$,($C_5O_5^{2-}$ = dianion of croconic acid).

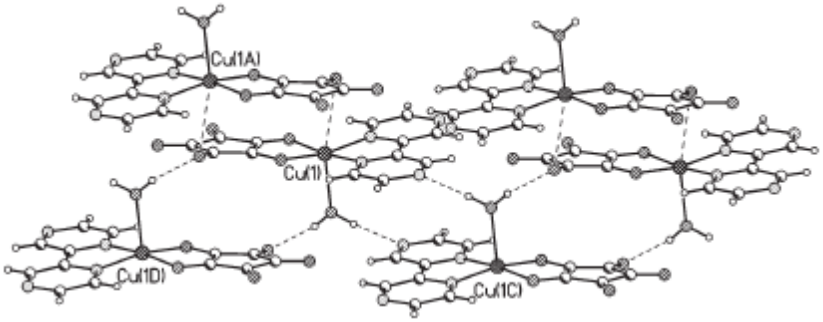

Fig 1.21: A view of the layer structure of $[Cu(bpz)(C_5O_5)(H_2O)]$ adopted from[{72}].

In 2004[{73}], 2,2'-bipyrazine -containing copper(ii) complexes of formula $[Cu(bpz)(ox)]_n$, $[Cu_2Cl_2(bpz)_2(H_2O)_2(ox)][Cu(bpz)(H_2O)_2(ox)]\cdot 2H_2O$ [bpz = 2,2'-bipyrazine; ox = oxalate] have been prepared and their structures have been determined by X-ray diffraction on single crystals.

The structure of $[Cu_2Cl_2(bpz)_2(H_2O)_2(ox)][Cu(bpz)(H_2O)_2(ox)]\cdot 2H_2O$ contains neutral $[Cu(bpz)\ (H_2O)_2(ox)]$ (mononuclear) and $[Cu_2(bpz)_2(H_2O)_2Cl_2(ox)]$ (dinuclear) units where the bpz acts as a bidentate ligand and the oxalate group adopts the bidentate (mononuclear) and bis-bidentate (dinuclear) coordination modes.

Magnetic susceptibility measurements for the two in the temperature range 1.9−290K reveal the occurrence of weak for$[Cu(bpz)(ox)]_n$ and strong for $[Cu_2Cl_2(bpz)_2(H_2O)_2(ox)]$ $[Cu(bpz)\ (H_2O)_2(ox)\ ]\cdot 2H_2O$) antiferromagnetic interactions between the copper(II) atoms in agreement with the out-of-plane $[Cu(bpz)(ox)]_n$ and in-plane $[Cu_2Cl_2(bpz)_2(H_2O)_2(ox)][Cu(bpz)(H_2O)_2\ (ox)]\cdot 2H_2O$) exchange pathways involved.

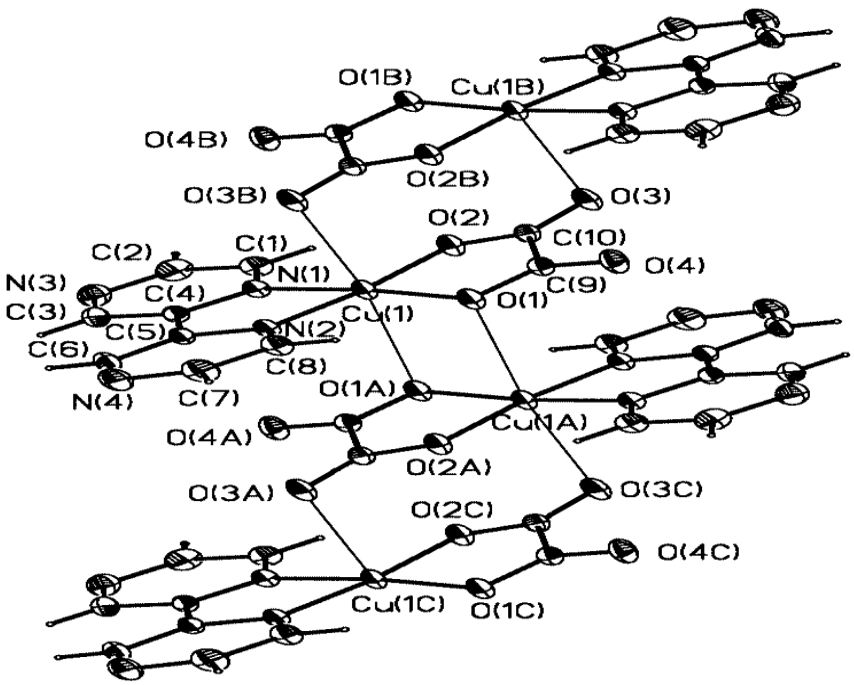

Fig 1.22: Section of the chain in $[Cu(bpz)(ox)]_n$ adopted from[73].

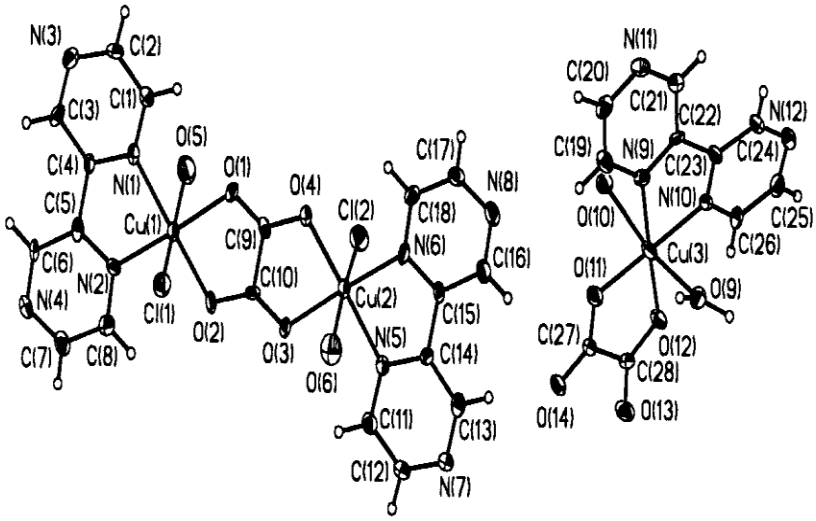

Fig 1.23: The dinuclear and mononuclear building blocks in $[Cu_2Cl_2(bpz)_2(H_2O)_2$-$(ox)][Cu(bpz)(H_2O)_2(ox)]\cdot 2H_2O$, adopted from[73].

Reactions of the *p*-sulfonatothiacalix[4]arene salt (Na_4H_4TCAS) and $CuSO_4$ in the presence of 2,2'-bipyrazine (2,2-bpz) generated 2D coordination networks formed by tetranuclear cluster subunits, $\{[Cu(2,2'\text{-}bpz)(H_2O)_3]^{2+}$ Є$[Cu_4(TCAS)(\mu 4\text{-}SO_4)(H2O)_4]^{2-}$

$\cdot 16H_2O\}n$. X-ray diffraction analyses reveal that this complex include metal–2,2'-bipyrazine complex into the hydrophobic cavities of *p*-sulfonatothiacalix[4]arenes as guests through supramolecular interactions[74].

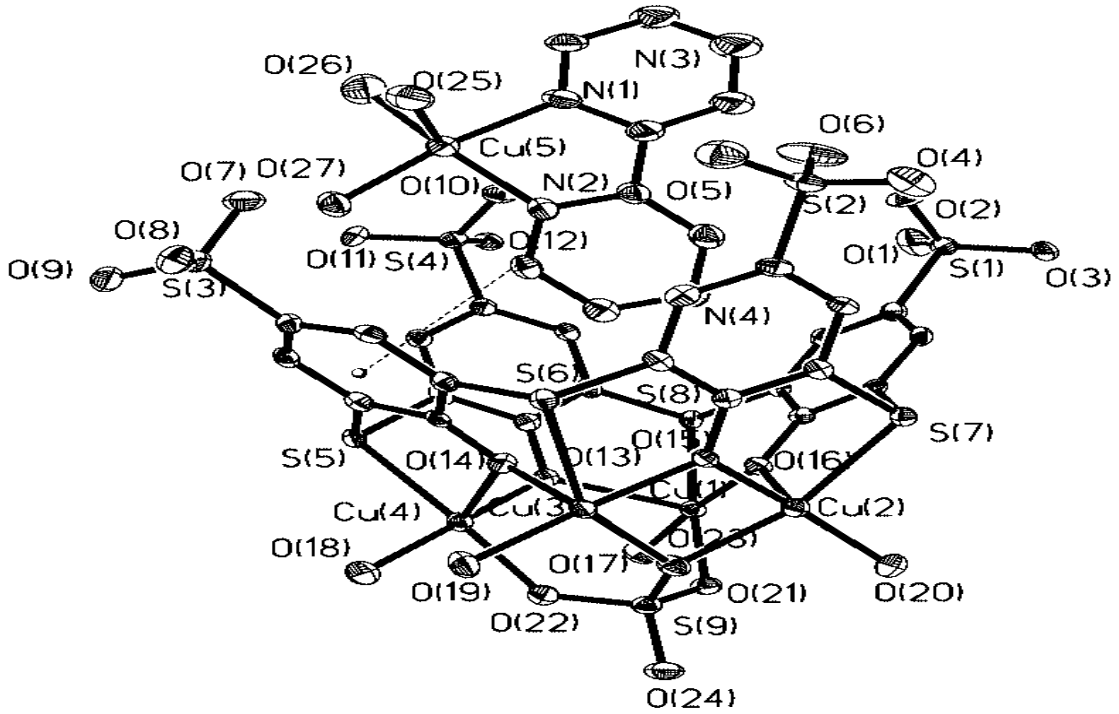

Fig 1.24: The X-ray asymmetric units of$\{[Cu(2,2'\text{- bpz})(H_2O)_3]^{2+}$ Є$[Cu_4$ (TCAS)(μ4-$SO_4)(H2O)_4]^{2-}\cdot 16H_2O\}n$, adopted from[74].

In 2008 C. Yuste et al[75], have been prepared and study the crystal structures and magnetic properties of the copper(II) complexes containing heterocyclic ligand one of them 2,2'-bipyrazine, reaction of copper(II) with 2,2'-bipyrazine results $[Cu_4(bpz)_4(tcm)_8]$(tcm = tricyanomethanide) The structure of this complex is made up of neutral centrosymmetric rectangles of (2,2-bipyrazine)copper(II) units at the corners, the edges being built by single- and double-μ-1,5-tcm bridges with copper–copper separations of 7.969 and 7.270A˚,respectively. Five- and six-coordinated copper atoms with distorted square pyramidal and elongated octahedral environments. The investigation of the magnetic properties' in the temperature range 1.9–295 K has shown the occurrence of weak ferromagnetic interactions (Fig 1.2.8.6) .

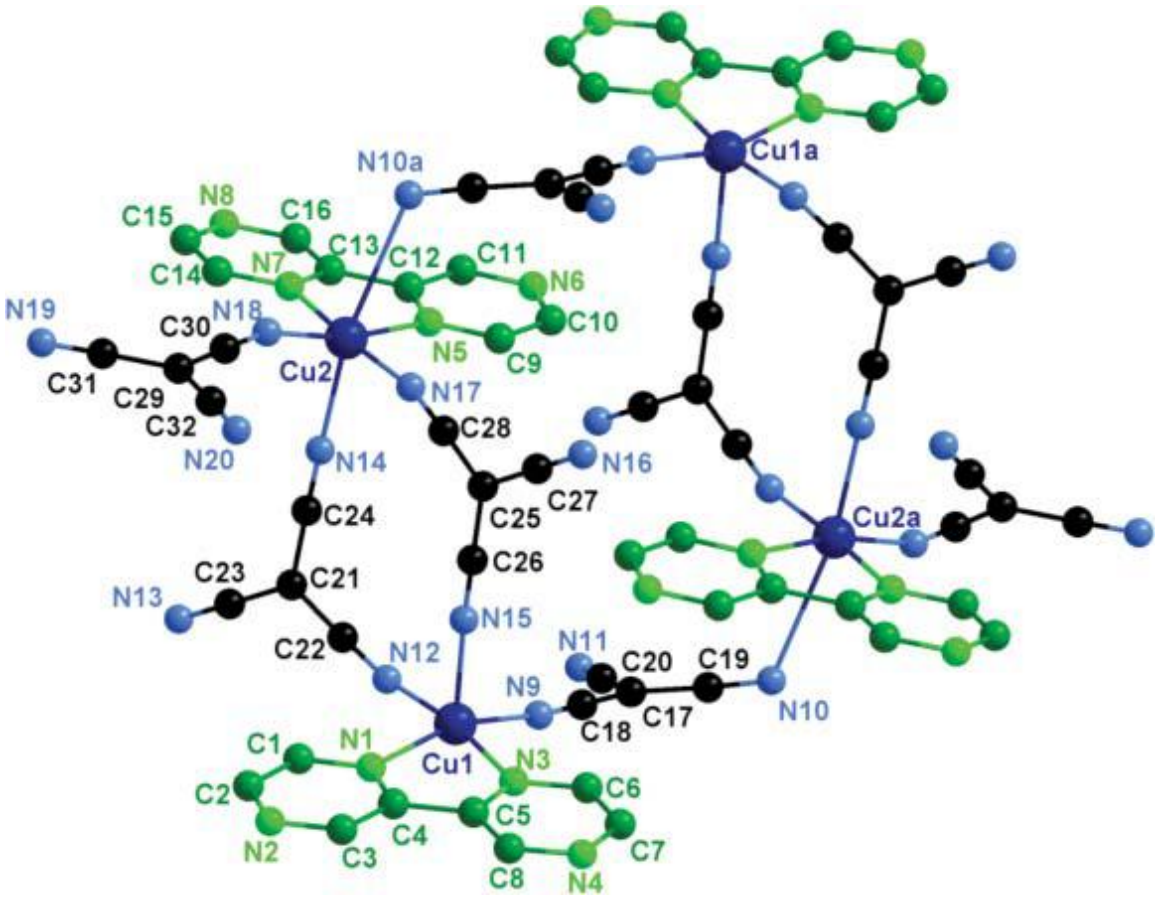

Fig 1.25: View of the tetranuclear $[Cu_4(bpz)_4(tcm)_8]$complex, adopted from[{75}].

Lippert group[{68}], prepare a discrete and polymeric heteronuclear constructs derived from triangular 2,2'-bipyrazine complexes of cis-a_2Pt^{II} (with a = NH_3 or a_2 = ethylenediamine) to get a decanuclear Pt_6Cu_4 complex, $[\{(en)Pt(2,2'\text{-}bpz)\}_3]_2Cu_4(H2O)_6(NO_3)_{20}\cdot 11H_2O$ with the appearance of a paddle wheel, a dodecanuclear Pt_6Cu_6 capsule with a Cu^{2+} ion in its interior and additional Cu^{2+} ions in its periphery giving a total composition of $[\{(en)Pt(2,2'\text{-}\ bpz)\}_3]_2Cu_{11}(NO_3)_{34}(H2O)_{18}\cdot 3H_2O$. The structures of this compound is dominated by host–guest interactions between the triangular metal vases of $[\{cis\text{-}Pt(NH_3)2(2,2'\text{-}bpz\text{-}N4,N4')\}_3]^{6+}$ and $[\{cis\text{-}Pt(en)\ (2,2'\text{-}bpz\text{-}N4,N4')\}_3]^{6+}$ and anions, respectively, as well as hydrogen bonding involving anions and water molecules and electrostatics. Preliminary AFM (atomic force microscopy) studies reveal that the +6 cations of $[\{cis\text{-}Pt(NH_3)2(2,2'\text{-}bpz\text{-}N4,N4')\}_3]^{6+}$ have a strong tendency to interact with double-stranded DNA with formation of condensed DNA states.

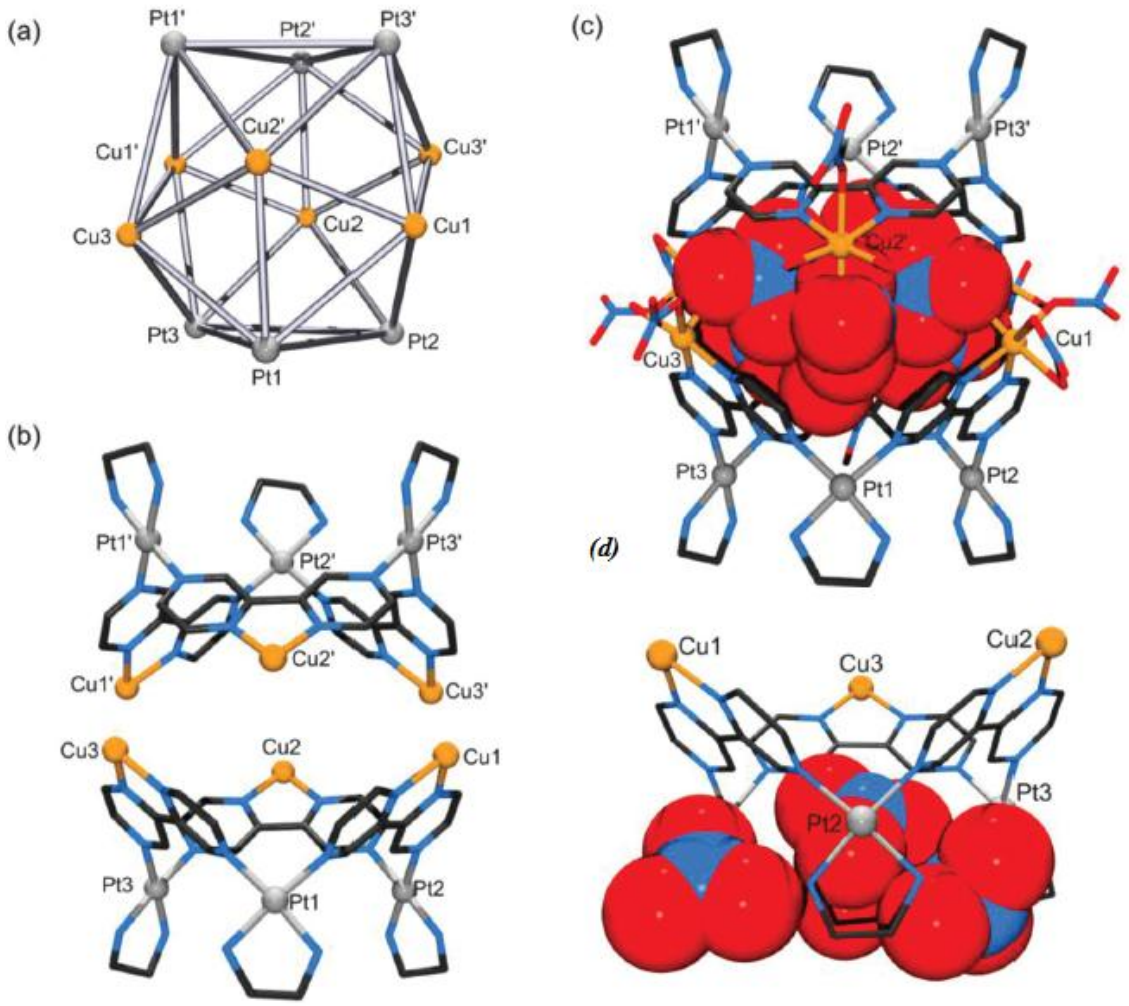

Fig 1.26: Details of container complex $[\{(en)Pt(2,2'\text{-}\ bpz)\}_3]_2Cu_{11}\ (NO_3)_{34}\ (H2O)_{18}\cdot 3H_2O$: (a) Pt_6Cu_6 icosahedral skeleton; (b) two Pt_3Cu_3 vases forming a capsule; (c) filled host cavity ;(d) View of the four nitrate anions hosted at the bottom of the Pt_3 in $[\{(en)Pt(2,2'\text{-}\ bpz)\}_3]_2Cu_{11}(NO_3)_{34}(H2O)_{18}\cdot 3H_2O$ adopted from[{68}].

1.2.9 Nickel complexes:

According to Cambridge crystallographic data centre, (CCDC) no any crystal structure for complex containing nickel and 2,2'-bipyrazine ligand. in 2004[{77}], 2007[{22}] and 2010[{76}] A. Klein group, have been prepared mixed ligand complexes contains 2,2'-bipyrazine ligand, but there is no single crystal X-ray analysis for any of them, due to

the equilibrium tends towards the starting materials, because of 2,2'-bipyrazine ligand is poor base[77] .

Organometallic nickel complexes with α-diimine have gained an enormous interest in the last decade. This is mainly due to a number of important catalytic processes like olefin oligoor polymerization, olefin/CO co-polymerization, and various (electro)catalytic C–C coupling reactions. Paralleling their use in catalysis[76], and to controlled the size of nickel nanoparticles by Thermal degradation of nickel(II) bipyridine complex[77].

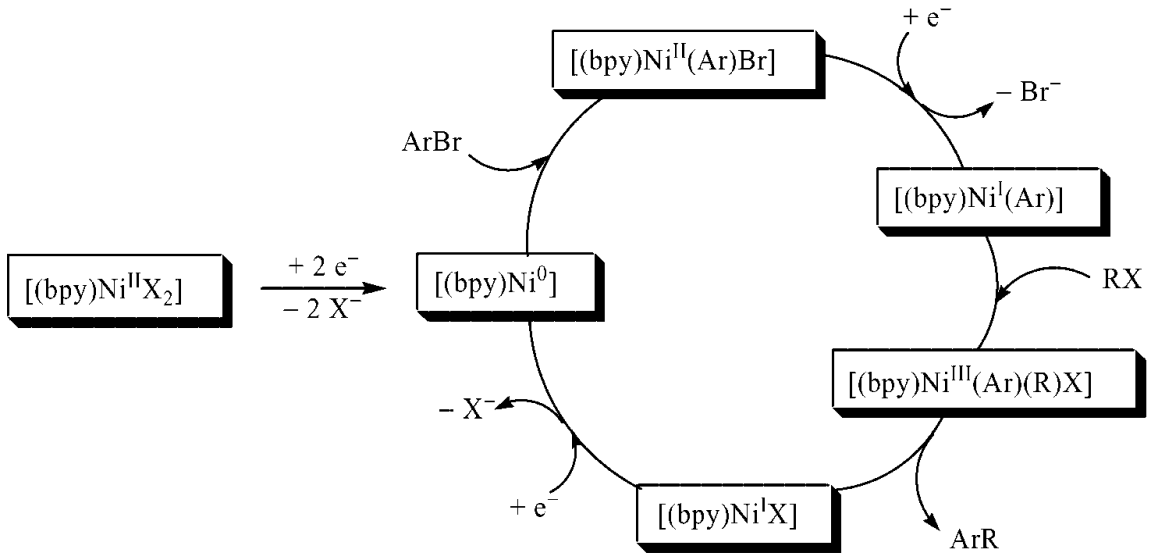

Scheme 1.13: Proposed mechanism for the C–C coupling reactions by nickel-α-diimine complex adopted from[22].

In 2004, A. Klein et al[78], prepared and characterized New organometallic nickel complexes of the type [(α-diimine)Ni(Mes)Br] and [(α-diimine)Ni$(Mes)_2$] (Mes = mesityl = 2,4,6-trimethylphenyl), α-diimine ligands is tmphen = 3,4,7,8-tetramethyl-1,10-phenanthroline, dmbpy = 4,4'-dimethyl-2,2'-bipyridine, bpy = 2,2'-bipyridine, bpym = 2,2'-bipyrimidine, bpm = 4,4'-bipyrimidine.

And in other work in 2007[22]the redox properties of this complexes have been studied in detail by various electrochemical and spectroelectrochemical (UV-Vis, NIR and EPR) methods. Electrochemical oxidation leads to formally trivalent nickel species, the metal contribution to the unpaired electron for the formally monovalent and trivalent nickel species.

1.3 Research Objectives:

- Synthesis of new mono and polynuculear coordination compounds containing copper(II) and nickel(II) metal ion and 2,2'-bipyrazine ligand.
- synthesis of new mixed ligand complexes containing nickel(II) and copper(II) with 2,2'-bipyrazine and other nitrogen bases.
- Characterization of the new complexes using X-ray diffraction (SCXRD), FTIR, UV-Vis spectroscopy and thermal analysis by differential scanning calorimetry (DSC).
- Study the structurally and magnetically prosperities of the new complexes.

Chapter two

Experimental (Instruments, materials and methods)

2.1 Instruments:

2.1.1 Single Crystal X-ray Diffraction (SCXRD):

This non-destructive technique and the most common experimental method of obtaining a detailed structure of a molecule, that allows resolution of individual atoms, single crystal X-ray diffraction (SXRD) is performed by analyzing the pattern of X-rays diffracted by an ordered array of many identical molecules (single crystal). This technique can reveal the chirality of molecule, molecular structure and packing of molecules.

- X-ray diffraction studies was done at University of Zaragoza – Spain- by Professor Pablo J. Sanz Miguel,data collection for three compounds were recorded at 100 K on an APEX-II diffractometer equipped with an area detector and graphite monochromated Mo Kα radiation (0.71073 Å). Data reduction of the diffraction images was performed using the APEX2 software. All the structures were solved by direct methods and refined by full-matrix least-squares methods based on F2 using the SHELXL-97 software. All distance and angle calculations were performed using the SHELXL-97 and WinGX programs.

2.1.2 Mercury - Crystal Structure Visualisation:

Mercury offers a comprehensive range of tools for 3D structure visualization, the exploration of crystal packing and the statistical analysis of CSD search data.

This program helps me in the Literature survey for this work and to open and collected data from cif file of crystallography analysis and display the figures and measurement of angles, distance and torsions used in this thesis.

2.1.3 Fourier transforms infrared spectroscopy (FT-IR):

FT-IR stands for Fourier Transform Infra Red, the preferred method of infrared spectroscopy. In infrared spectroscopy, IR radiation is passed through a sample. Some of

the infrared radiation is absorbed by the sample and some of it is passed through (transmitted). The resulting spectrum represents the molecular absorption and transmission, creating a molecular fingerprint of the sample. Like a fingerprint no two unique molecular structures produce the same infrared spectrum. This makes infrared spectroscopy useful for several types of analysis.

- FT-IR analysis was performed at research and development laboratory in Beit Jala Pharmaceutical Company (BJP) using Nicolet Avatar 320 FT-IR Spectrometer.

2.1.4 Differential Scanning Calorimetry (DSC) Thermal Analysis:

- DSC analysis was done in Nanotechnology Center in Al-Quds University using DSC 4000 System, 100-240V/50-60Hz.

2.1.5 Melting Point Determination (capillary method):

This technique was used to study thermal behaviour of the compounds, and the change that occurs to the sample by heat. The inorganic complexes usually have high melting point, most of them have decomposition point.The melting points were recorded on a hot stage melting point apparatus.

- Melting point determination was done in Chemistry & chemical technology laboratories in Al-Quds University using BARNSTEAD Mel-Temp 1001D Electrothermal Melting Point Apparatus.

2.1.6 Ultraviolet-visible spectrophotometry (UV-Vis):

There are three electronic transitions involved in the coordination complexes in solid state: (1) a d-d transition or an f-f transition on the metal ion. Such transition is called ligand-field transition. The absorption band is called ligand-field absorption band. It often occurs in the visible and near infrared regions, and the intensity of the band is weak; (2) a L-L transition, charge transfer based on the ligand, this charge transfer is similar to that of a general organic compound, often occurs in the Ultraviolet region; (3) charge-transfer absorption spectra are produced by charge transfer between the ligand and metal ion, concretely including two types: (1) metal-to-ligand charge transfer (MLCT); (2) ligand-to-metal charge transfer (LMCT), which often occur in the ultraviolet and visible regions.

- UV-Vis analysis was done in Chemistry & chemical technology laboratories in Al-Quds University using PERKIN-ELMER, Lambda 5, UV-Vis Spectrophotometer.

2.2 Materials:

Metal salt Copper(II) perchlorate hexahydrate $[Cu(H_2O)_6](ClO_4)_2$ and Nickel(II) perchlorate hexahydrate $[Ni(H_2O)_6](ClO_4)_2$, N,N-Diethylethylenediamine ($(C_2H_5)_2N$ $-CH_2CH_2NH_2$), 2,2´-Dipyridylamine ($C_{10}H_9N_3$), copper(II) carbonate hydroxide [$Cu_2(OH)_2CO_3$], 2-pyrazinecarboxylic acid ($C_5H_4N_2O_2$), chloroform, toluene, methanol, were purchased from sigma Aldrich. and used as received.

2.3 Methods:

2.3.1 Synthesis of 2,2'-bipyrazine (bpz)($C_8H_6N_4$):

Synthesis was done according to reported procedure[{24}], by reacting 4.1 gram (0.0185) mol of copper(II) carbonate hydroxide with 9.2 gram (0.074) mol pyrazinecarboxylic acid in 150 ml water, the mixture stirred for 16.5 hour at room temperature, the blue precipitate was filtrated with washing with small amount of water.

The product Bis(2-pyrazinecarboxylato)copper(II) was dried in oven at 40 °C for 2 days, then dry Bis(2-pyrazinecarboxylato)copper(II) was putted in a Pyrex boat which placed in 1.0 m Pyrex tube with diameter 2 cm. The boat was heated under argon atmosphere with Bunsen burner, to pyrolysis the copper complex, 2,2'-bipyrazine and pyrazine sublimed on to the side of the Pyrex tube during the pyrolysis, after 20 min of burning the sublimation is finish, the colour of copper complex changed to black, after cooling at room temperature, the boat was removed and air passed through the tube to remove most of the pyrazine impurity. The remain sublimated solid in the Pyrex washed out by 50 ml chloroform, the chloroform was evaporated at room temperature. The product 2,2'-bipyrazine recrystallized by 80 ml toluene, after evaporated the toluene at room temperature the yellow plat crystal collected as 2, 2'-bipyrazine. The percentage yield was10.567% .

2,2'-bipyrazine was characterized by FTIR spectroscopy and Ultraviolet-visible spectrophotometry (UV-Vis).

2.3.2 Synthesis of coordination complexes:

2.3.2.1 Synthesis of $[Cu(bpz)(OH)(ClO_4)(H_2O)]_2.H_2O$ (1):

The $[Cu(bpz)(OH)(ClO_4)(H_2O)]_2.H_2O$ complex was prepared by dissolve 37 mg (0.1 mmol) Copper(II) perchlorate hexahydrate $[Cu(H_2O)_6](ClO_4)_2$ and 15.9 mg (0.1 mmol) 2,2'-bipyrazine in 15 ml of deionizied water and stirred with reflux at 70 °C for 2h, to the clear solution (pH= 3.11), 11.62 mg (0.1 mmol) of N,N-diethylethylenediamine was added, the stirring was continuous for half hour (pH = 7.32). A clear blue solution was filtrated and left to evaporate at room temperature until most of the solvent was evaporated. A blue block single crystal suitable to X-ray analysis was filtrated off and air dried. The percentage yield of this complex is 57.2%.

2.3.2.1.1 Calculated elemental analysis:

Table 2.1: Calculated elemental analysis for **(1)**:

Molecular formula: $C_{16}H_{22}N_8 O_{14}Cu_2Cl_2$

Element	Mass g/mol	Percentage %
C	16x12.011=192.176	25.68%
H	22x1.008=22.176	2.96%
N	8x14.007=112.056	14.97%
O	14x15.999=223.986	29.93%
Cu	2x63.546=127.092	16.98%
Cl	2x35.45=70.9	9.47%
Overall	748.386 g/mol	99.99%

2.3.2.1.2 Crystal Data:

A summary of the key crystallographic information is given in (Table 2.2) for complex **(1)**.

2.3.2.2 Synthesis of $[Cu(dipyam)_2](ClO_4)_2$ (2):

The $[Cu(dipyam)_2](ClO_4)_2$complex was prepared by dissolving 37 mg (0.1 mmol) Copper(II) perchlorate hexahydrate $[Cu(H_2O)_6](ClO_4)_2$ and17.12 mg (0.1 mmol) 2,2´-dipyridylamine ($C_{10}H_9N_3$) in 15 ml of deionizied water and stirred with reflux at 70 °C

for 1hour, to the clear solution, 17.12 mg (0.1 mmol) of N,N-2,2´-dipyridylamine was added, stirring was continued for 1 hour. A clear blue solution was filtrated and left to evaporate at room temperature until most of the solvent was evaporated. A prism blue single crystal suitable to X-ray analysis was filtrated off and air dried. The percentage yield of this complex is 38.79%.

2.3.2.2.1 Calculated elemental analysis:

Table 2.3: Calculated elemental analysis of **(2)**.

Molecular formula: $C_{20}H_{18}N_6O_8CuCl_2$

Element	Mass g/mol	Percentage %
C	20x12.011=240.22	39.72%
H	18x1.008=18.14	3.00%
N	6x14.007=84.04	13.89%
O	8x15.999=127.99	21.16%
Cu	1x63.546=63.546	10.51%
Cl	2x35.45=70.9	11.72%
Overall	604.836 g/mol	100.00%

2.3.2.1.2 Crystal Data:

A summary of the key crystallographic information is given in (Table 2.4) for complex **(2)**.

2.3.2.3 Synthesis of $[Ni(bpz)_3](ClO_4)_2.H_2O$ (3):

47.7 mg (0.3 mmol) solid 2,2'-bipyrazine was added in three equally portion to 15 ml of light green aqueous solution of 36.5 mg (0.1 mmol) nickel(II) perchlorate hexahydrate $[Ni(H_2O)_6](ClO_4)_2$ under stirring with reflux at 70 °C until the dissolving of the solid. A dark yellow solution was filtrated and left to evaporate at room temperature until most of the solvent was evaporated. A brown prism single crystal suitable to X-ray analysis was filtrated off and air dried. The percentage yield of this complex is 82%.

2.3.2.3.1 Calculated elemental analysis:

Table 2.5: Calculated elemental analysis for complex **(3)**:

Molecular formula: $C_{24}H_{20}N_{12}O_9NiCl_2$

Element	Mass g/mol	Percentage %
C	24x12.011=288.264	38. 34%
H	20x1.008=20.16	2.69%
N	12x14.007=168.084	22.41%
O	9x15.999=143.991	19.19%
Ni	1x58.6934=58.6934	7.82%
Cl	2x35.45=70.9	9.45%
Overall	750.0924 g/mol	99.9%

2.3.2.3.2 Crystal Data:

A summary of the key crystallographic information is given in (Table 2.6) for complex **(3)**.

Chapter Three

Result and Discussion

3.1 2,2'-bipyrazine (bpz) ligand :

An impressive amount of work has been devoted to magneto-structural studies of 2,2'-bipyrazine (bpz) due to structural flexibility of bpz, whereas two pyrazine rings rotate with respect to each other enables many possibilities to bind metals, and the structure of 2,2'-bipyrazine can coordinate to transition metals as σ-doner or π-doner from the ligand to the metal center[{11}], and shows that the ligand adopts a planar structure with the two pyrazine rings related to each other by an inversion centre. As a result the ligand adopts an arrangement such that the two central nitrogen atoms are placed *anti* to each other as observed in the structure of 2,2'-bipyridyl[{12,66}] (Fig. 3.2). The 2,2'-bipyrazine molecules are stacked with a ring centroid to plane separation of 3.36 Å representing a significant π–π interaction[{66}]. Additionally the 2,2'-bipyrazine transition metal complexes are attracting considerable interest due to peculiar electrochemical, spectroelectrochemical, magnetic, optical, and medicinal properties[{24-44}].

3.1.1 Infrared Spectroscopy:

The infrared absorption frequencies obtained for the free 2,2'-bipyrazine are listed in (Table 3.1), and spectra are given in (Fig 3.1).

Table 3.1: Infrared frequencies (cm^{-1}) for the free 2,2'-bipyrazine and assignments.

Frequencies (cm^{-1})	Assignment
3077 w, 3049 w and 3013w	υ C– H
1571 m and 1523 m	υ C ⋯ N
1364s and 1392s	υ C ⋯ C)
1464s	δ ring
1272w and 1284w	β CH
1151s and 1091s	β ring, breathing
1051w, 1028s, 1018vs	ring-H in-plane bending vibrations

702w and 644w	β ring
847s, 750w and 712w	out-of-plane ring-H bending and τ ring

FTIR spectra for 2,2'-bipyrazine have the following characteristic bands: (υ(C− H), υ(C ⋯ C), υ(C ⋯ N), δ ring, ring-H in-plane bending vibrations and out-of-plane ring-H bending, β ring and ring torsion vibrations).

A three weak bands at 3077, 3049 and 3013 cm^{-1} which attributed to υ(C− H) and two medium and two strong bands at 1571, 1523 cm^{-1}, 1364 and 1392 cm^{-1} related to (C ⋯ C) (C ⋯ N) stretching, and strong sharp band at 1464 cm^{-1} mainly ring deformation vibrations.

Additionally, two strong bands 1151 and 1091 cm^{-1} composite C ⋯ C, C ⋯ N and H-C ⋯ C bending modes and strong 1028 , 1051 and very strong 1018 cm^{-1} bands which attributed to ring-H in-plane bending vibrations, and two weak bands at 702,712 and strong at 847 cm^{-1} mainly out-of-plane ring-H bending and ring torsion vibrations.

The vibrations of the bpz ligand, whose assignment is made having in mind the detailed analysis carried out for biphenyl[{79,80}] and 2,2'-bipyridine[{81}].

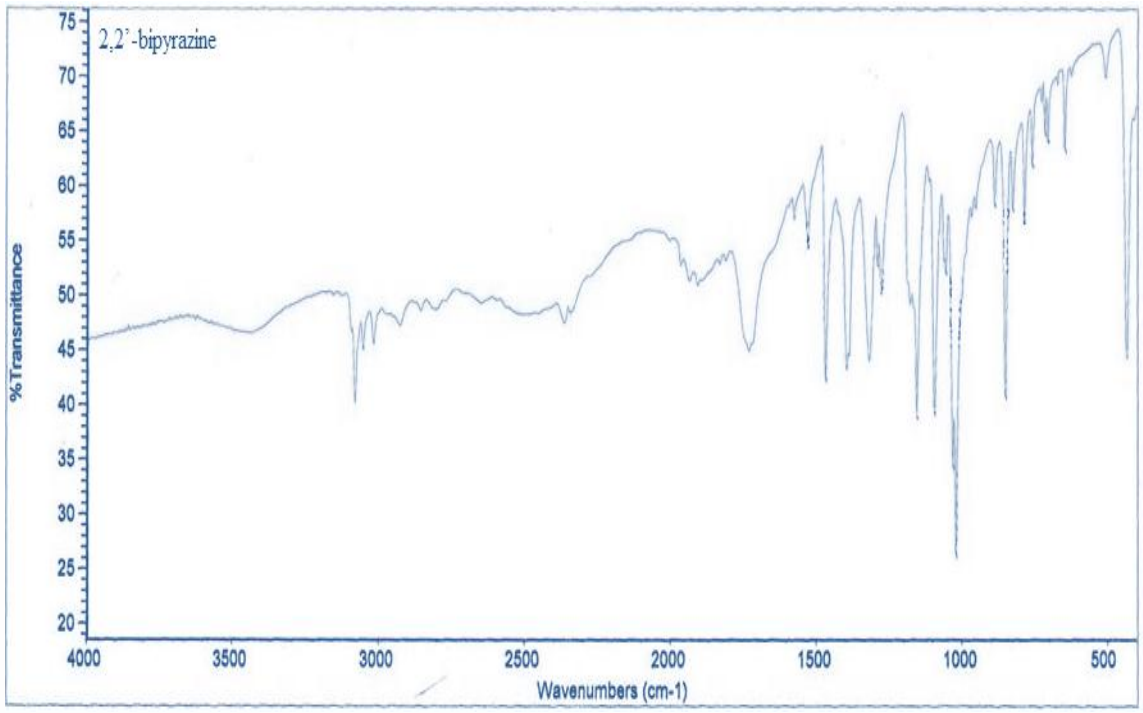

Fig. 3.1: FT-IR spectra for 2,2'-bipyrazine ligand.

3.1.2 Ultraviolet-visible spectrophotometry (UV-Vis):

Electronic spectral for free 2,2'-bipyrazine ligand have been obtained from dimethyl sulfoxide solutions are shown in (Fig. 3.1b). Free 2,2'-bipyrazine ligand showed a broad absorption bands centered at 290 nm, it may be assigned to L→ L transitions.

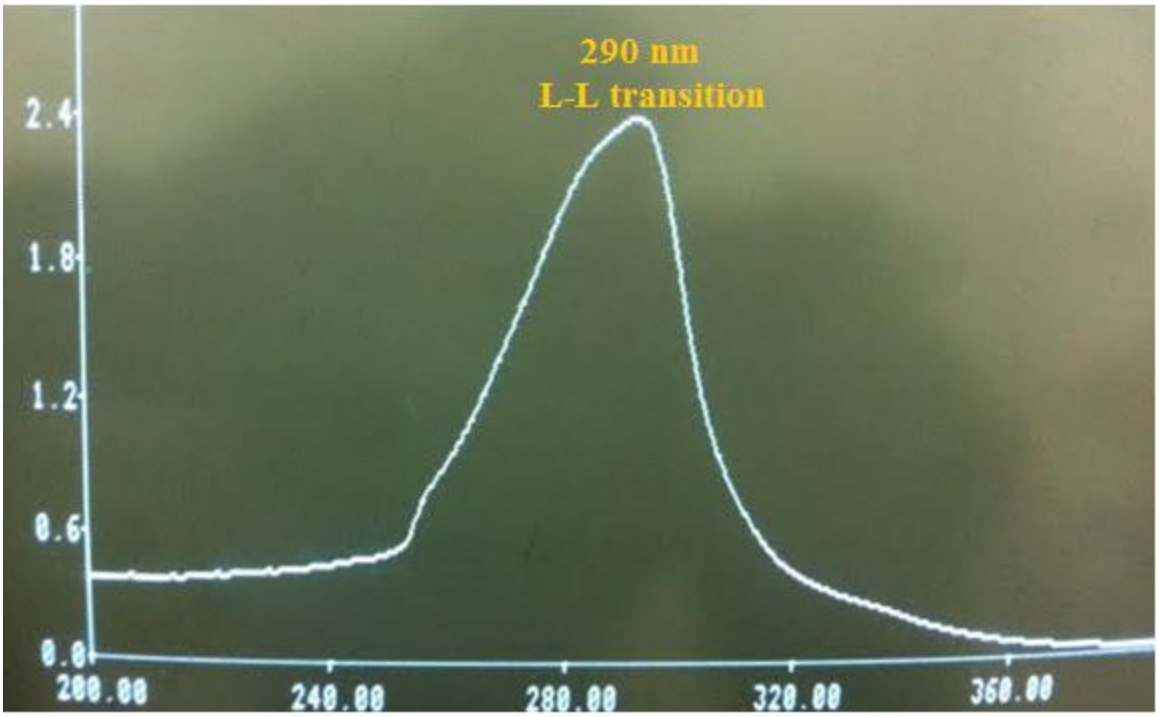

Fig. 3.1a: Electronic spectra of free 2,2'-bipyrazine ligand.

3.1.3 Crystal structure for 2,2'-bipyrazine ligand:

The structure of 2,2'-bipyrazine showed that the ligand adopts a planar structure with the two pyrazine rings related to each other by an inversion centre. The main C-C bond distances in pyrazine ring 1.402 Å similar to the C-C aromatic bond length 1.40 Å, but the C-C near two nitrogen atoms shorter than C-C far two nitrogen atoms, this difference due to the two nitrogen atoms which effected in the charge distribution in the ring, the bridging C-C distance connecting the two aromatic rings is 1.484 Å and is as expected for a singles C–C bond[{148, 151}] (Fig 3.2 and Table 3.3).

The bond angles, bond distances and torsions for free 2,2'-bipyrazine (bpz) ligand were calculated by Cambridge Crystallographic Data Centre (CCDC), CSD version 5.38 (November 2016), as shown in (Table 3.2, Table 3.3, and Table 3.4).

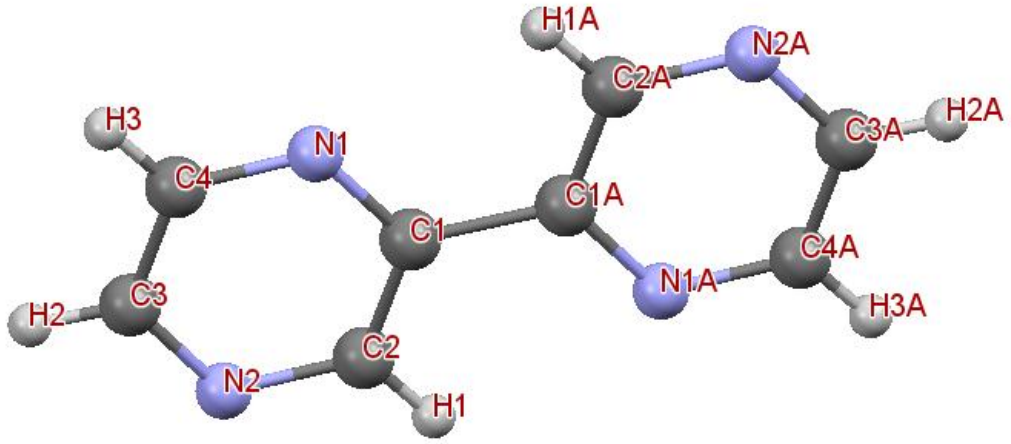

Fig. 3.2: Crystal structure of 2,2'-bipyrazine ligand{66} with the atom numbering scheme adopted from Cambridge Crystallographic Data Centre (CCDC),CSD version 5.38 (November 2016).

3.2 Copper (II) complexes:

The magnetic properties of copper(II) complexes have been an attractive area of research. This is due to the fact that copper(II) (d^9) has a single unpaired electron and therefore can be used as a model system for probing the nature of magnetic exchange interactions between single unpaired electrons on two or more metal centres, and in particular, how this interaction is mediated by the ligands that bridge the metal centres{82-84}.

The study of magnetic interactions in polynuclear coordination complexes has played a significant role in the development of magnetochemistry{85}. Much effort has centred on the synthesis and modification of such complexes with detailed examination of their structures and properties. In general, structure–function correlations cannot be considered to be actually contributing in an engineering sense, they can identify particular systems as being of greater potential in the development of, for example, molecular ferromagnetic materials{86}. However, preparation of polynuclear compounds with special topological features has to be confronted with many great challenges because crystal structures are

affected by multiple factors such as pH value, metal ions, organic ligands, reaction conditions[87].

In this work two copper(II) coordination compound were prepared, first with 2,2'-bipyrazine ($C_8H_6N_4$) (bpz) ligand, and the second coordination compound with 2,2´-dipyridylamine ($C_{10}H_9N_3$)(dipyam) ligand. These coordination compounds were characterized by Fourier transforms infrared spectroscopy (FTIR), ultraviolet-visible spectrophotometry (UV-Vis) and single crystal X-ray diffraction, in addition the thermal stability was recorded in the 20 - 450 °C range.

3.2.1 $[Cu(bpz)(OH)(ClO_4)(H_2O)]_2.H_2O$ (1):

Hydroxo-bridged metal complexes, in which the metal atoms are linked by hydroxo-bridge, is one of the most active research areas in chemistry of materials, coordination chemistry and supramolecular chemistry[87-90]. This activity has been fuelled by the development of novel extended supramolecular architectures of widespread use in a variety of technological applications[91], photophysical[92], DNA cleavage due to the advantages in electronic and structural diversity and it has high nucleolytic efficiency[93], and their different magnetic properties, on based di-μ-hydroxo- bridged copper(II) dinuclear compounds exhibits an antiferromagnetic interaction, while others exhibit a ferromagnetic interaction[94]. Additionally, the data obtained have been used to develop empirical correlations of the strength of magnetic coupling with key structural descriptors of the Cu–OH–Cu bridging unit[95-97]. For the dihydroxo-bridged copper(II) dinuclear species, the linear correlation between the Cu–O–Cu bridging angle and the singlet–triplet energy gap (J), $J = -74.53\ (\theta) + 7270\ cm^{-1}$ (in which (θ) is the Cu–O–Cu angle) was first observed by Hodgson and co-workers[98,99].

An antiferromagnetic interaction is found when the Cu– O–Cu angle is larger than 97.5°, but when the Cu–O–Cu angle is smaller than 97.5°, a ferromagnetic interaction would be expected.

Several theoretical approaches were applied to understand the behavior of the antiferromagnetic and ferromagnetic interaction of such dihydroxo- bridged copper(II) dinuclear species[99]. The earlier studies have also revealed that the nature of exchange

coupling strongly influenced by the nature of the terminal ligands, the geometry of the copper environment, the coordination of counter ions and solvent molecules[{100}].

More recently, different density functional methods were used to extend the study on the magnetic behaviour and introduced some additional parameters concerning the non planarity of the Cu_2O_2 core and the out-of-plane displacement angle of the hydroxo hydrogen atom and showed that greater out-of-plane shifts reduce the anti and ferromagnetic components[{101-103}].

3.2.1.2 Infrared Spectroscopy:

The infrared spectrum of complex **(1)**, (Fig 3.3) shows a strong and broad absorption centerd at 3417 cm^{-1} owing to symmetric and antisymmetric OH stretching of the hydroxo-bridges and/or lattice water and/ or coordinated water[{99, 104}], a weak intensity peak at 656 cm^{-1} composite wagging frequencies both coordinated water[{105}], and two medium intensity peaks at 1637 cm^{-1} and 866 cm^{-1} have been assigned to H-O-H bending of lattice water and deformation vibrations of hydroxo-bridges respectively[{19,105,106}]. The coexistence of coordination perchlorate is consistent with the occurrence of a very strong and broad absorption at 1097 cm^{-1}, a medium intensity peak at 940 cm^{-1} and a strong intensity peak at 623 cm^{-1} owing to Cl–O in ClO_4^- stretching, O-ClO_3^- bending respectively[{106-109 }].

Additionally, the IR spectrum of the complex **(1)**, shows two new medium intensity characteristic peaks near far IR region at 512 and 460 cm^{-1} related to Cu-O and Cu-N respectively[{110-114}].

The IR spectrum of the complex **(1)**, was compared with that of free 2,2'-bipyrazine ligand (Table 3.5), (Fig 3.1) and (Fig 3.3). In fact most of the peaks that are present in the free ligand are also observed in the spectrum of the complex, but with a small shift to lower wave number due to the new charge distribution in the coordinated ligand and crystal packing.

Table 3.5: Comparison of infrared frequencies (cm^{-1}) for 2,2'-bipyrazine in complex **(1)**, with the free 2,2'-bipyrazine ligand and assignments.

Frequencies (cm^{-1}) for complex	Assignment	Frequencies (cm^{-1}) for free 2,2'-bipyrazine
3007 w, 3117 w, 3072w, 3050w and 2926w	υ C– H	3077 w, 3049 w and 3013w
1536 m, 1489 m and 1480	υ C ⋯ N	1571 m and 1523 m
1341m and 1318m	υ C ⋯ C)	1364s and 1392s
1413 s	δ ring	1464s
1283 w	β CH	1284w
1152 s	β ring	1151s and 1091s
1051s ,1000 w	ring-H in-plane binding vibrations	1051w, 1028s, 1018vs
698 w, 753 w and 856 s	out-of-plane ring-H bending and τ ring	702w, 750w and 847s

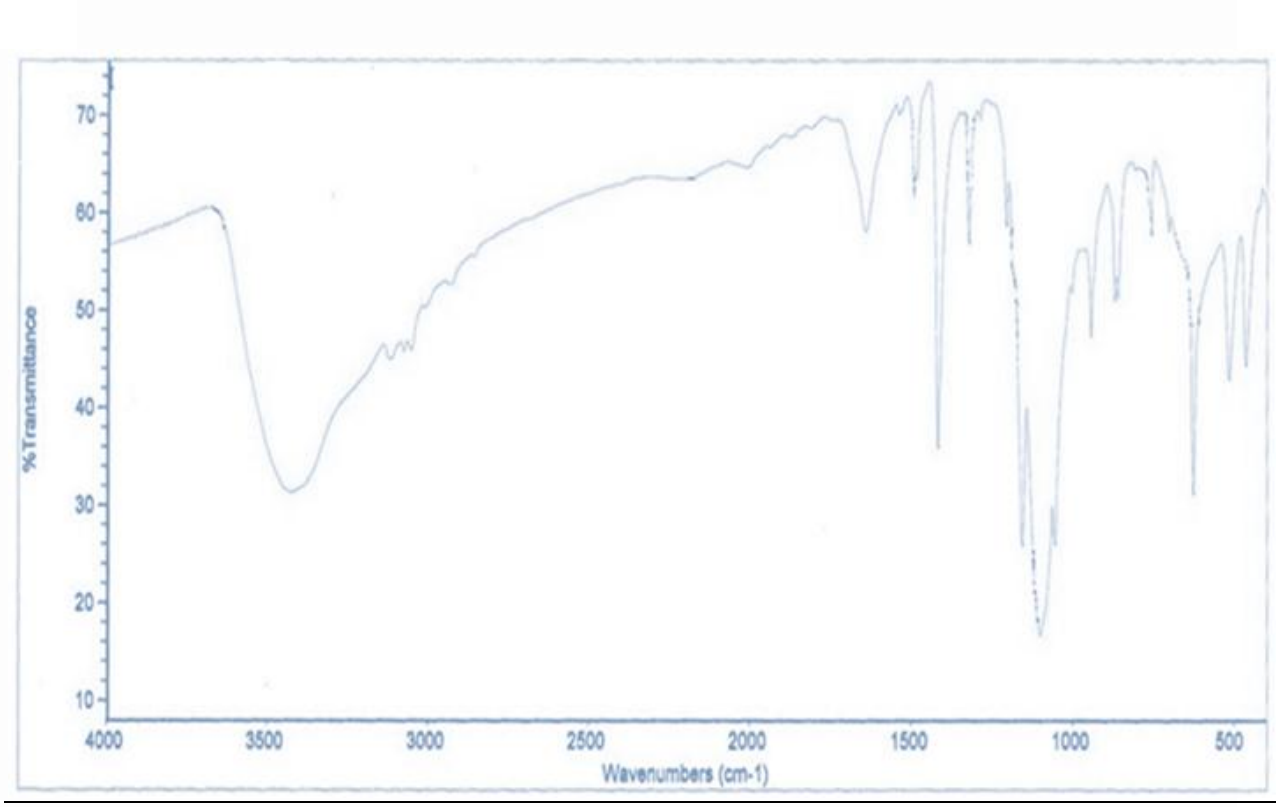

Fig. 3.3: FT-IR spectra for complex**(1)**.

3.2.1.3 Ultraviolet-visible spectrophotometry (UV-Vis):

The electronic absorbtion spectra of **(1)**, (Fig. 3.3b) have been obtained from dimethyl sulfoxide solutions at room temperature. The spectra shows a broad band at 719 nm consistent with the distorted elongated octahedral geometry[{156-158, 66}]. Broad band maxima are also observed at 292 nm and 215 nm, which could result from ligand – ligand (L-L) transitions.

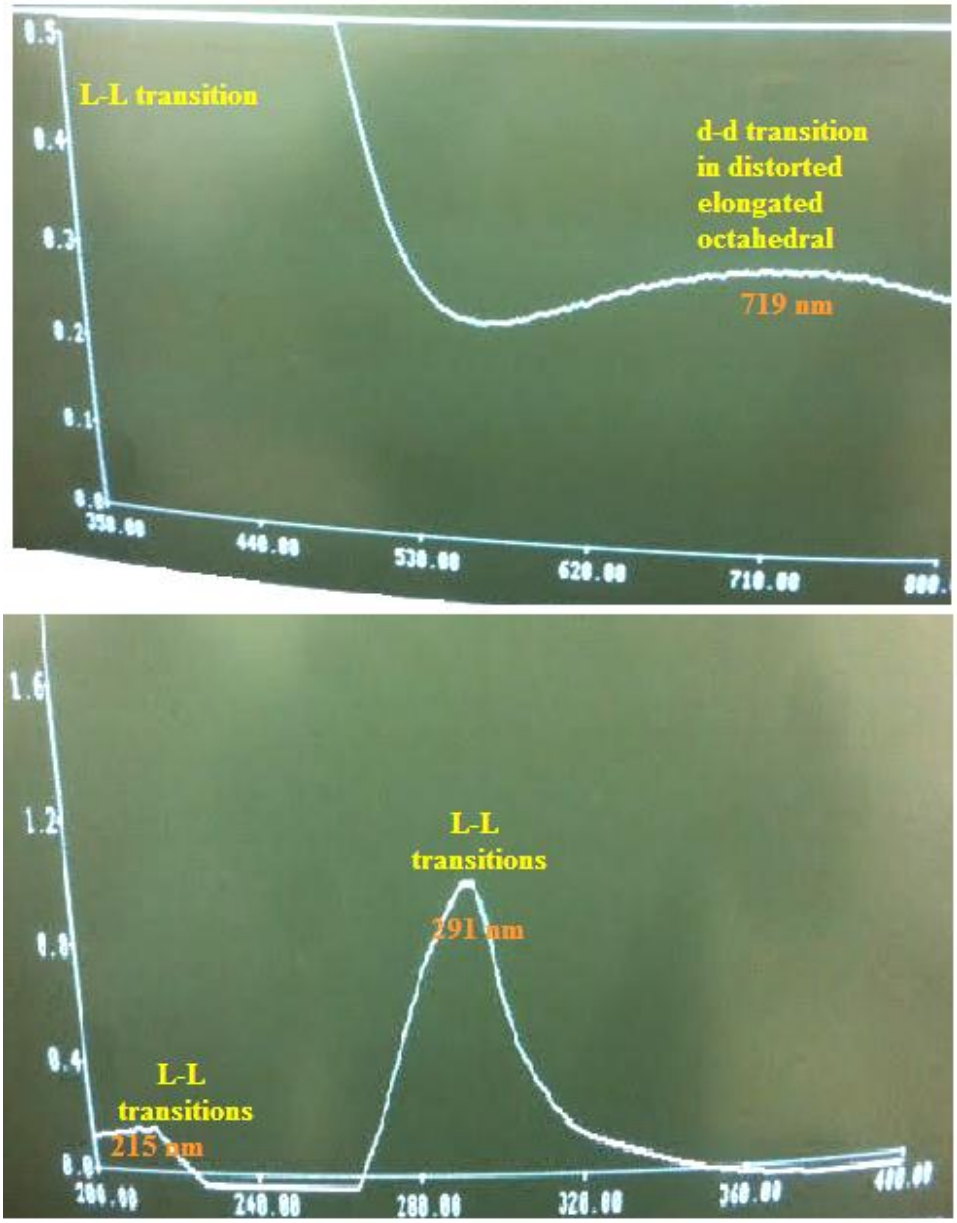

Fig. 3.3a: Electronic spectra of **(1)**, shows d-d transition band (up) and L-L transition bands (bottom).

3.2.1.4 Thermal analysis:

The thermal study of **(1)**, include capillary melting point determination method, Differential Scanning Calorimetry (DSC) Thermal Analysis.

Capillary melting point of **(1)**, showed change in color of the sample at 220 °C the colour goes to dark blue to black, after 300 °C to 400 °C the colour dark blue to black and no change.

The sample in DSC instrument was heated at a rate of 5 °C/min, from 20 to 450 °C in nitrogen gas flowing at a rate of 25ml/min, then cooling in the same range.

The DSC curve (Fig 3.4) shows endothermic peak associated with enthalpy of 2076.55 J/g at 220-297 °C at T_{max} = 272.45 °C that corresponds to melting point process.

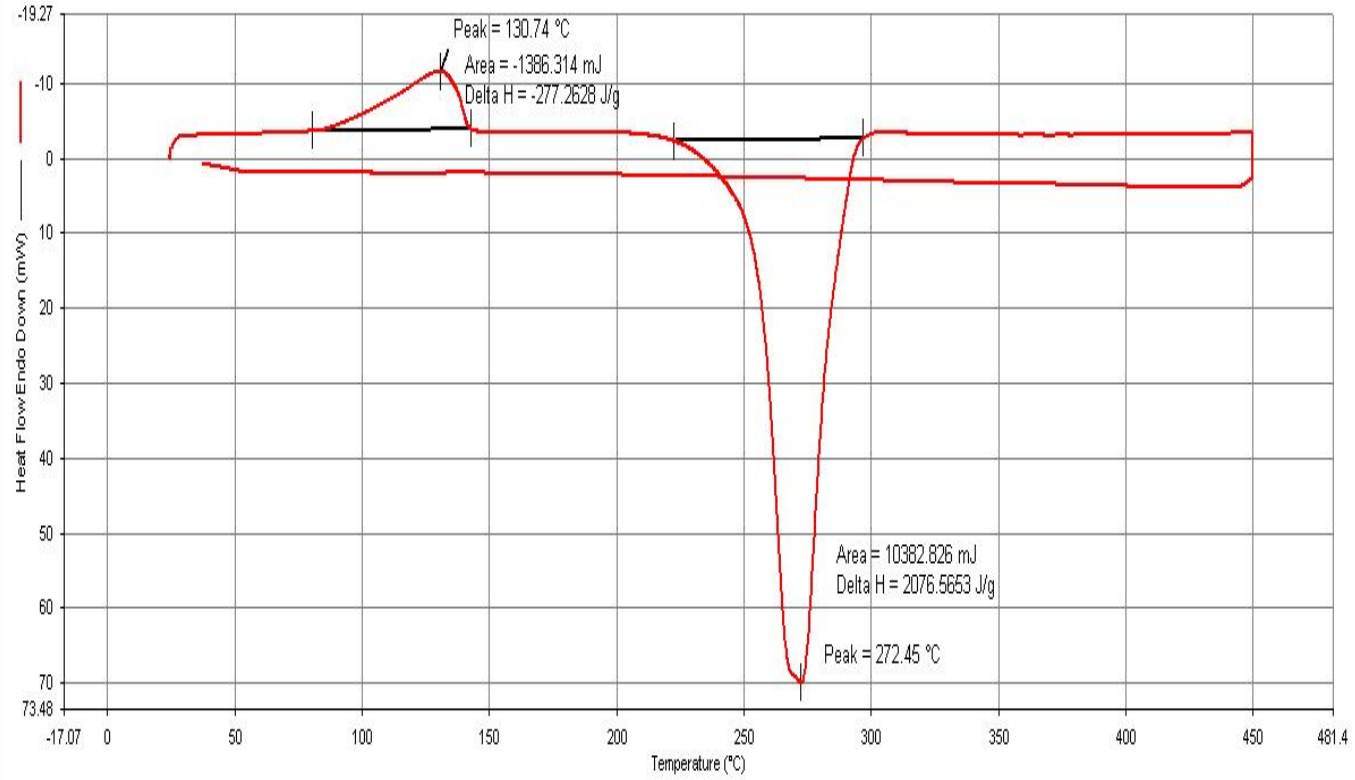

Fig. 3.4: Differential Scanning Calorimetry (DSC)of **(1)**.

3.2.1.5 Crystal structure for (1):

The structure of complex **(1)**, is made up of discrete centrosymmetric bis(μ-hydroxo) copper(II) dimers, with 2,2'-bipyrazine as the terminal bidentate ligand in equatorial position, two weakly coordinated water molecules and two monodentate perchlorate

groups in axial position, and water of crystallization molecules. A perspective view of this complex, with the atom-numbering scheme, is depicted in **(**Fig 3.5).

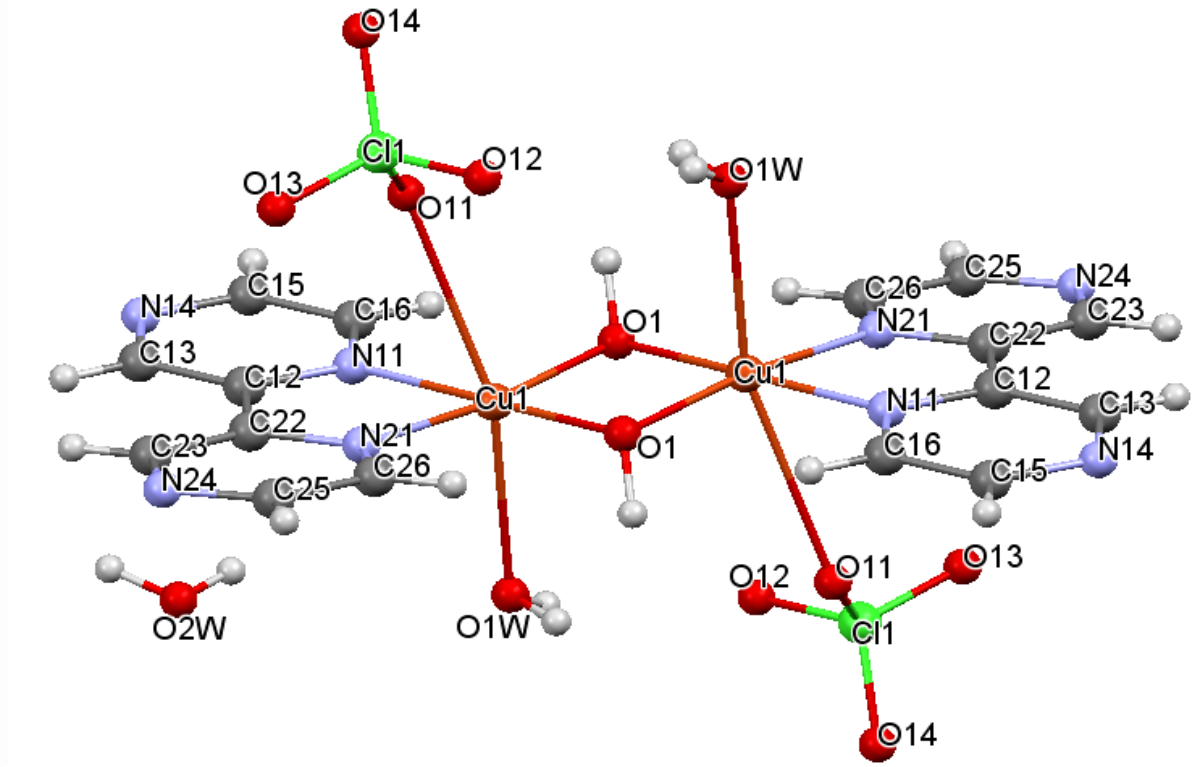

Fig. 3.5: Perspective view of **(1)** with the atom numbering scheme.

The coordination geometry around each copper(II) ion is distorted elongated tetragonal octahedral, CuN_2O_4: the equatorial positions are occupied by the two nitrogen atoms of 2,2'-bipyrazine and the two oxygen atoms of the bridging hydroxo groups, whereas the axial sites are filled by oxygen atoms of water and perchlorate molecules.

The Cu-N distances, 1.994 and 2.009 Å for Cu(1)-N(21) and Cu(1)-N(11) respectively (Fig. 3.6, Table 3.8), are very close to those found in 2 2'-dipyridylamine, 2,2'-bipyridine and 2,2'-bipyrimidine-containing copper(II) complexes[{100, 115-119}]. The Cu-O (hydroxo bridge) distances, 1.934 and 1.917 Å (Fig. 3.6, Table 3.8), are slightly shorter than found in 2,2'-bipyrimidine-containing copper(II) complexes[{115, 118}], but very close to those observed in 2 2'-dipyridylamine and 2,2'-bipyridine[{100, 117}]. The Cu1 axial bonds is much longer [2.472 Å for Cu(1)-O(1w) and 2.746 Å for Cu(1)-O(11)] than the equatorial metal-to-ligand distances (Fig. 3.6).

The tetragonality parameter, T (defined as the ratio between the in-plane and out-of-plane average Cu− X bond lengths) [91, 116], is 0.7526. In the CuN_2O_4 coordination environment the two axial Cu1−O11 and Cu1−O1w distances are different (Δd = 0.274 Å), resulting in a 4 + 1 + 1 coordination environment (Fig. 3.6). Distortion from a regular octahedral geometry is observed for the CuN_2O_4 coordination environment, with a cis X−Cu1−X angle range 72.89−104.53° and a trans X−Cu1−X angle range 162.70−176.11°(Table 3.7).

The Cu–Cu distance within the dinuclear unit is 2.826 Å ,while the Cu(1)–O(1)–Cu(1) angle is 94.40° as in (Fig.3.6, Table 3.7 and Table 3.8). To the best of my knowledge, this is the shortest distance and smallest angle was obtained until now and indicating a stronger Cu(II)–Cu(II) interaction in comparable with the Cu(II)–Cu(II) distance and angles in the reported structure[115-122, 86, 91].

As a result of Cu–Cu distance and Cu–O–Cu angle the exchange interaction should be ferromagnetic[99].

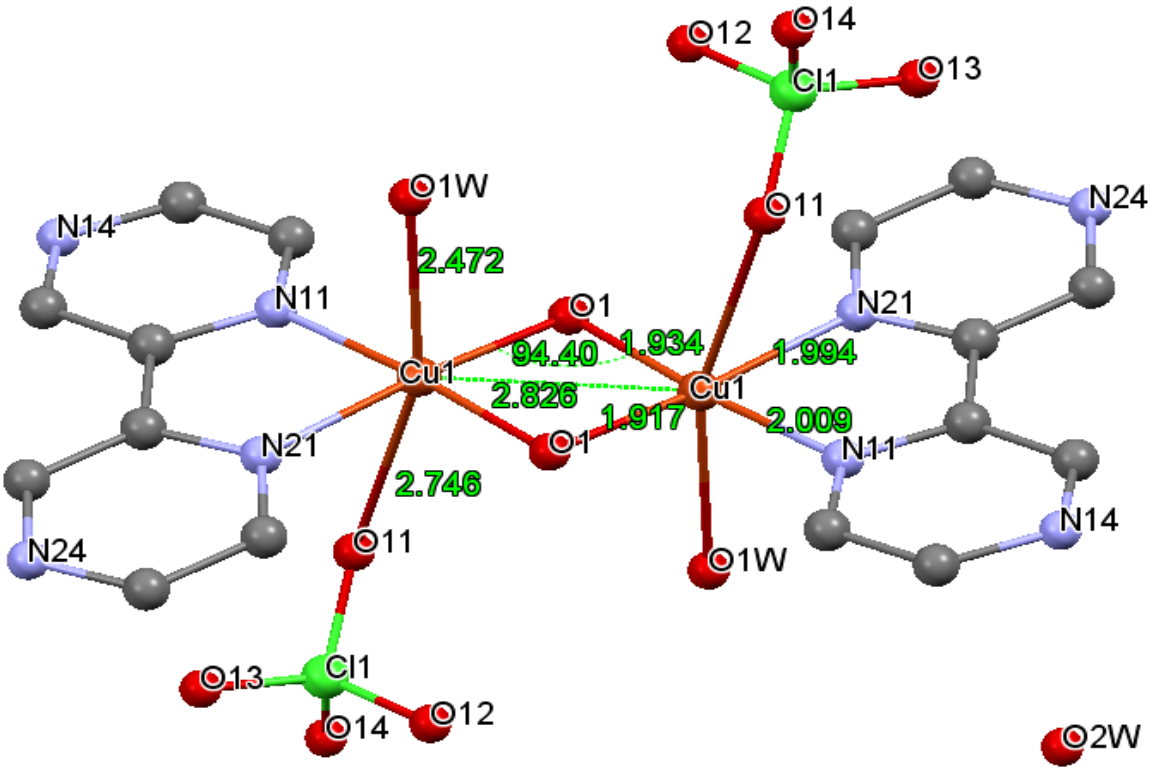

Fig. 3.6: A structure of **(1)**, containing some important distance and angels according to the X-ray analysis.

The four equatorial atoms are practically coplanar with deviations from the equatorial plane around copper(II) atom which define as (N11, N21, O1, O1) 0.041 Å in N(21) and 0.039 Å in N(11), the copper atom being displaced 0.076 Å towards the axial (O1w) oxygen atom, and the oxygen atom in the bridge deviated from the plane by 0.040 Å towards the axial (O1w) oxygen atom (Fig 3.7). The pyrazine rings of the 2,2'-bipyrazine ligand are planar as expected with a very small deviations from the mean planes not greater than 0.003 Å. However, they are not coplanar, each 2,2'-bipyrazine ligand is buckled so that its outer carbon and nitrogen atoms are displaced towards the axial atoms [O(11) and O1w respectively] of the distorted octahedral arrangement about the copper atom; the dihedral angle between the planar six-membered pyrazine rings is 6.44°. The N(11)-Cu(1)-N(21) angle is 81.10° and O(1)-Cu(1)-O(1) angle is 85.60° are significantly smaller than the ideal value of 90°, due to the steric requirements of the geometrical constraints of a 2,2'-bipyrazine ring system. The dihedral angle between the equatorial N(21) N(11) O(1) O(1) and bpz mean planes is 4.04° (Fig 3.7). And the dihedral angle between equatorial planes (O1,Cu,O1) and (N11,Cu,N21) is 6.98°. additionally the hydroxo-bridged are coplanar. All of the upper measurements of dihedral angles and atom deviations and angles N(11)-Cu(1)-N(21) and O(1)-Cu(1)-O(1) are strongly influenced in the magnetic behavior according to recent studies[101-103].

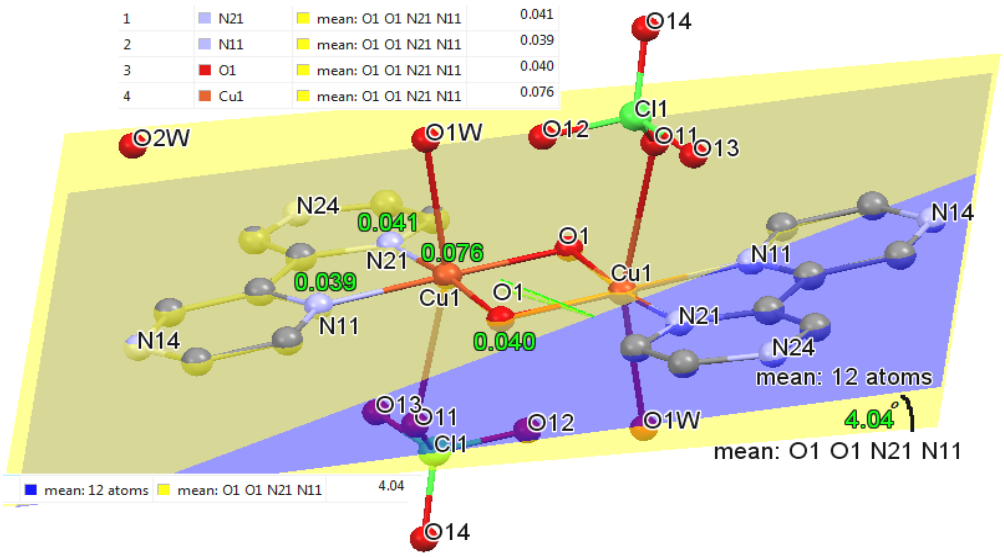

Fig. 3.7: A projection show the dihedral angle between the mean 2,2'-bipyrazine plane and the equatorial plane around Cu(II) cation, and nitrogen, hydroxido bridge deviations from the equatorial plane in **(1)**.

Both types of water molecules, crystallization (O2w) and coordinated (O1w) together, and the crystallization water (O2w) with the hydroxide, nitrogen in 2,2'-bipyrazine ligand and perchlorate ligand, are involved in waek/moderate hydrogen bonds[{123}]. The corresponding D-H, H···A and D···A bond distances and D−H···A bond angles are shown in (Fig.3.8, Table 3.6).

The perchlorate ligand of one chain acts as a hydrogen bond acceptor of coordinated water molecules [O1w−H···O12] (Table 3.6). The nitrogen in 2,2'-bipyrazine ligand acts as a hydrogen bond acceptor of crystallization water molecules [O2w−H3w···N14 and O2w−H4w···N24], additionally the crystallization water molecules act as hydrogen bond acceptor of the hydroxido bridge [O1−H1···O2w] and coordination water molecules [O1w−H1w···O2w] of a different chain (Table 3.6).

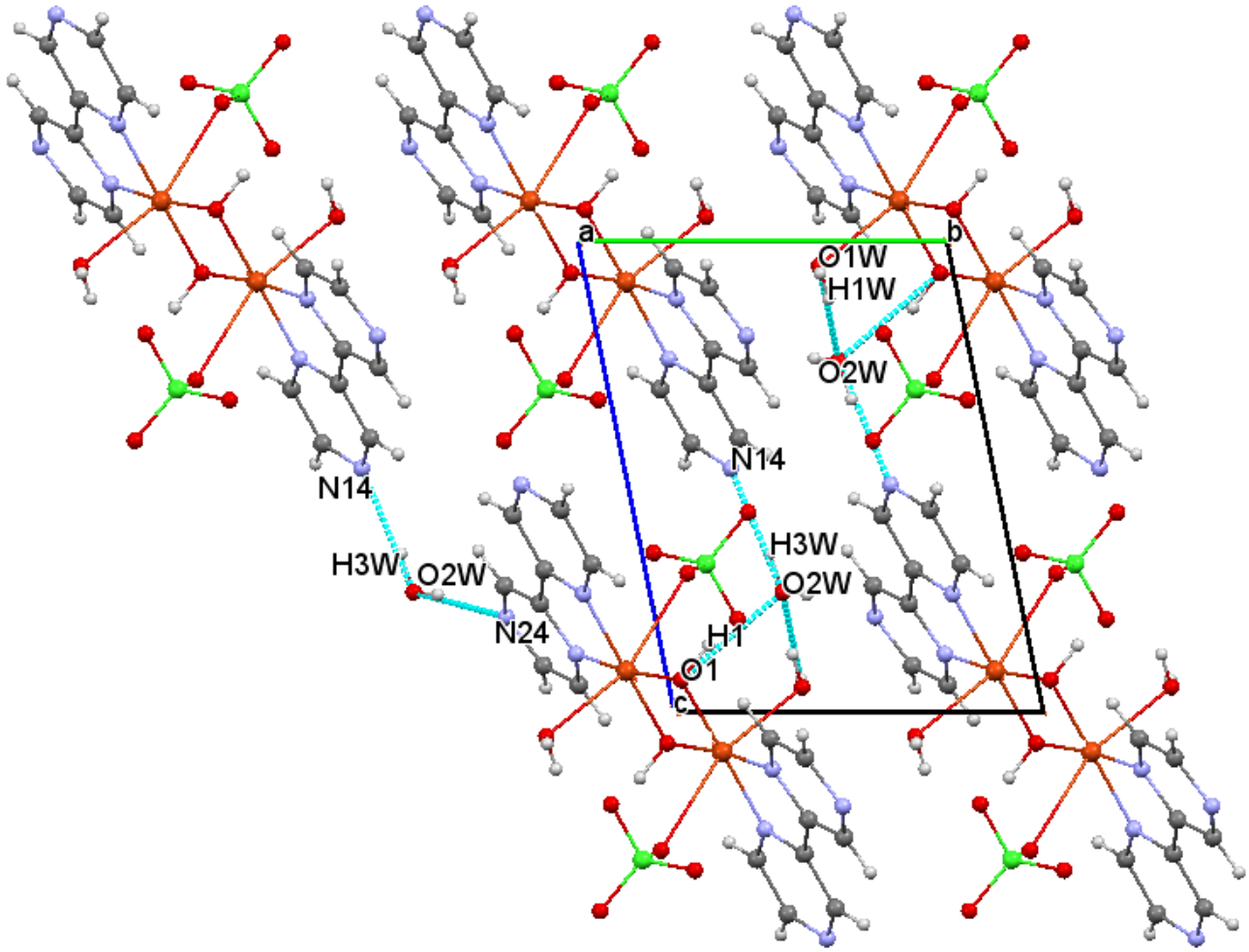

Fig. 3.8: Crystal packing of **(1)**, view along the a axis showing the inter-intrachain H-bonds and unit cell.

The structure of **(1)**, is replete with hydrogen bonding interactions involving the crystallization water molecules and the complex and forms a 2D sheet, with adjacent sheets then linking into 3D (Fig. 3.11) through perchlorate oxygen atoms interactions involving C–H(bpz) …. O(ClO^-_4) with C….O distances in the ranges 3.068-3.258 Å and [C–H(bpz) …. O1w] 3.412 Å (Fig. 3.9). Adjacent Cu chains interdigitate through π–π stacking interactions involving each 2,2'-bipyrazine ligand 3.299 Å separation at closest contact, and leads to the formation of 2D sheets(Fig. 3.10).

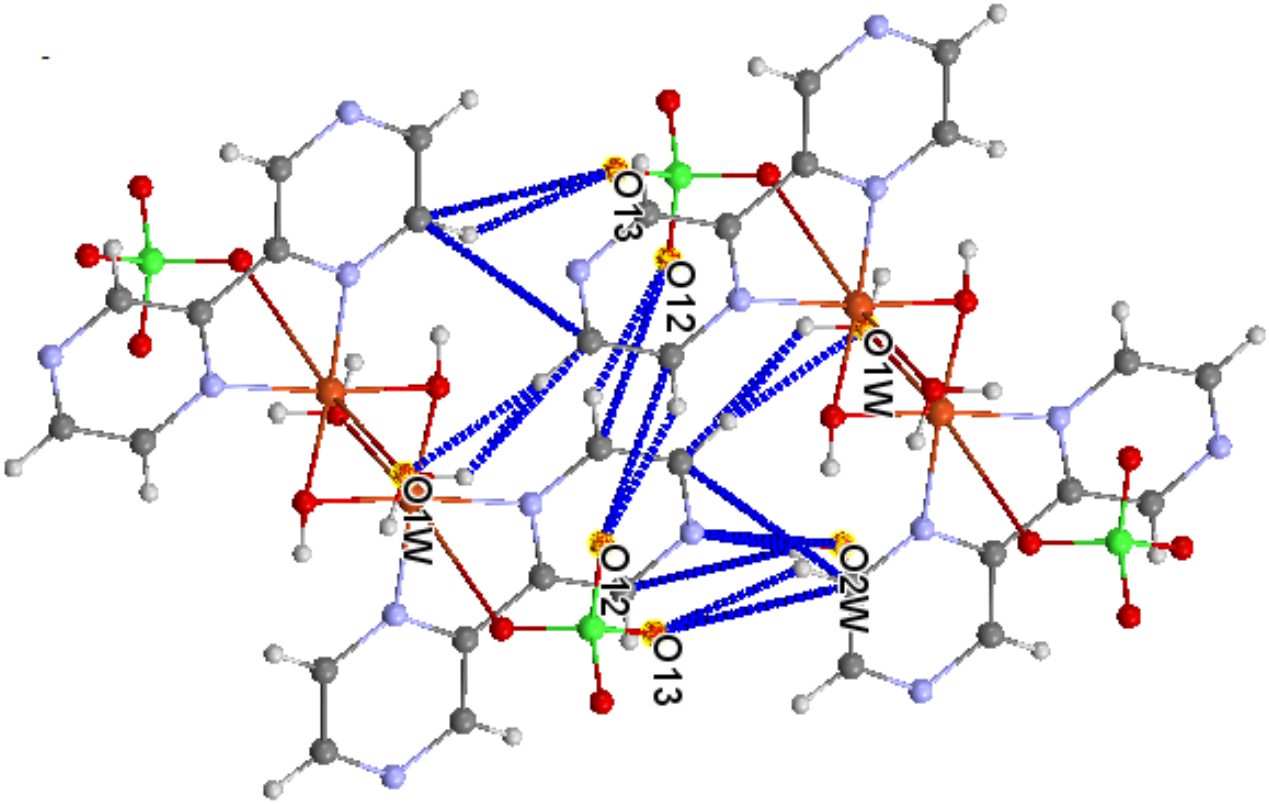

Fig. 3.9: View of the network around the monodentate perclorate and coordination water in complex **(1)**.

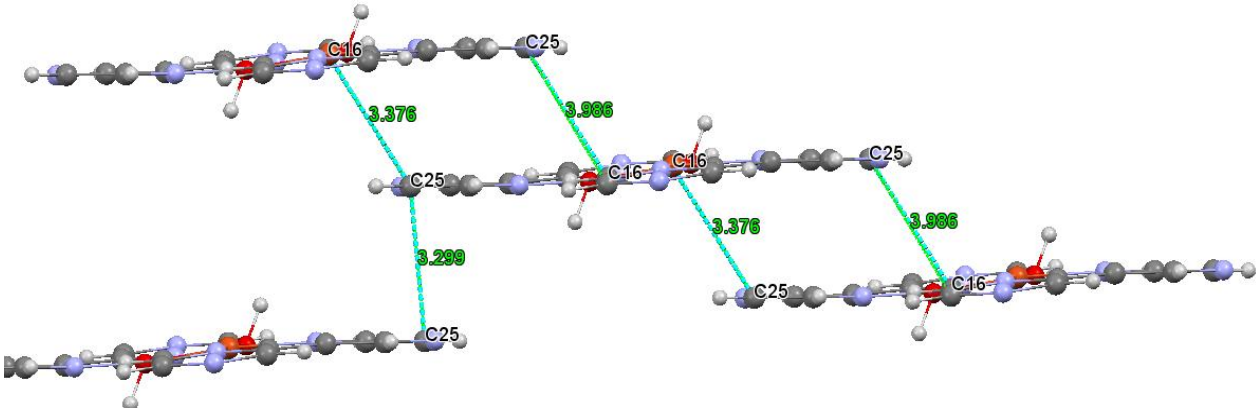

Fig. 3.10: View of the π–π stacking interactions distance between 2,2'-bipyrazine ligand in complex **(1)**.

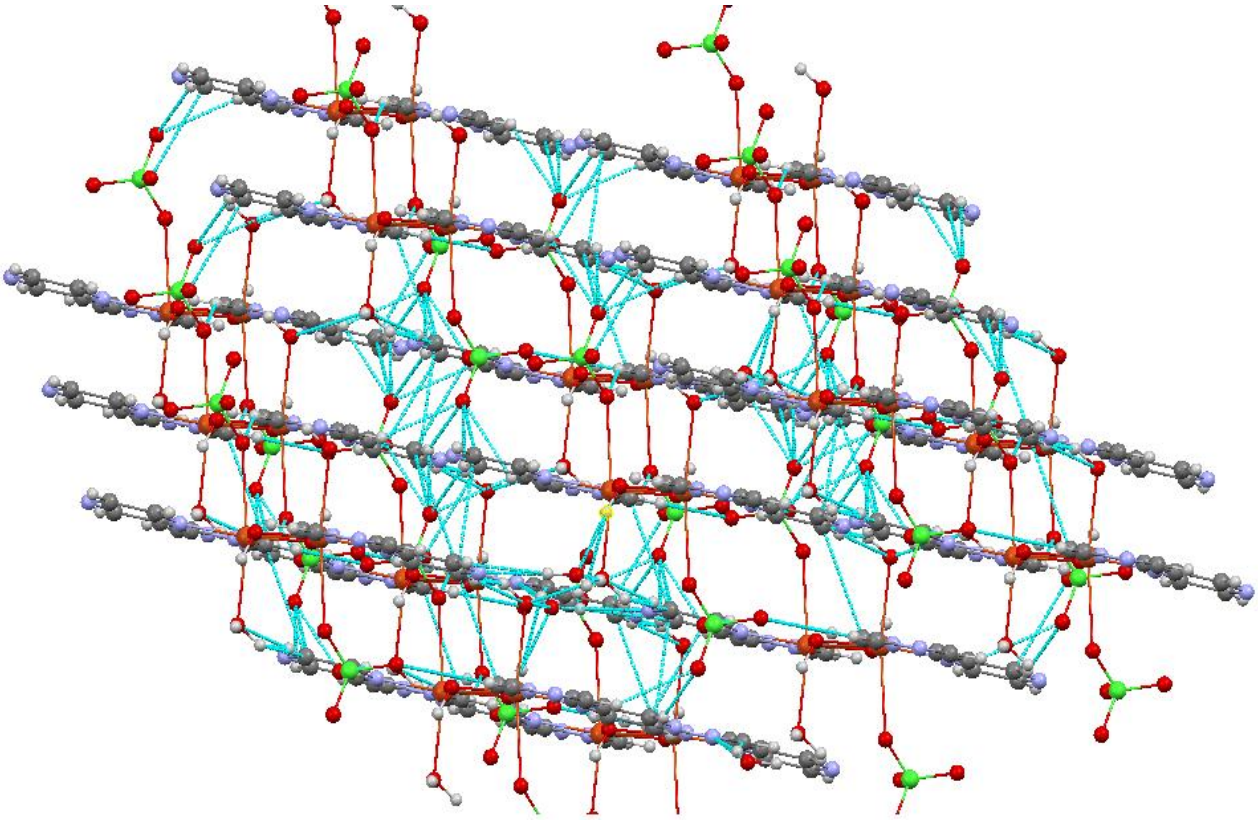

Fig. 3.11: View of a three-dimensional network structure of **(1)**.

3.2.1.6 Magnetically characterization according to crystal structure for (1):

As seen from (Table 3.10) most ferromagnetic compounds with the planar Cu_2O_2 chromophore, of which both the X-ray crystal structure and the magnetism are available, are bis(bidentate)-related compounds. Comparing the observed magnetism and the empirical correlation formula for all compounds, a difference is observed.

For example compound $[Cu(bipy)(OH)(CF_3SO_3)]_2$[124] which has an observed value for *J* of +17 cm^{-1} and a calculated value, according to the empirical formula, of *J* = -71 cm^{-1}. This difference proves again that even minor structural effects do have an influence on the magnetic susceptibility, and in $[Cu(dmbipy)(OH)(CF_3SO_3)]_2$[94], the observed value for *J* of +148 cm^{-1} and a calculated value 227 cm^{-1} this difference is due to additional structural effects, such as H-bonds, non-planarity, additional bridges, and terminal ligand.

In this work we present the synthesis, infrared spectroscopy, thermal analysis and X-ray crystal structure of the compound **(1)**, the first X-ray structure of a dinuclear Cu(II) compound with 2,2'-bipyrazine ligand containing hydroxo-bridge, and exhibiting the smallest Cu–O–Cu angle and shortest Cu….Cu distance reported so far (Table 3.10). where the Cu–O–Cu angle is 94.40° and Cu….Cu distance 2.826 Å and the coordination geometry around copper(II) ion is distorted elongated tetragonal octahedral, and coordination of water solvent molecule and perchlorate counter ions, and planer Cu_2O_2 is predicted a strong ferromagnetic interaction.

Table 3.10: Relevant data for the structurally and magnetically characterized copper(II) hydroxo-bridged containing bis(bidentate) ligands, and different coordinated and uncoordinated counter ions.

Compound	Cu-O/ Å	Cu....Cu/ Å	Cu-O-Cu /°	calculated J/cm^{-1}	observed J/cm^{-1}	Ref.
$[Cu_2(bipy)_2(OH)_2](CF_3SO_3)_2$	1.927	2.920	98.5	-71.205	+17	124
$[Cu_2(bipy)_2(OH)_2](ClO_4)_2$	1.918	2.871	96.9	+48.043	+93	125,126
$[Cu_2(bipy)_2(\mu OH)_2(HPO_4)(H_2O)]\cdot 4H_2O$	1.962	2.906	96.52	+76.364	+184	86
$[Cu_2(bipy)_2(OH)_2]\ SO_4.5H_2O$	1.939	2.893	96.5	+77.85	+49	125, 127
$[Cu_2(bipy)_2(OH)_2](PF_6)_2$	1.953	2.914	96.5	+77.85	+12	101

$[Cu(bipy)(OH)(SO_4)]_2.5H_2O$	1.926	2.893	96. 5	+77.85	+37	94
$[Cu_2(bipy)_2(OH)_2]C_4O_4.4H_2O$	1.927	2.870	96.4	+85.30	+145	128
$[Cu_2(biypm)(OH)_2(NO_3)_2].2H_2O$	1.926	2.886	96. 2	+100.21	+184	115
$[Cu_2(bipym)(H_2O)_2(OH)_2]\ (NO_3)_2$	1.922	2.854	95.9	+122.57	+148	115
$[Cu(bipym)(OH)(H_2O)(NO_3)]_2$ $.4H_2O$	1.923	2.881	95.7	+137.47	+114	115
$[Cu_2(bipy)_2(OH)_2](NO_3)_2$	1.922	2.847	95.6	+144.93	+172	125, 129
$[Cu_2(bipym)_2(H_2O)_4\ (OH)_2](\ ClO_4)_2$ $.2H_2O$	1.950	2.870	95.0	+189.65	+147	118
$[Cu_2(bipym)(OH)_2(H_2O)_2(NO_3)_2].2$ H_2O	1.940	2.862	95.0	+189.65	+160	115
$[Cu(dmbipy)(OH)(CF_3SO_3)]_2$	1.932	2.8383	94.5	+226.91	+148	94
$[Cu(bpz)(OH)(ClO_4)(H_2O)]_2.\ H_2O$	1.934	2.826	94. 40	+234.37		This work

(bipym = 2,2'-bipyrimidine), (bipy=2,2'-bipyridine), (dmbipy=4,4'-dimethyl-2,2'-bipyridine). Calculated J where the singlet–triplet energy gap $J = -74.53\ (\theta) +7270$ cm−1.

3.2.1.7 Synthesis for (1):

In preparation of this complex the N,N-Diethylethylenediamine was used to prepare mixed ligand complex but the single crystal X-ray diffraction reveals the N,N-diethylethylenediamine do not exist in crystal structure, and when prepared the complex without using N,N-diethylethylenediamine the reaction product is viscous semisolid. When tracking the pH of the reaction was found the N,N-diethylethylenediamine raised the pH of the reaction from 3.11 after the 2,2’-bipyrazine react to 7.32, and when used other bases to adjustment the pH of the reaction the complex does not obtaind.

I can say the N,N-Diethylethylenediamine essential to synthesis the $[Cu(bpz)(OH)(ClO_4)(H_2O)]_2.H_2O$ complex, to adjustment pH of the reaction and the N,N-Diethylethylenediamine volatile so they leave the reaction solution easily in evaporation stage.

3.2.2 $[Cu(dipyam)_2]$ $(ClO_4)_2$ (2):

Bis(2-pyridyl)amine ligand has attracted interest in the molecular self assembling processes that lead to macromolecular architectures, because this property was used in this research to prepared mixed ligands copper complexes, by using 2,2'-dipyridylamine and the main ligand in this work 2,2'-bipyrazine, but unfortunately the single crystal X-ray diffraction reveals that it contains only 2,2'-dipyridylamine ligand and the single crystal X-ray diffraction was performed in 1971 by Johnson et al[{130}], and in 2001 by Miao et al,[{131}].

The complex **(2)** in this work was prepared in a new procedure and characterized in details by infrared spectroscopy, UV-Vis spectroscopy and thermal analysis by differential scanning calorimetry (DSC) and capillary melting point, this is the difference between this study and previous studies of this complex in 2001 and 1971.

3.2.2.2 Infrared Spectroscopy:

The infrared spectrum of **(2)** (Fig 3.12) shows a weak absorption peaks at 3326, 3221, 3154, 3095 and 2921 cm^{-1} which attributed to symmetric and asymmetric C-H and N-H stretching, weak and strong intensity peaks at 1644 to 1483 cm^{-1} assigned to ring stretching[{131, 132}],and two medium intensity peaks at 1235 and 1443 cm^{-1} have been assigned to symmetric and antisymmetric C-N stretching vibrations respectively, of carbon in pyridyl ring and nitrogen out the ring. Additionally, a strong and sharp peaks at 1119 to 1166 cm^{-1} mainly out-of-plane ring-H bending and weak from 850 to 910cm^{-1} composite ring-H in-plane binding vibrations.

The IR spectrum of the **(2)**, was compared with that of the free 2,2'-dipyridylamine ligand (Fig. 3.12). Most of the peaks were shifted to lower or to higher wave number, due to the metal coordination and crystal packing.

The pattern of the vibrations of the perchlorate ion in the IR spectrum of **(2)**, shows a strong absorption at 1089 cm^{-1} related to Cl–O stretching, a weak intensity peak at 931 cm^{-1} owing to ClO_4^- stretching, and a medium intensity peak at 619 cm^{-1}, is characteristic of the presence of uncoordinated perchlorate and did not appear in free ligand[{107-109}]. The vibration bands of metal-nitrogen are located at 435 cm^{-1} with medium intensity[{110-114}].

The infrared spectra of complex **(2)**, are given in (Fig 3.12).

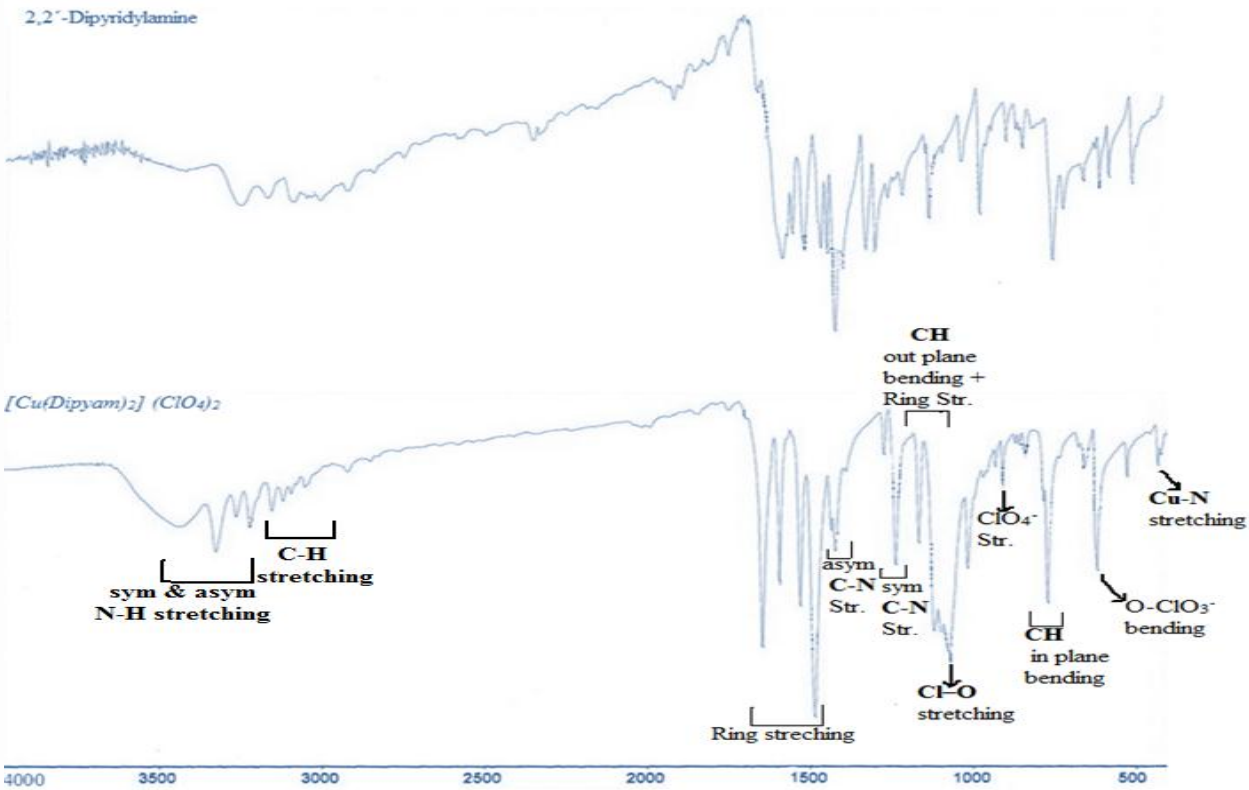

Fig. 3.12: FT-IR spectra of (2), (Down) and 2,2´-dipyridylamine ligand(Upper). And definition of characteristic peaks.

3.2.2.3 Ultraviolet-visible spectrophotometry (UV-Vis):

The absorption spectra of complex **(2)**, (Fig. 3.12b) in the visible domain contain a wide band, centered at 688 nm, which can be observed only at higher concentrations of the complexes and was attributed to the d-d transition of the electrons which suggests a $^2T_{2g} \rightarrow {}^2E_g$ transition, specific for Cu(II) complexes with distorted tetrahedral[{159,160}]. A second absorption band for this complex is found at about 414 nm, can be attributed to charge transfer[{70}]. An absorption band below 400 nm is associated with ligand- ligand transition.

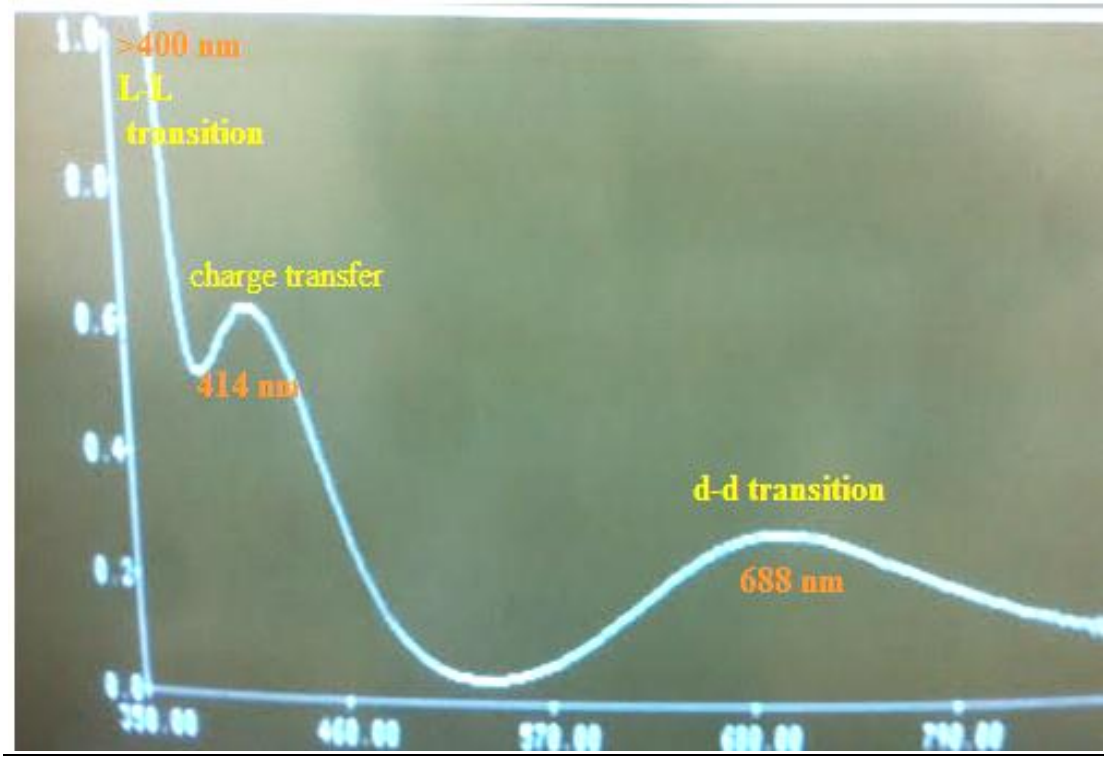

Fig. 3.12a: Electronic spectra of complex **(2)**.

3.2.2.4 Thermal analysis:

The thermal study of **(2)**, include capillary melting point determination method, Differential Scanning Calorimetry (DSC) Thermal Analysis.

Capillary melting point of complex **(2)**, shows no changes in the sample color before 305 °C but at this temperature the sample explosive and melt as blue liquid along the capillary tube wall.

The sample in DSC instrument was heated at a rate of 5 °C/min, from 20 to 450 °C in nitrogen gas flowing at a rate of 25 ml/min, then cooling in the same range.

The DSC curve (Fig 3.13) show endothermic peak associated with enthalpy of 2054.6528 J/g at 289-318 °C at T_{max} = 308.65 °C that expect to melting point process.

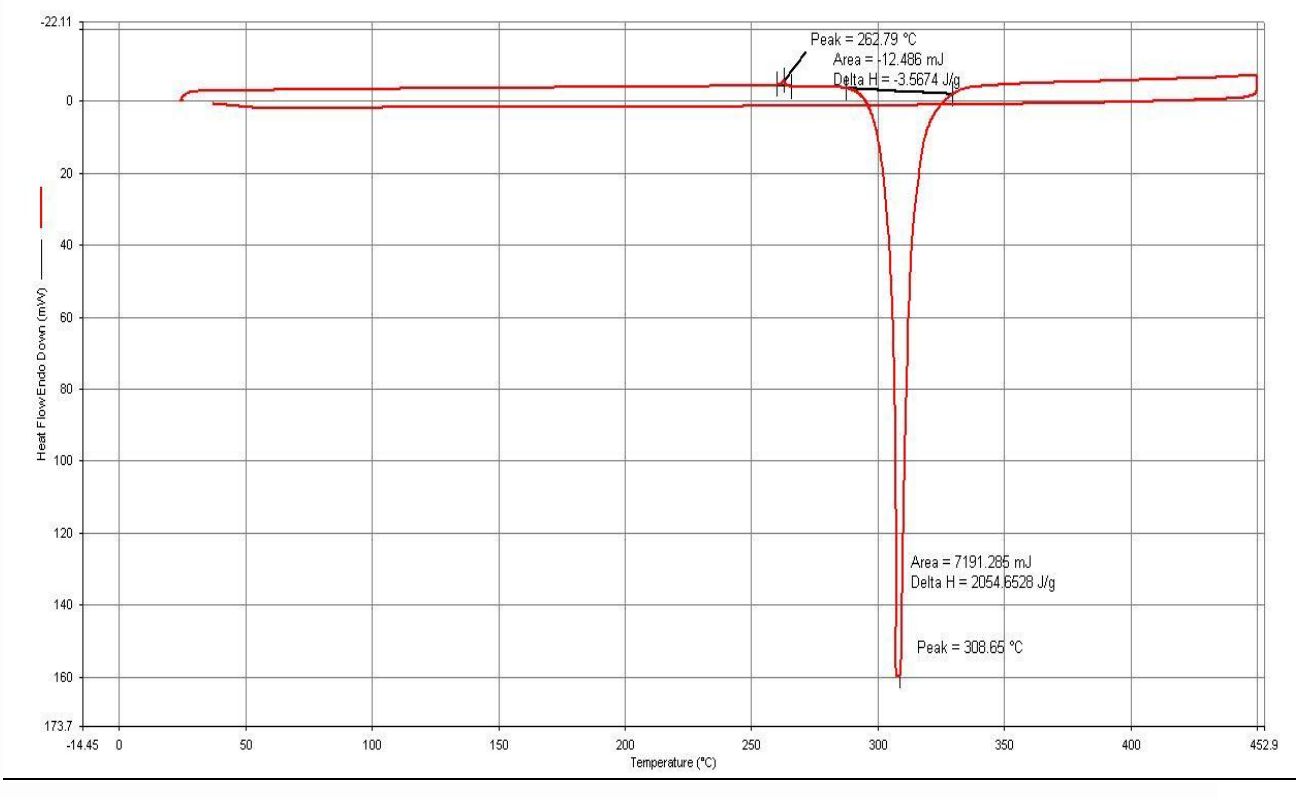

Fig. 3.13: Differential Scanning Calorimetry (DSC) of **(2)**.

3.2.2.5 Crystal structure of (2):

In the structure of **(2)**, the Cu(II) center is four-coordinated with the nitrogen donors of the pyridine rings of the 2,2′-dipyridylamine ligand, by trans-trans mode (Fig. 3.14). The crystal structure reveals that the CuN_4 coordination sphere has a distorted tetrahedral coordination geometry (Fig. 3.14). There are six cation $[Cu(dipyam)_2]^{+2}$ and eight anion (ClO^-_4) per unit cell the relative arrangement of the constituents units in the unit cell are shown in (Fig. 3.15).The perchlorate anions link the complex cations to form a chain structure through C-H$^{\cdots}$O close contacts and N-H$^{\cdots}$O hydrogen bonds (Fig. 3.17).

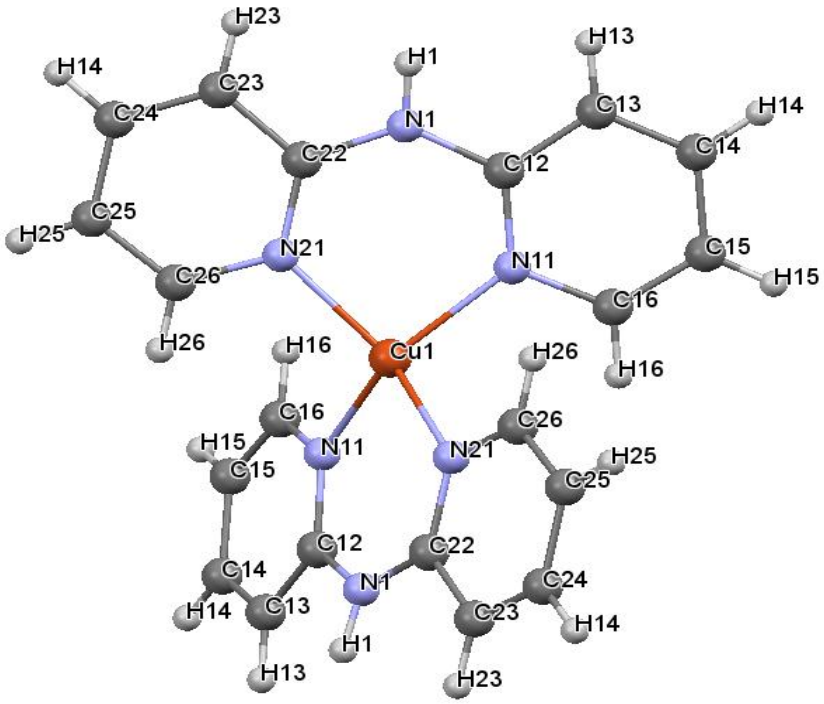

Fig. 3.14: Perspective view of **(2)**, cation with the atom numbering scheme.

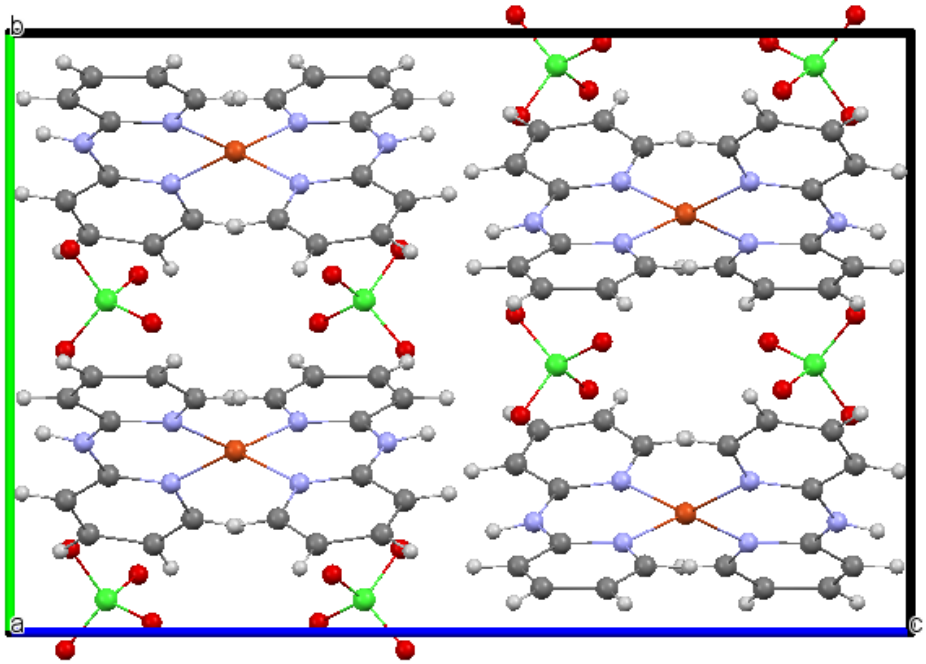

Fig. 3.15: A projection of the crystal in unit cell packing of **(2)**,down the a-axis.

The degree of distortion from planar towards tetrahedral can be reflected by the dihedral angle between the N11-Cu-N21 and N11-Cu-N21in other ligand planes 54.04 ° is smaller than in the perfect tetrahedral.

The Cu-N bond distances (Fig. 3.16, Table 3.13) are 1.968 and 1.962 Å Cu-N21 ,Cu-N11 respectively, which are almost equivalent to the value of the analogous complexes[133, 134]. They involve bite angle [N(11)–Cu–N(21)] of 93.98° (Fig. 3.16, Table 3.12), slightly more than 90°. The N(11) … N(21) bite distances 2.874 Å (Fig. 3.16). are significantly increased with respect to the bite value of the uncoordinated 2,2'-dipyridylamine (2.6 Å) which evaluated by A. N. Chernyshev et al,[135].

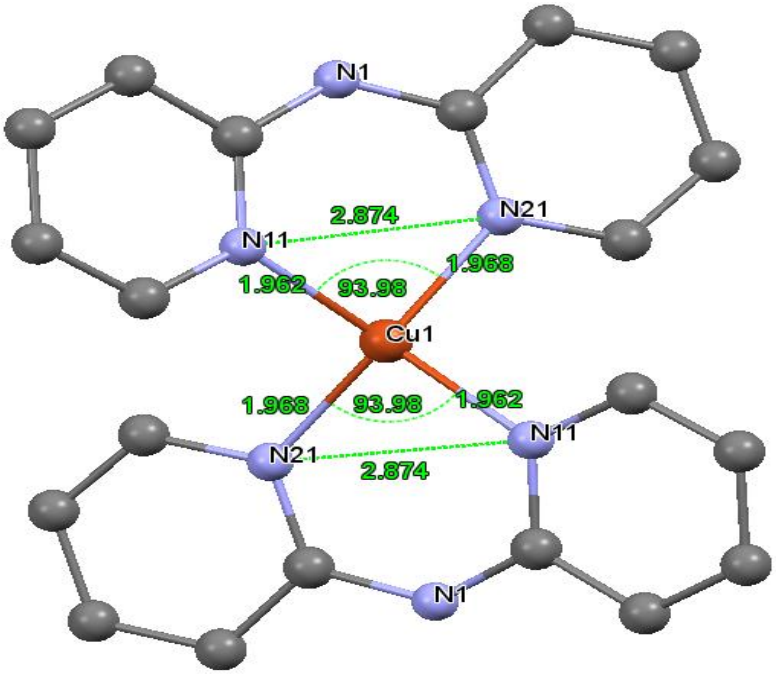

Fig. 3.16: Ionic structure of **(2)**, containing some important distance and angels.

The dihedral angle between the mean planes of two dipyam ligands is 55.61°, the dipyam groups are not planar, the dihedral angle between the mean planes of the pyridine rings is 9.91°, but pyridine rings are essentially planar (the largest deviation being 0.014 Å at the N11 atom).

The perchlorate anions act as bridges to link the complex cations through N-H…. O hydrogen bonds (Table 3.11) and C-H….O close contacts (Fig. 3.17), forming a three dimensional network structure, as shown in (Fig. 3.18). The perchlorate oxygen atoms participate in weak supramolecular interactions of the type C–H(dipyam) …. O(ClO^-_4)

with C….O distances in the ranges 3.198 - 3.458 Å (Table 3.13), which are in the normal range of the weak interactions[{136,137}]. Furthermore, the complex cations of **(2)**, are stacked in the closest approach between the pyridine rings of 4.112 Å, indicating no significant π----π stacking interactions.

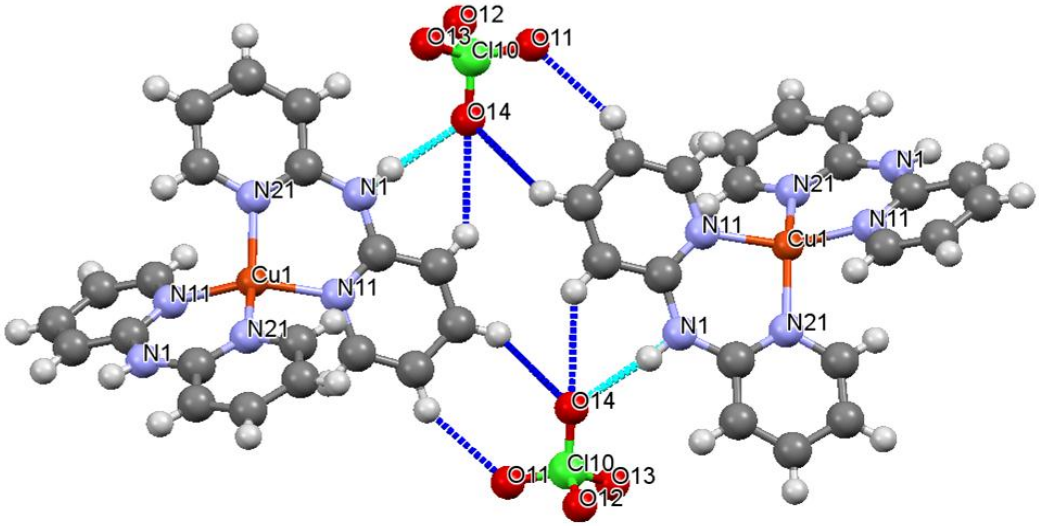

Fig. 3.17: View of the chain structure of **(2)**, showing the supramolecular C–H(dipyam) ….O(ClO^-_4) type interactions (blue line) and the hydrogen bond links the perchlorate anion with one nitrogen atoms in dipyam ligand (light blue line).

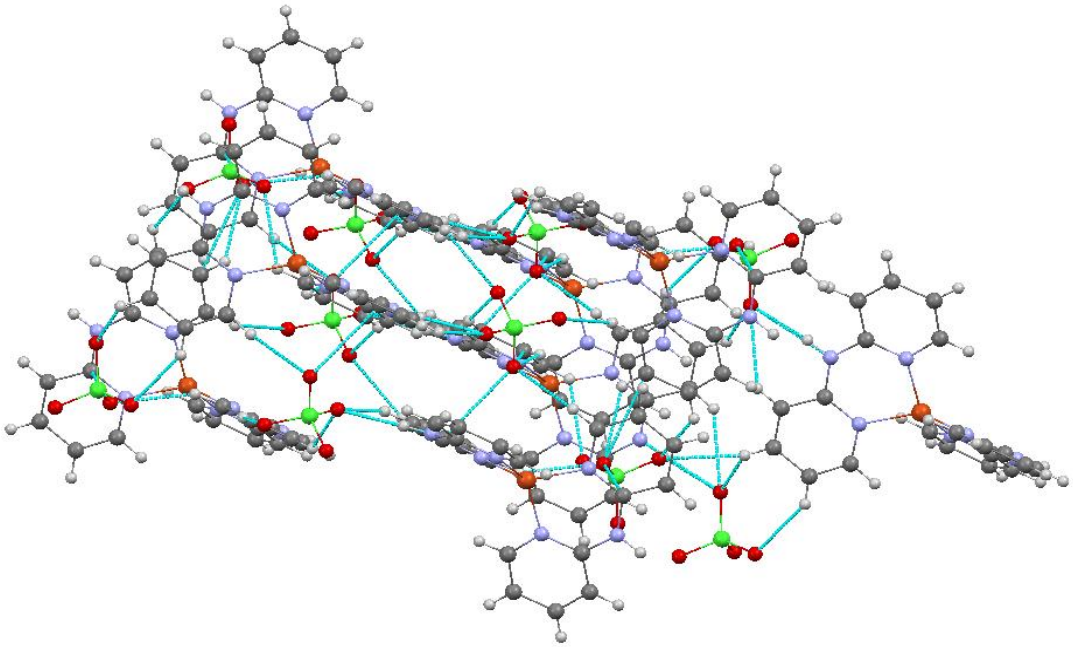

Fig. 3.18: View of a three-dimensional network structure of **(2)**.

3.3 Nickel(II) complexes:

3.3.1 $[Ni(bpz)_3](ClO_4)_2.H_2O$ (3):

Nickel complexes have been receiving much attention, due to biological applicability such as antiepileptic[{138}], anticonvulsant[{139}], antibacterial[{140}], antifungal[{140}], antimicrobial[{141}], and anticancer/antiproliferative[{142, 143}], activities. Nickel complexes can inhibit DNA repair mechanism due to interfering with enzymes or proteins synthesis involved in DNA replication or DNA repair[{144}].

Polypyridyl Ni(II) complexes show good affinity in DNA binding to exert biological effects. DNA is a target molecule for cancer therapy, therefore, the experimental and theoretical investigations of interaction of DNA with suitable molecules is very important to the design of pharmaceutical molecules[{145, 146}]. The organonickel(II) complexes are widely used as catalysts in olefin polymerization[{22}], and in control the size of nickel nanoparticles by thermal degradation of nickel(II) polypyridyl complex.

In this research we present the synthesis, and characterization of the first Ni(II) transition metal with 2,2'-bipyrazine ligand.

3.3.1.2 Infrared Spectroscopy:

FTIR spectra of **(3)**, (Fig. 3.19) show a medium and broad characteristic peak at 3432 cm^{-1} is due to the O–H stretching of water of crystallization molecules involved in hydrogen bonds, and a medium intensity peak at 1638 cm^{-1} owing to H-O-H bending of water of crystallization[{105}]. The pattern of the vibrations of the perchlorate ion in the IR spectrum of **(3)**, shows a very strong and broad absorption at 1089 cm^{-1}, a weak intensity peak at 862 cm^{-1} and a strong intensity peak at 622 cm^{-1}, is characteristic of the presence of uncoordinated perchlorate[{107}].

The vibration bands of the 2,2'-bipyrazine ligand are located at 3082 cm^{-1} which attributed to υ(C– H), and the bands of υ(C ⋯ N), υ(C ⋯ C) was found at 1490 cm^{-1}, 1478 cm^{-1}, 1323 cm^{-1} and 1341 cm^{-1} respectively, and 1408 cm^{-1} a strong and sharp peak which attributed to CCH deformation vibrations, and a strong sharp peak at 838 cm^{-1} related to ring torsion vibrations, and 750, 697 cm^{-1} mainly out-of-plane ring-H bending, this bands are shifted to lower wave number due to the new charge distribution in the ligand and crystal packing in complex, additionally, 1154 cm^{-1} composite ring bending

modes and 1042s cm^{-1} which attributed to ring-H in-plane binding vibrations, this bands are similar as ligand but number of band decreases.

FTIR spectra of **(3)**, show up a bands near far IR region at 464-444 $cm^{-1}$and this bands doesn't appear in ligand IR spectrum so this bands related to Ni-N[110, 147].

The infrared spectra of **(3)**, are given in (Fig. 3.19).

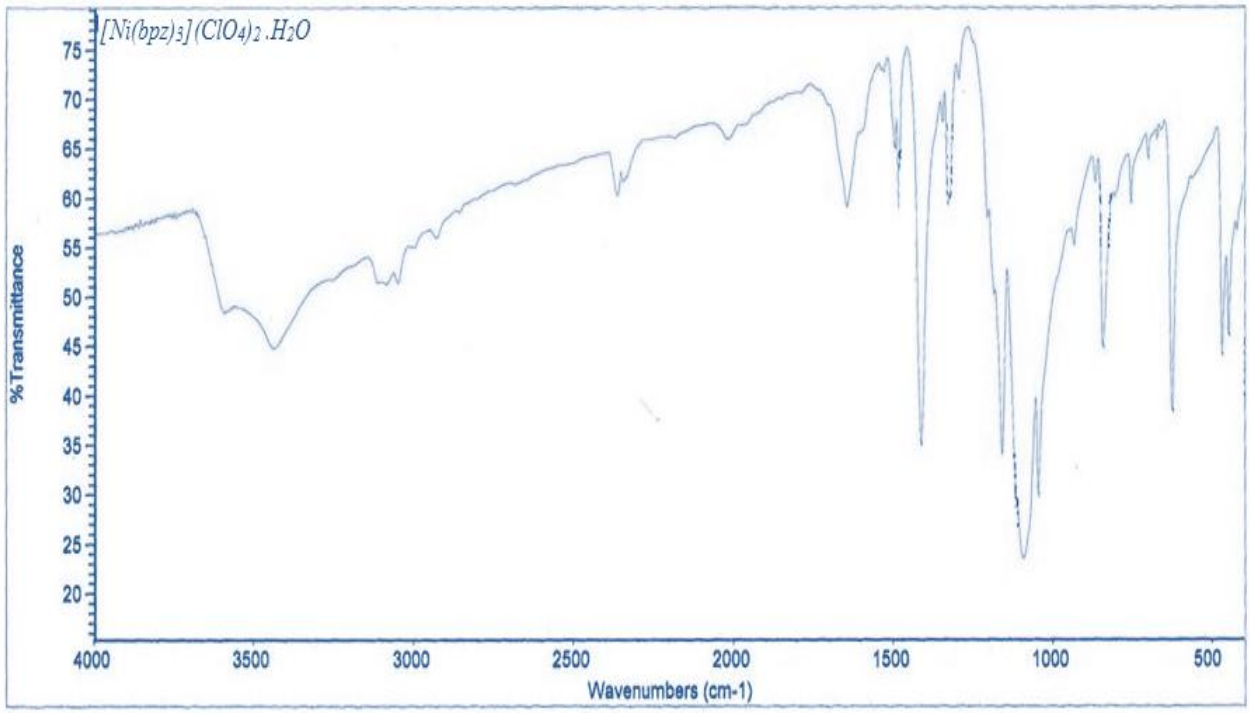

Fig. 3.19: FT-IR spectra for **(3)**.

3.3.1.3 Ultraviolet-visible spectrophotometry (UV-Vis):

Electronic spectral of **(3)**, have been obtained from dimethyl sulfoxide solutions and are presented in (Fig. 3.19b). The complex **(3)**, is colored, and there are spatial configuration of d^8 track in the Ni(II) ion, and the d orbital is not filled, d-d electronic transition can occur in three bands, but only two absorption bands observed in the visible region for the Ni(II) complex. In details, the electronic spectrum of **(3)**, displays one broad band at 606 nm and one weak broad absorption band at 763 nm which is assigned to d-d transition. These bands are typical for all the octahedrally coordinated Ni(II) complexes[154,155]. The bands at 264, 215 nm and a shoulder peak at 290 nm are assigned to ligand-centered ($\pi \rightarrow \pi^*$ and $n \rightarrow \pi^*$) transitions, these bands were found in the electronic spectra of free 2,2'-bipyrazine ligand.

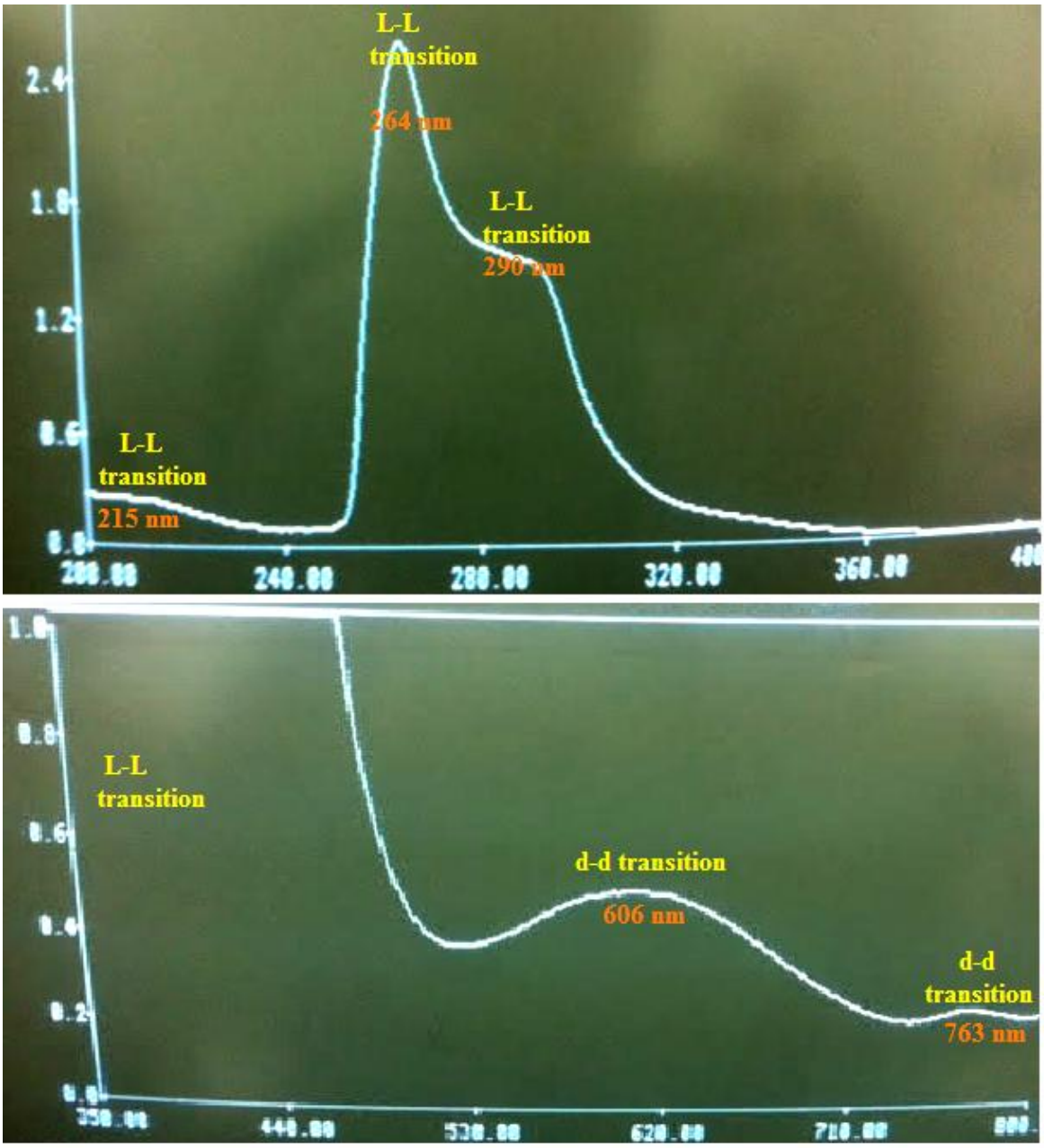

Fig. 3.19a: Electronic spectra of **(3)**, shows ligand-centered (LC) bands (up) and d-d transition (bottom).

3.3.1.4 Thermal analysis:

The thermal study of **(3)**, include capillary melting point determination method, Differential Scanning Calorimetry (DSC) Thermal Analysis.

Capillary melting point of the **(3)**, shows a change in color of the sample from yellow to brown at 280 °C then the color goes to dark brown to 350 °C , from 350 °C to 400 °C the color changed to dark brown and no change.

The sample in DSC instrument was heated at a rate of 5 °C/min, from 20 to 450 °C in nitrogen gas flowing at a rate of 25 ml/min, then cooling in the same range.

The DSC curve (Fig. 3.20) shows endothermic peak associated with enthalpy of 1474.2728 J/g at 248-395 °C at T_{max} = 334.15 °C that correspond to melting point process. There is a hysteresis in the transformation on heating and cooling which is notable.

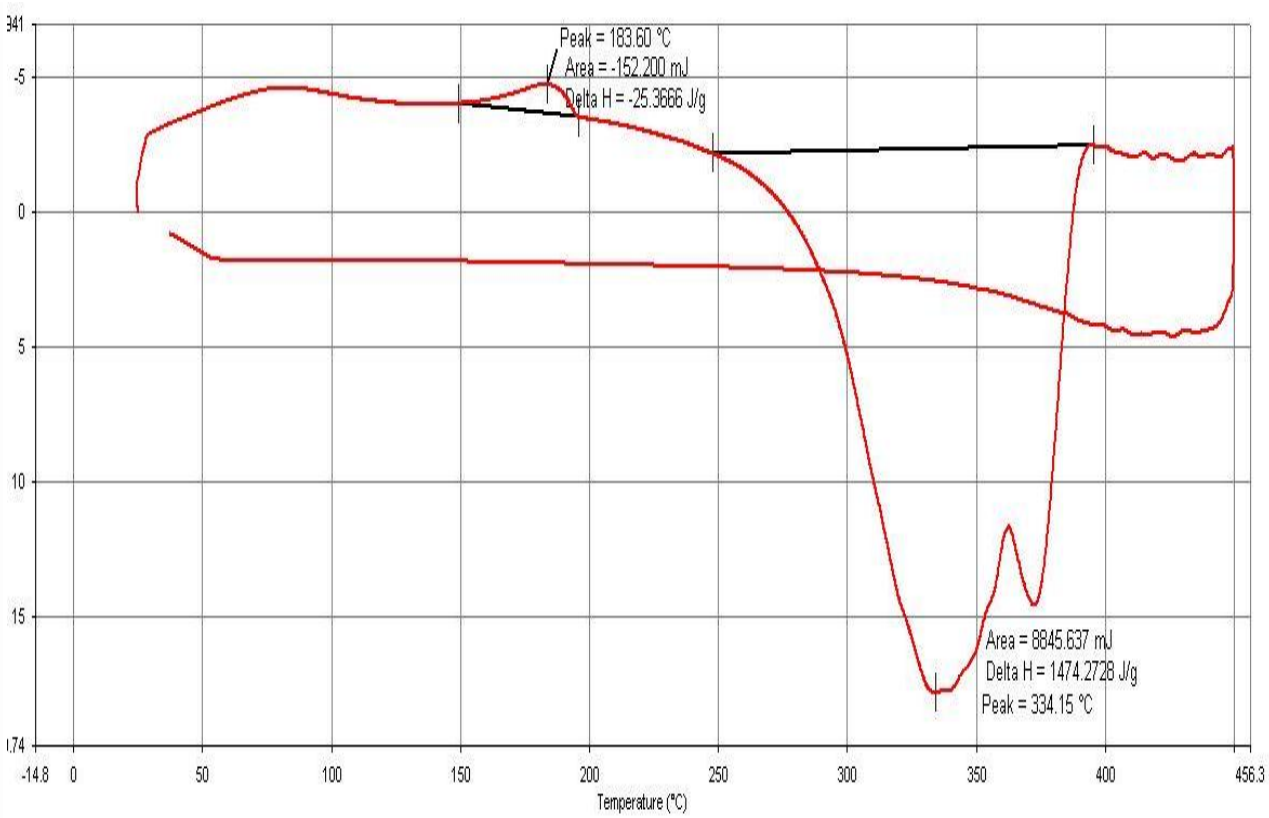

Fig. 3.20: Differential Scanning Calorimetry (DSC) of **(3)**.

3.3.1.5 Crystal structure of (3):

The structure of the nickel(II) complex is made up of discrete $[Ni(bpz)_3]^{+2}$ cations, uncoordinated perchlorate anions and water molecules of crystallization which are linked together by electrostatic interactions, such as hydrogen bonds (involving the water molecule and one of the pyrazine nitrogen atoms and perchlorate oxygen atoms) and Van

der Waals forces. There are four molecules per unit cell. A perspective view of the complex cation with the atom numbering scheme is shown in (Fig. 3.21) and the relative arrangement of the constituents units in the unit cell are shown in (Fig. 3.22).

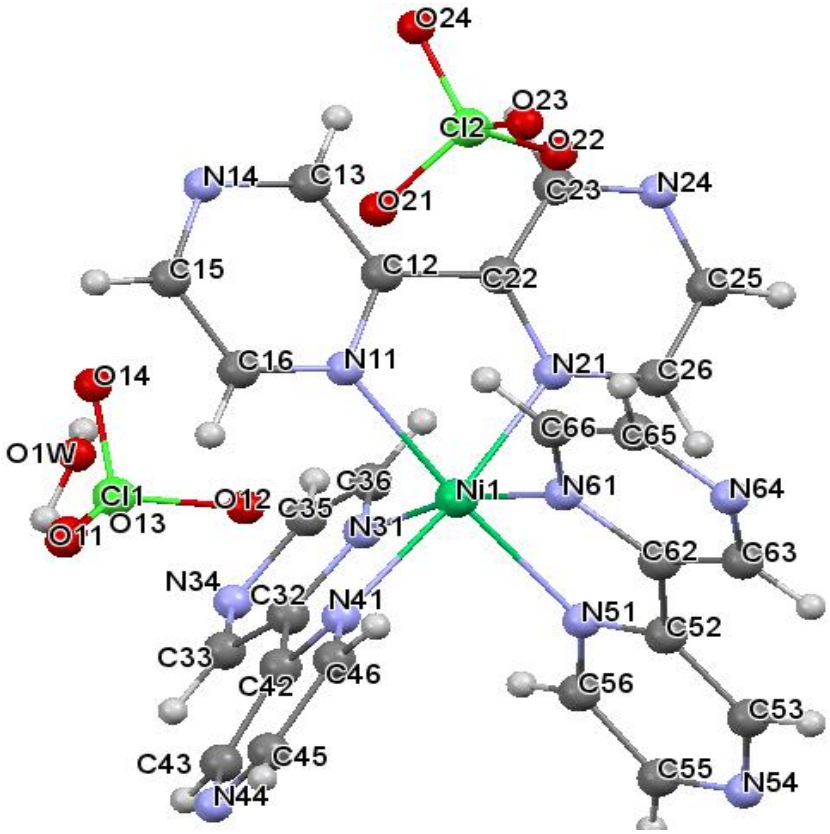

Fig. 3.21: Perspective view of **(3)**, with the atom numbering scheme.

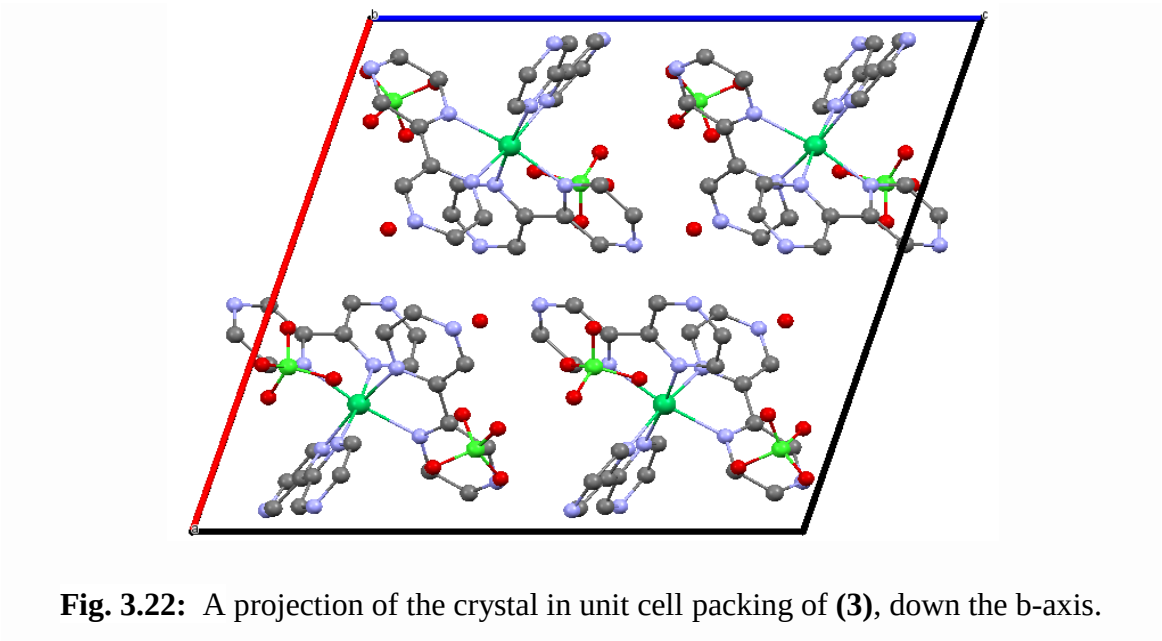

Fig. 3.22: A projection of the crystal in unit cell packing of **(3)**, down the b-axis.

The three bpz ligands form a propeller-like trigonal arrangement around the metal atoms. The coordination by the six nitrogen atoms is trigonally distorted octahedral owing to the fact that the ligand bite distance is too short to fit a perfect octahedron (Fig. 3.23).

Three 2,2'-bipyrazine ligands are bonded to Ni(II) forming five-member chelate rings, with Ni–N distances are within the range 2.068(3) - 2.104(3) Å with an average of 2.081 Å (Table 3.18, Fig. 3.23), this value compares well with that reported for tris-chelated the nickel (II) complexes[{148, 149}] (Table 3.16).

The main distortion from the octahedral geometry is observed in the values of the angles subtended by bpz at the metal atom (78.92°, 78.51° and 79.14° for N(11)–Ni–N(21), N(51)–Ni– N(61) and N(31)–Ni–N(41) respectively, (Table 3.19, Fig. 3.23).

The theoretical models predict a distortion towards trigonal- prismatic geometry for tris(bidentate chelate) complexes, which subtend angles less than 90° at the coordination metal atom[{148}].

The 2,2'-bipyrazine ligands is clearly distorted because of its coordination to nickel (II): the N(11) … N(21), N(31) … N(41) and N(51) … N(61) bite distances (2.641(7), 2.640(7) and 2.648(7) Å, respectively) (Fig. 3.23) Are significantly reduced with respect to the bite value of the free 2,2'-bipyrazine (2.82 Å) (Table 3.16) which evaluated by A. J. Blake et al[{66}].

From the Ni–N bond length, apparently, the central atoms are displaced from the midpoint of the octahedral and the coordination sphere is rather flexible and can be adjusted within certain limits to suit packing requirements, the (Ni-N51) is the longest bond distance (Fig 3.23, Table 3.19), thereby the ligand is pushed further away may be because the perchlorate anions adjacent the other two bpz ligands.

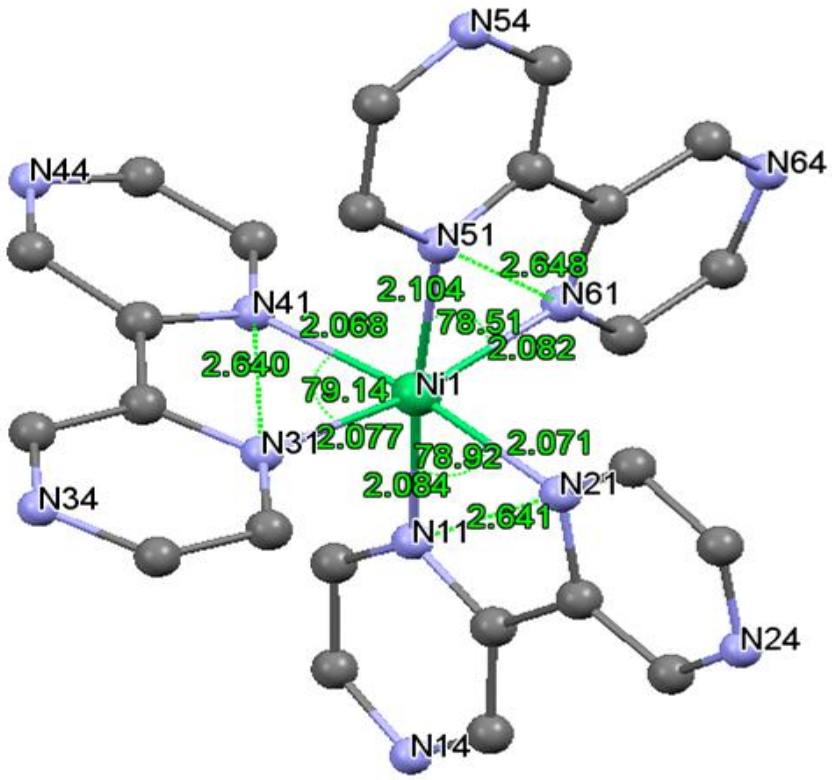

Fig. 3.23: Ionic structure of **(3)**, containing some important distance and angels.

The best mean plane around the Nickel atom is defined by the N(51), N(61), N(11) and N(31) set of atoms with the largest deviation being 0.066 Å at the N(51) atom.

The metal atom is displaced by 0.003 Å from this mean plane. The pyrazine rings of bpz deviate somewhat from planarity (the largest deviation being 0.028 Å at the C(42) atom), except those containing N(31) and N(34) atoms which are planar. One of the three bpz groups are essentially planar (those containing N(11) and (21)) with dihedral angle between the mean planes of the pyrazine rings are 4.72°) whereas the other two bpz (which containing N(31) and N(41), N(51) and N(61)) are not planar the dihedral angle in this two bpz between the mean planes of the pyrazine rings are(6.99°, and 10.12° respectively.

The dihedral angle between the mean bpz planes (which containing N(31) and N(41) with N(51) and N(61)) is 77.41°, which containing N(31) and N(41) with N(21) and N(11) is 85.83°, and between bipyrazine ligands planes containing N(51) and N(61) with N(21) and N(11)) is 88.90°, with average value of the dihedral angle between the mean bpz planes is 84.05° (Fig. 3.24).

In the cationic complexes $[Ni(bpz)_3]^{+2}$, there are little deviation from linearity for the trans N atoms with angles N51–Ni–N11, N41–Ni–N21and N31–Ni–N61 at 175.02°, 171.84° and 169.26° respectively, owing to the rigidity of bipyrazine ligands.

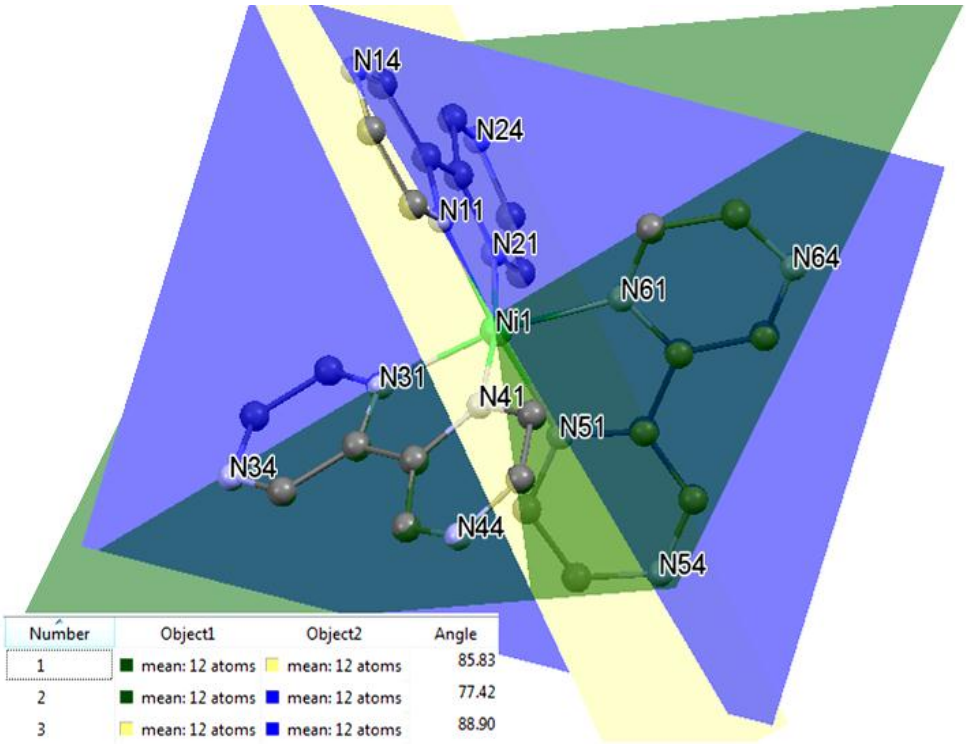

Fig. 3.24: A projection show the dihedral angle between the mean 2,2'-bipyrazine planes, blue plane contain (N51,N61), green (N31,N41) and yellow contain (N11,N21) bpz ligand in complex **(3)**.

The perchlorate anions have a tetrahedral geometry, with mean Cl–O bond distances and O–Cl–O bond angles of 1.430(7) Å, and 109.8° at Cl(1) and 1.428(4) Å and 109.3(3)° at Cl(2) (Table 3.19, Table 3.18, Fig. 3.25).

A moderate hydrogen bond[{123}] links the water molecule [O(1W)] and one of the pyrazine nitrogen atoms [2.962 Å for O1w–H1w ... N14], and hydrogen bond between the water molecule and the perchlorate oxygen atoms[2.992 Å for O1w–H2w ... O22] (Table 3.15, Fig. 3.25), and interestingly, the perchlorate oxygen atoms participate in weak supramolecular interactions of the type C–H(bpz) …. O(ClO^-_4) with C….O distances in the ranges 3.234-3.372 Å (at Cl(1)) and 3.364-3.119 Å [at Cl(2)] (Fig. 3.25).

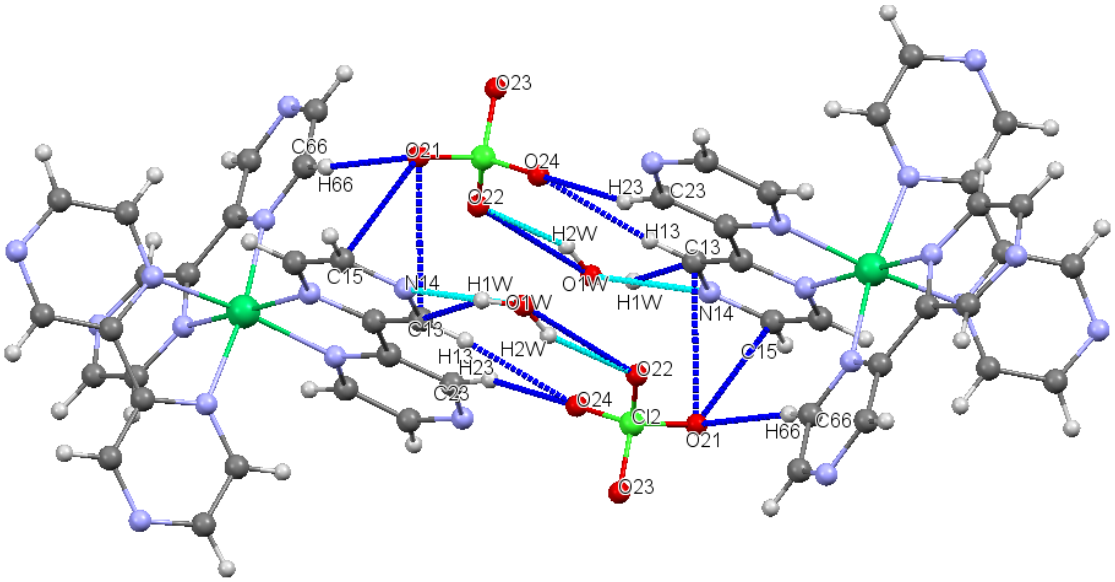

Fig. 3.25: View of the chain structure of **(3)**, showing the supramolecular C–H(bpz) ….O(ClO^-_4) type interactions (blue line) and the hydrogen bond links the water molecule with one of the pyrazine nitrogen atoms [O1w–H1w ... N14] and the hydrogen bond links the water molecule with perchlorate anion [O1w–H2w ... O22] (light blue line).

A short intermolecular attraction between the 2,2'-bipyrazine rings in $[Ni(bpz)_3]^{+2}$ cations forms a weak hydrogen bonds of the types CH----π, C–H···N–C[{123}] , acts as a significant contributor in the construction of supramolecular in the crystal packing, the distance between aromatic ring (less than or slightly larger than 3.0 Å) is an indication for the occurrence of C–H----π, C–H···N–C hydrogen bonds (Fig. 3.26)[{148,150,152}]. The intermolecular CH----π distances are smaller than 3.0 Å, where the distance of C25-H25---- π cloud at pyrazine ring containing (C33) and C65-H65---- π cloud at pyrazine ring containing (C55) 2.845 Å and 2.887 Å respectively. The C–H···N–C mean distances 3.2616 Å (Table 3.15, Fig. 3.26). Database surveys on transition metal complexes gave evidence of the C–H----π and C–H···N–C hydrogen bond being an important factor in controlling the crystal packing and molecular structure[{153}].

The packing structures of **(3)**, show that the rings of the polypyrizyl ligands are stacked in two set between bpz ligands in complex with parallel displaced form interaction. The mean π----π interactions distances 3.1613 Å (Fig.3.26 and Fig.3.27).

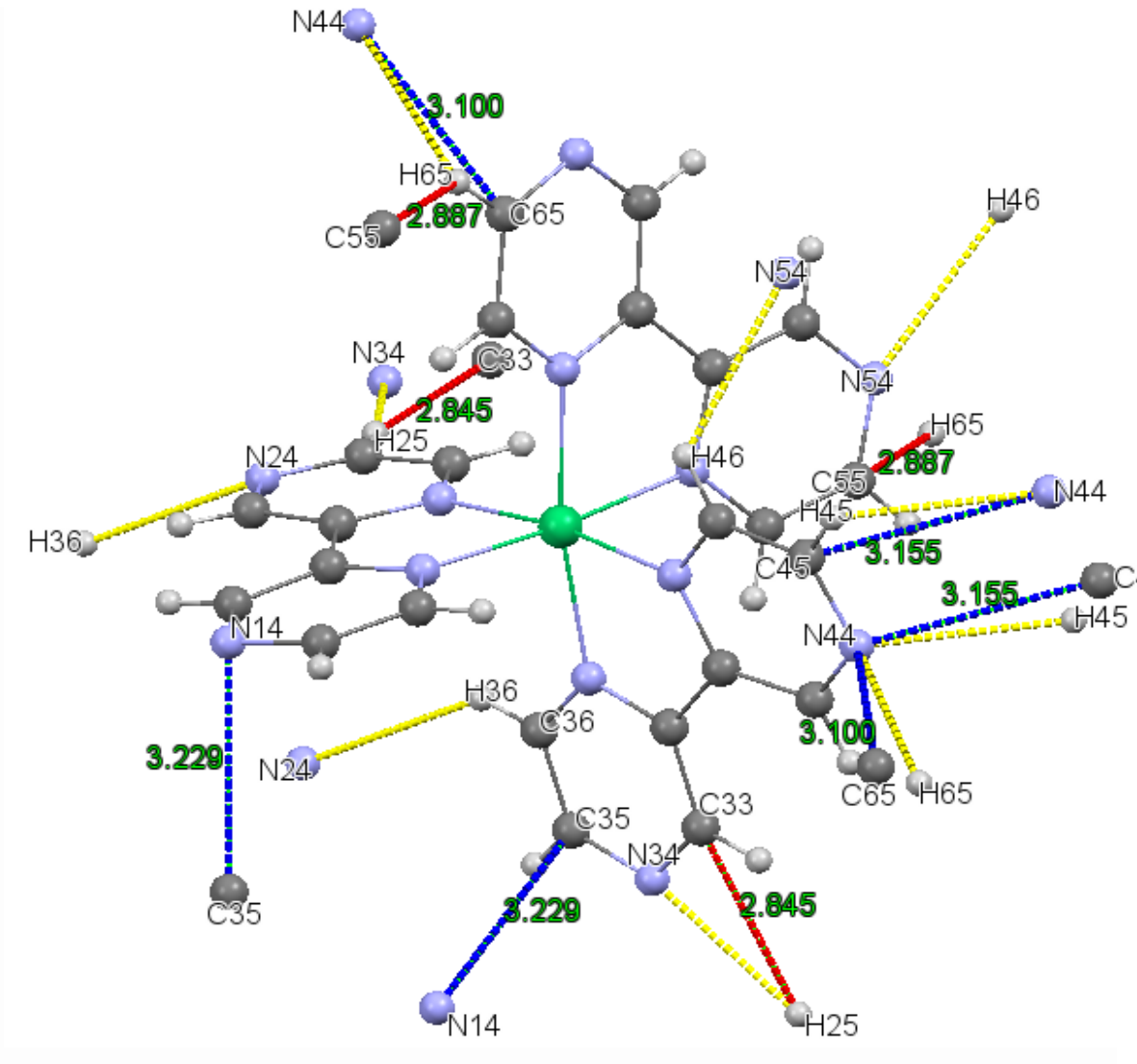

Fig. 3.26: View of the interaction between the bpz ligand in **(3)**, showing C–H----π (red line) distance, C–H···N–C (yellow line), hydrogen bonds interaction , and π ---- π interactions (blue line) distance.

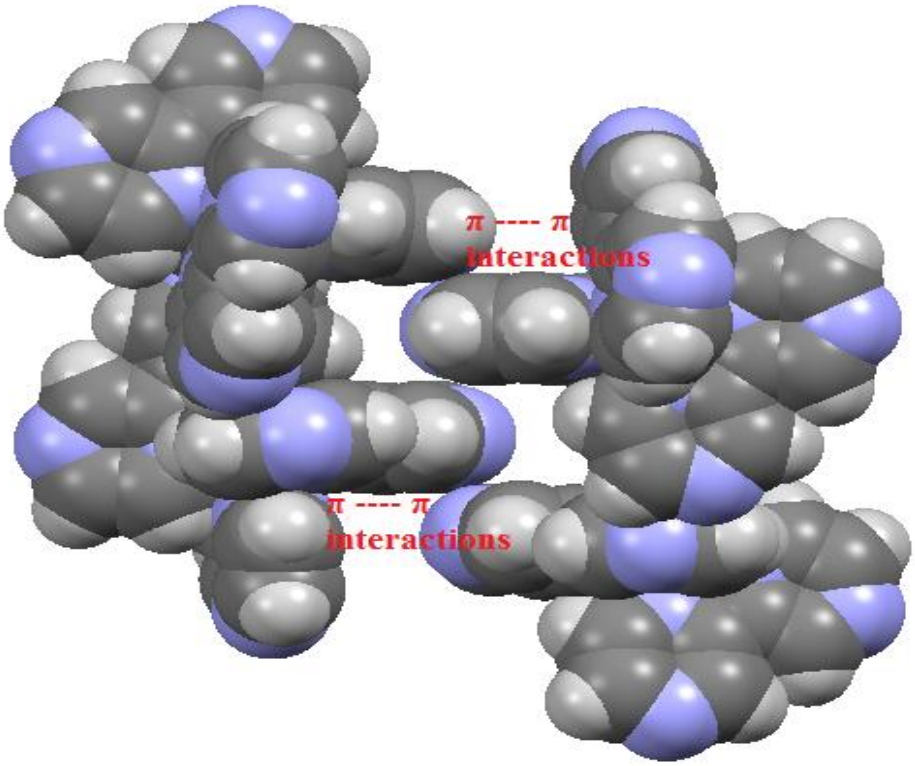

Fig. 3.27: Space-filling packing diagram of the complex cation, displaying the π ---- π interactions of adjacent cations in **(3)**.

Comparison of **(3)**, with the isomorphous compounds $[Fe(bpz)_3]$ $(ClO_4)_2.H_2O$[69], $[Ru(bpz)_3]$ $(PF_6)_2$[151], $[Ni(bpy)_3](PF_6)_2$[148] and Free bpz ligand[66]:

Bond lengths and bond angles of similarly attached atoms are compared in (Tables 3.16 and 3.17). Entries were averaged in cases where there was more than one equivalent bond distance or angle for a given cation. The ligand bite and M-N distance increases on going from $[Fe(bpz)_3]$ $(ClO_4)_2.H_2O$ to $[Ni(bpz)_3](ClO_4)_2.H_2O$, this trend reflects the size of the central cation.

The bpz and bpy ligands can act either as a σ-donor or a π-acceptor, and differ in their character , the Ni(II)–N bond in these complexes is constituted by a σ–bond and π – bonding. The weaker σ bonding in the series bpy > bpz is balanced by the stronger π bonding in the series bpz > bpy such that the ligand bite and the interatomic Ni(II)–N distance is essentially the same[148, 151]. The average bridging C-C distance connecting the two aromatic heterocyclic rings of coordinated bpz is 1.450 Å, 1.482 Å and 1.473 Å

the values very close to that observed in the free bpz (1.484 Å) (Tables 3.16) and which is as expected for a single C–C bond.

The angles which obtained in this work of **(3)**, compares well with the related angles in the tris-chelated complexes in (Table 3.17), and it's in the range of angles of tris-chelated complexes.

Table 3.16: Bond distances (Å) Comparisons $[Ni(bpz)_3](ClO_4)_2.H_2O$ with $[Fe(bpz)_3]$-$(ClO_4)_2.H_2O$[69], $[Ru(bpz)_3]$ $(PF_6)_2$[151], $[Ni(bpy)_3](PF_6)_2$[148] and Free bpz ligand[66]

Bond length	$[Fe(bpz)_3]$-$(ClO_4)_2.H_2O$	$[Ru(bpz)_3]$-$(PF_6)_2$	$[Ni(bpz)_3]$-$(ClO_4)_2.H_2O$	$[Ni(bpy)_3]$ $(SO_4)_2.H_2O$	Free bpz Ligand
M–N	1.961	2.051	2.081	2.094	
–C–N–	1.341	1.354	1.332	1.343	1.363
–C–N|	1.322	1.332	1.330		1.337
–C–C–	1.379	1.401	1.379	1.366	1.396
>C–N–	1.357	1.330	1.349	1.347	1.340
>C–C<	1.450	1.482	1.473	1.482	1.484
Bite distances	2.563	2.589	2.643	2.649	

–N– ***(Bonding to metal)*** –N\| ***(Nonbonding to metal)*** –C– ***(Carbon in ring)*** >C– ***(Bridgehead carbon) .***

Table 3.17: Bond Angle (deg) Comparisons $[Ni(bpz)_3](ClO_4)_2.H_2O$ with $[Fe(bpz)_3]$-$(ClO_4)_2.H_2O$[69], $[Ru(bpz)_3]$ $(PF_6)_2$ [151], $[Ni(bpy)_3](PF_6)_2$[148] and Free bpz ligand[66]:

Angles position	$[Fe(bpz)_3]$-$(ClO_4)_2.H_2O$	$[Ru(bpz)_3]$-$(PF_6)_2$	$[Ni(bpz)_3]$-$(ClO_4)_2.H_2O$	$[Ni(bpy)_3]$ $(SO_4)_2.H_2O$	Free bpz ligand
–N–M–N–	174.95	172.37	172.04	169.87	
N (C, C)	116.20	119.73	117.19	118.63	116.62

	115.39	117.83	116.38	-----	116.30
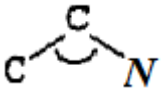	125.14	122.14	120.37	-----	121.08
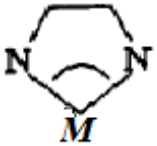	81.59	78.61	78.85	78.50	
	4.30	6.64	7.27	6.99	0.00

The average bond distances and bond angles to the $[Fe(bpz)_3](ClO_4)_2.H_2O$[69], $[Ru(bpz)_3]\ (PF_6)_2$[151], $[Ni(bpy)_3](PF_6)_2$[148] complexes and Free bpz ligand[48] in Table 3.16 and Table 3.17 was calculated according to bond angle and bond distance in the Cambridge Crystallographic Data Centre (CCDC), CSD version 5.38 (November 2016).

Chapter Four

Conclusion and future work

4.1 Conclusion:

The research work of this thesis is divided in two parts; the first one is synthesis of coordination compounds containing mono and dinuclear copper and nickel with 2,2'-bipyrazine and other nitrogen base ligands. The second part is the characterization, using single crystal X-ray diffraction, FTIR spectroscopy, Electronic spectral by Ultraviolet-visible spectrophotometry (UV-Vis), and Thermal analysis (DSC), and the characterization in detail of the 2,2'-bipyrazine ligand by FTIR spectroscopy and X-ray diffraction.

All synthetic work was carried out under normal laboratory conditions.

All coordination compounds when prepared were first characterized by FTIR spectroscopy and electronic spectra, the confirmation of the coordination behavior was based on energy shift in electronic spectra of the final product compared to the free ligand and the d-d absorption.

The 2,2'-bipyrazine is a ligand containing four nitrogen atoms, have attracted a great interest to form macromolecular architectures and bonding in DNA due to different coordination modes and outer nitrogen atoms.

The coordination modes between metal ions (copper(II) and nickel(II)) and 2,2'-bipyrazine and 2,2′-dipyridylamine ligands are known coordination modes in the literature.

In this research we are synthesized and characterized three coordination compounds which is $[(bpz)Cu(OH)(ClO_4)(H_2O)]_2.H_2O$ **(1)**, $[Cu(dipyam)]_2(ClO_4)_2$ **(2)** and $[Ni(bpz)_3](ClO_4)_2.H_2O$ **(3)**, where (bpz=2,2'-bipyrazine and dipyam=2,2′-dipyridylamine).

The crystal structure of **(1)**, is a novel dinuclear copper(II) complex with distorted elongated tetragonal octahedral geometry around each copper ion, the crystal structure shows the first example of di-μ-hydroxo-copper(II) dimer with 2,2'-bipyrazine as outer ligand.

Although the structure of this compound showed the Cu–O–Cu angle is 94.40° and Cu….Cu distance is 2.826 Å, to the best of our knowledge, this is the shortest distance and smallest angle was obtained until now and indicating a stronger Cu(II)–Cu(II) interaction in comparable with the Cu(II)–Cu(II) distance and angles in the reported structures[{115-122, 86, 91}]. The planar Cu_2O_2 network of copper(II) dinuclear and unexpected coordination of water solvent molecule and perchlorate counter ions.

According to the relevant data for the structurally and magnetically predicted a strong ferromagnetic interaction material of widespread use in a variety of technological applications. The packing structure shows the rings of the polypyrizyl ligands are interact through π----π interactions and replete with hydrogen bonding interactions, the water of crystallization and the complex forms a 2D sheet, with adjacent sheets then linking into 3D through perchlorate oxygen atoms interactions and π----π interactions.

In preparation of **(1)**, the N,N-diethylethylenediamine essential to adjustment of the reaction pH and when other bases were used such as sodium hydroxide, sodium carbonate…etc, to adjustment pH the product is unsuitable to X-ray diffraction analysis may be due to the N,N-diethylethylenediamine is volatile and leave the reaction solution easily in evaporation stage.

The synthesis of **(1)**, must confront with many great challenges because crystal structures are affected by multiple factors such as pH value, metal ions, organic ligands, reaction conditions and so on.

To design further synthetic work its essential to choose the appropriate pH.

The second coordination compound is **(2)**, the single crystal X-ray diffraction reveals that the complex was performed in 1971by Johnson et al, and in 2001 by Miao et al, but the new in this research is the preparation method, thermal analysis by differential scanning calorimetry (DSC) and characterization in detail by FTIR spectroscopy and Ultraviolet-visible spectrophotometry (UV-Vis).

the crystal structure reveals that the Cu(II) center is four-coordinated by the nitrogen donors of the pyridine rings of the 2,2′-dipyridylamine ligand, by trans-trans mode, and the CuN_4 coordination sphere has a distorted tetrahedral coordination geometry. The perchlorate anions link the complex cations to form a chain structure through C-H$^{\cdots}$O and N-H$^{\cdots}$O hydrogen bonds, and no indication to π ---- π stacking interactions.

This complex unexpected and serendipitous when prepared mixed ligand copper(II) complex using 2,2'-bipyrazine the main ligand of this work and 2,2′-dipyridylamine, the single crystal X-ray diffraction reveals the 2,2'-bipyrazine does not exist in the crystal structure.

The third crystal structure is mononuclear Ni(II) complex, $[Ni(bpz)_3](ClO_4)_2.H_2O$, is the first nickel(II) complex containing 2, 2'-bipyrazine ligand, and this type of coordination compound have been an attractive area of research due to important applications.

The crystal structure shows the geometry around nickel(II) is a trigonal distorted octahedral and the crystal packing reveals interesting crystal packing contains a weak hydrogen bonds of the types CH----π, C–H···N–C, and the 2,2'-bipyrazine ligand are stacked in two set with parallel displaced form interaction forming π----π interactions distances 3.1613 Å.

This coordination compound has a relative high melting point due to high intermolecular attraction.

4.2 Future work:

As a sequel to this work, I suggest to do father characterization and may be very important characterization such as magnetic susceptibility at different temperature, to study the applications of $[(bpz)Cu(OH)(ClO_4)(H_2O)]_2.H_2O$ complex, whereas the di-μ-hydroxo-copper(II) dimer with heterocycle ligands complexes have a wide technological applications, photophysical, DNA cleavage due to the advantages in electronic and structural diversity and it has high nucleolytic efficiency. Study the applications of the $[Ni(bpz)_3](ClO_4)_2.H_2O$ coordination compound, where as the reported application for tris-chelated nickel(II) complexes which has a structure like this complex, show good affinity in DNA binding to exert biological effects and the DNA is a target molecule for cancer therapy, therefore, the experimental and theoretical investigations of interaction of DNA with suitable molecules is very important to the design of pharmaceutical molecules to inhibit DNA repair mechanism due to interfering with enzymes or proteins synthesis involved in DNA replication or DNA repair. The metal complexes containing 2,2'-bipyrazine ligand showed important application in solar cell and catalysts in polymerization reactions and interesting magnetic, optical, and medicinal properties.

I suggest to proposed a new synthetic procedure to prepare a new di-μ-hydroxo-copper(II) dimer with 2,2'-bipyrazine ligand, but using different volatile bases to the adjustment of the pH such as N,N,N′,N′-tetramethylethylenediamine and N,N-dimethylethylenediamine…etc, and repeat the reaction with diffrent solvent such as methanol and ethanol …etc, I think these reactions produce a suitable single crystal for X-ray diffraction analysis.

For example in this research work I repeated the synthetic procedure for **(1)**, complex using N,N,N′,N′-Tetramethylethylenediamine as a base to adjust the pH, a suitable single crystal of X-ray diffraction analysis was produces and characterized by FTIR, the resulting product a new coordination compound with significant different with FTIR spectrum of **(1)**.

If we do this work we can get additional information about the mechanism of this type of reaction and a very important information about structural and magnetical prosperities of this kind of coordination compounds.

Also I suggest to use **(1)**, **(2)** and **(3)**, as starting material to prepare Supramolecular compounds continues multinuclear, such as the reaction of the above complexes with silver(I) salts.

Chapter Five

References:

[1] J.M. Lehn, Supramolecular Chemistry, VCH, Weinheim, 1995.
[2] J.P. Sauvage (Ed.), Transition Metals in Supramolecular Chemistry, Wiley, Chichester, 1999.
[3] M. Fujita, Struct. Bond. 96, 2000 177.
[4] (a) B. Olenyuk, A. Fechtenko¨ tter, P.J. Stang, J. Chem. Soc. Dalton Trans. 1998, 1707;
(b) P.J. Stang, Chem. Eur. J. 4,1998 19
(c) S. Leininger, B. Olenyuk, P.J. Stang, Chem. Rev. 100, 2000, 853.
[5] G.F. Swiegers, T.J. Malefetse, Chem. Rev. 100, 2000, 3483.
[6] J.A.R. Navarro, B. Lippert, Coord. Chem. Rev. 185–186, 1999, 653.
[7] Various articles in: Inorganic Crystal Engineering, Dalton Discussion No. 3, J. Chem. Soc. DaltonTrans, 2000, 3705.
[8] (a) R.K.O. Sigel, S.M. Thompson, E. Freisinger, F. Glahe´, B. Lippert, Chem. Eur. J. 7, 2001, 1968;
(b) S. Metzger, A. Erxleben, B. Lippert, JBIC 2, 1997, 256.
[9] M. Fujita, O. Sasaki, T. Mitsuhashi, T. Fujita, J. Yazaki, K. Yamaguchi, K. Ogura, Chem.Commun, 1996, 1535.
[10] R.D. Schnebeck, L. Randaccio, E. Zangrando, B. Lippert, Angew. Chem. Int. Ed. Engl. 37, 1998, 119.
[11] (a) A.R. Katritzky, Advances in Heterocyclic Chemistry, vol. 58, Elsevier, 1993.
(b) W.R. Browne, R. Hage, J.G. Vos, Coord. Chem. Rev. 250, 2006, 1653.
[12] M. H. Chisholm, J. C. Huffman, I. P. Rothwell, P. G. Bradley, N. Kress and W. H. Woodruff, J. Am. Chem. Soc. 1981, 103, 4945.
[13] A. Galstyan, W.Shen, E. Freisinger, H. Alkam,W. Hiller, P. J. S.Miguel, Markus Sch_rmann, and B. Lippert .Chem. Eur. J. 2011, 17, 10771 – 10780,.
[14] H. Hadadzadeh, M.M. Olmstead, A.R. Rezvani, N. Safari, H. Saravani . Inorganica Chimica Acta. 359, 2006, 2154–2158.
[15] B.Qiu, L. Guo, C. Guo, Z. Guo, Z. Lin, G. Chen. Biosensors and Bioelectronics. 26, 2011, 2270–2274.
[16] V. Rajendiran, M. Palaniandavar, V. S. Periasamy, M. A. Akbarsha. Journal of Inorganic Biochemistry. 116, 2012, 151–162
[17] Ke-Jie Du, Jin-Quan Wang, Jun-Feng Kou, Guan-Ying Li, Li-Li Wang, Hui Chao, Liang-Nian Ji. European Journal of Medicinal Chemistry. 46, 2011, 1056e1065.
[18] S.G.Camera, H.E.Toma , Jornal of photo chemistry and photobiology A:Chemistry. 151, 2002, 57-5-65.
[19] M. J. Belousoff, B. Graham, B. Moubaraki, K. S. Murray, and L. Spiccia. Eur. J. Inorg. Chem. 2006, 4872–4878.
[20] H.H.Alkam, A.Hatzidimitriou, C.C.Hadjikostas, C.Tsiamis.Inorganica Chimic Acta. 256, 1997, 41-50
[21] F. H. Haghighi, H. Hadadzadeh, F. Darabi, Z. Jannesari, M. Ebrahimi, T. Khayamian, M. Salimi, H. A. Rudbari. Polyhedron. 65, 2013, 16–30.

[22] A. Klein, A. Kaiser, B. Sarkar, M. Wanner and J.Fiedler, Eur. J. Inorg. Chem. 2007, 965–976.
[23] J. J. Lafferty and F. H. Case. J. Org. Chem. 1967, 32, 1591.
[24] R. J. Crutchley and A. B. P. Lever. Inorg. Chem. 1982, 21, 2276-2282.
[25] D. P. Rillema, G. Allen, T. J. Meyer, and D. Conrad. Inorg. Chem. 1983, 22, 1617-1622.
[26] N. V. Lebedeva, R. D. Schmidt, J. J. Concepcion, M. K. Brennaman, I. N. Stanton, M. J. Therien, T. J. Meyer, and M. D. E. Forbes. J. Phys. Chem. A 2011, 115, 3346–3356.
[27] P.K. Ghosh and A.J. Bard. J. Electroanal. Chem., 169, 1984, 113-128.
[28] A. Rugge , C. D. Clark a Morton, Z. Hoffman, D. P. Rillema. lnorganica Chimica Acta 279, 1998, 200-205.
[29] P. A. Anderson, R. F. Anderson, M. Furue, P. C. Junk, F. R. Keene, B. T. Patterson, and B. D. Yeomans. Inorg. Chem. 2000, 39, 2721-2728.
[30] T. S. Akasheh and Z. M. Egahmed. CHEMICAL PHYSICS LETTERS, Volume 152. number 4,5.
[31] I. Jibril, T. S. Akasheh and A. M. Shraim. Polyhedron Vol. 8, No. 21, pp. 2615-2619, 1989.
[32] T. S. Akasheh, and N. A. F. ALRawashdeh. Journal of Photochemistry and Photobiology, A: Chernisby, 54, 1990, 283-292
[33] T. S. Akasheh, I. Jibril and A. M. Shraim. Inorganica Chimicu Acta, 175, 1990, 171-180.
[34] T. Iguro, N. Ikeda, T. Ohno. Inorganica Chimica Acta 226, 1994, 203-211.
[35] T. K. Mallick, P. K. Das, S. Sinha and B. K. Ghosh. Polyhedron Vol. 13, No. 12, pp. 1817-1823.1994.
[36] P. Thanasekaran, S. Rajagopal,R. Ramaraj and C. Srinivasan. Radiat. Phys, Chem. Vol. 49, No. 1, pp. 103-106, 1997.
[37] K.C. Zheng, J.P. Wang, W.L. peng, X.W. Liu, F.C. Yun. Journal of molecular structure (Theochem), 582, 2002, 1-9.
[38] B. D. Alexander and T. J. Dines. Inorganic Chemistry, Vol. 43, No. 1, 2004.
[39] B. V. Bergeron and G. J. Meyer. J. Phys. Chem. B 2003, 107, 245-254.
[40] M.E. G. Posse, M. M. Vergara, F. Fagalde, N.E. Katz. Polyhedron 22, 2003, 465-471.
[41] M. Kuss-Petermann and O. S. Wenger. J. Phys. Chem. Lett. 2013, 4, 2535−2539.
[42] O. S. Wenger. Chem. Eur. J. 2011, 17, 11692 – 11702.
[43] C. Bronner and O. S. Wenger. Phys. Chem. Chem. Phys., 2014, 16, 3617-3622.
[44] C. Bronner and O. S. Wenger. J. Phys. Chem.Lett. 2012, 3, 70−74.
[45] D. M. Schultz, J. W. Sawicki and T. P. Yoon. J. Org. Chem. 2015, 11, 61–65.
[46] S. Ernst, Y. Kurth, and W. Kaim. Journal of Organometallic Chemistry, 302, 1986, 21l-21 5.
[47] S. Ernst, S. Kohlmann and W. Kaim. Journal of Organometallic Chemistry 354, 1988, 177-192.
[48] D. M. Baird, F. L. Yang, D. J. Kavanaugh, G. Finness and K. R. Dunbar.Polyhedron Vol.15, No. 15, pp 2597 2606. 1996.
[49] W. A. Fordyce and G. A. Crosby. Inorg. Chem. 1982, 21, 1023-1026.

[50] A. Furlani, R. Paolesse, M. V. Russo, A. Camus and N. Marsich. POLYMER, 1987, Vol 28.
[51] M. Ladwig and W. Kaim. Journal of Organometallic Chemistry, 419, 1991, 233-243.
[52] K.Kalyanasundaram. J. Chem. SOC., Faraday Trans. 2, 1986,82, 2401-2415.
[53] W. Kaim, H. E.A. Kramer, C. Vogler, and J. Rieker. Journal of Organometallic Chemistry, 367, 1989, 107-115.
[54] R. Kirgan, M. Simpson, C. Moore, J. Day, L. Bui, C. Tanner, and D. P.l Rillema. Inorg. Chem. 2007, 46, 6464-6472.
[55] C. Bronner and O. S. Wenger. Inorg. Chem. 2012, 51, 8275−8283.
[56] V. Christou and G. B. Young. Journal of Organometaliic Chemistry, 368, 1989, 391-399.
[57] R-D. Schnebeck, L. Randaccio, E. Zangrando, and B. Lippert. Angew. Chem. Int. Ed. 1998, 37, No. ½.
[58] R-D. Schnebeck, E. Freisinger, and B. Lippert. Angew. Chem. Int. Ed. 1999, 38, No. ½.
[59] R-D. Schnebeck, E. Freisinger, F. Glahe´, and B. Lippert. J. Am. Chem. Soc. 2000, 122, 1381-1390.
[60] A. Galstyan, P. J. S. Miguel, and B. Lippert. Chem. Eur. J. 2010, 16, 5577 – 5580.
[61] R-D. Schnebeck, E. Freisinger and B. Lippert. Eur. J. Inorg. Chem. 2000, 1193-1 200.
[62] M. Willermann, C. Mulcahy, R. K. O. Sigel, M. M. Cerda`, E. Freisinger, P. J. S. Miguel, M. Roitzsch, and B. Lippert. Inorg. Chem. 2006, 45, 2093-2099.
[63] M. E. Kelly, S. G-Ruiz, R. Kluge, K. Merzweiler, D. Steinborn, C. Wagner, H. Schmidt. Inorganica Chimica Acta 362, 2009, 1323–1332.
[64] A. Galstyan, P. J. S. Miguel and B. Lippert. Dalton Trans., 2010, 39, 6386–6388.
[65] A. J. Blake, N. R. Champness, P. A. Cooke and J. E. B. Nicolson. Chem. Commun., 2000, 665–666.
[66] A. J. Blake, N. R. Champness, P. A. Cooke, J. E. B. Nicolson and C. Wilson. J. Chem. Soc., Dalton Trans., 2000, 3811–3819.
[67] T-T.Yeh.J-Y.Wu,Y-S.Wen,Y-H.Lui,J.Twu,Y-T.Tao,K-L.Lu, The Royal Society Of Chemistry, 2005,656-658.
[68] A. Galstyan, P. J. S. Miguel, K. Weise and B. Lippert. Dalton Trans., 2013, 42, 16151.
[69] L. M. Toma, C. Eller, D. P. Rillema, C. Ruiz-Pe'rez, M. Julve. Inorganica Chimica Acta 357, 2004, 2609–2614.
[70] J-Y. Wu, H-Y. Hsu, C-C. Chan, Y-S. Wen, C. Tsai and K-L. Lu. Crystal Growth & Design, Vol. 9, No. 1, 2009.
[71] J. Mathieu, A. Marsura, N. Bouhmaida, and N. Ghermani. Eur. J. Inorg. Chem. 2002, 2433-2437.
[72] J. Carranza, C. Brennan, J. Sletten, B. Vangdal, P. Rillema, F. Lloret and M. Julve. New J. Chem., 2003, 27, 1775–178.
[73] J.Carranza, H. Grove, J. Sletten, F. Lloret, M. Julve, P. E. Kruger, C. Eller, and D. P. Rillema. Eur. J. Inorg. Chem. 2004, 4836-4848.
[74] M. Wu, D. Yuan, L. Han, B. Wu, Y. Xu, and M. Hong. Eur. J. Inorg. Chem. 2006, 526–530.

[75] C. Yuste, D. Armentano, N. Marino, L. Ca˜nadillas-Delgado, F. S. Delgado, C. Ruiz-P´erez, D. P. Rillema, F. Lloret and M. Julve. Dalton Trans., 2008, 1583–1596.
[76] A. Klein, A-K. Schmieder, N. Hurkes, C. Hamacher, A. O. Schüren, M. P. Feth and H. Bertagnolli. Eur. J. Inorg. Chem. 2010, 934–941.
[77] N. Parveen, R. Nazir, M. Mazhar. J Therm Anal Calorim.2012.
[78] A. Klein, M. P. Feth, H. Bertagnolli, and S. Za´lis. Eur. J. Inorg. Chem. 2004, 2784-2796.
[79] G. Zerbi, S. Sandroni, Spectrochim. Acta 24A, 1968, 483.
[80] G. Zerbi, S. Sandroni, Spectrochim. Acta 24A, 1968, 511.
[81] J. Strukl, J.L. Walter, Spectrochim. Acta 27A, 1971, 209.
[82] M. Julve, M. Verdaguer, O. Kahn, A. Gleizes, M. Philoche-Levisalles, Inorg. Chem. 1983, 22, 368.
[83] O. Kahn, Inorg. Chim. Acta 1982, 62, 3.
[84] O. Kahn, J. Galy, Y. Journaux, J. Jaud, I. Morgenstern-Badarau, J. Am. Chem. Soc. 1982, 104, 2165.
[85] (a) O. Kahn, Molecular Magnetism, VCH, New York, Weinheim and Cambridge, 1993;(b) Magnetism: Molecules to Materials, ed. J. S. Miller and M. Drillon,Wiley-VCH,Weinheim, 2001. (c) Magneto- Structural Correlations in Exchange Coupled Systems, ed. R.D.Willett, D. Gatteschi and O. Kahn, NATO ASI Series, Ser. C, Reidel, Dordrecht, 1985, vol. 140.(d) Research Frontiers in Magnetochemistry, ed. C. J. O'Connor, World Scientific, Singapore, 1993.
[86] R. P. Doyle, M. Julve, F. Lloret, M. Nieuwenhuyzen and P. E. Kruger, Dalton Trans., 2006, 2081–2088 | 2081.
[87] (a) Evans, O. R.; Lin, W. Acc. Chem. Res. 2002, 35, 511. (b) Moulton, B.; Zaworotko, M. J. Chem. ReV. 2001, 101, 1629. (c) Swiegers, G. F.; Malefeste, T. J. Chem. ReV. 2000, 100, 3483. (d) Kaes, C.; Katz, A.; Hosseini, M. W. Chem. ReV. 2000, 100, 3553.
[88] (a) Carlucci, L.; Ciani, G.; Moret, M.; Proserpio, D. M.; Rizzato, S. Angew. Chem., Int. Ed. 2000, 39, 1506. (b) Zaworotko, M. J. Angew. Chem., Int. Ed. Engl. 2000, 39, 3052. (c) Batten, S. R.; Robson, R. Angew. Chem., Int. Ed. 2000, 37, 1460. (d) Hagrman, P. J.; Hagrman, D.; Zubieta, J. Angew. Chem., Int. Ed. 1999, 38, 2638.
[89] Rosi, N. L.; Eckert, J.; Eddaoudi, M.; Vodak, D. T.; Kim, J.; O'Keeffe, M.; Yaghi, O. M. Science 2003, 300, 1127.
[90] H. Hadadzadeh, Gh. Mansouri, A. Rezvani, H.R. Khavasi, B.W. Skelton, M. Makha, F. Rostami Charati, Polyhedron 30, 2011, 2535.
(b) M. Daryanavard, H. Hadadzadeh, A. Dehno Khalaji, M. Weil, Transition Met. Chem. 34, 2009, 779.
(c) H. Hadadzadeh, M.M. Olmstead, A. Rezvani, N. Safari, H. Saravani, Inorg. Chim. Acta 359, 2006, 2154.
[91] C. J. Gómez-García, E. Escrivà, S. Benmansour, J. J. Borràs-Almenar, J-V Folgado, and C. R. de Arellano, Inorg. Chem. 2016, 55, 2664−2671.
[92] S.W. Jones, L.M. Vrana, K.J. Brewer, J. Organomet. Chem. 554, 1998, 29.
[93] Ying Shao · Jingwen Chen, J Solution Chem, 2009, 38: 1357–1367.
[94] G. A. van Albada, I. Mutikainen, U. Turpeinen, J. Reedijk, Inorganica Chimica Acta 324, 2001, 273–277.
[95] M. F. Charlot, S. Jeannin, O. Kahn, J. Lucrece-Abaul, Inorg. Chem. 1979, 18, 1675.

[96] V. H. Crawford, H. W. Richardson, J. R. Wasson, D. J. Hodgson, W. E. Hatfield, Inorg. Chem. 1976, 15, 2107.
[97] M. J. Belousoff, M. B. Duriska, B. Graham, S. R. Batten, B. Moubaraki, K. S. Murray, L. Spiccia, Inorg. Chem. 2006,45,3746.
[98] V.H. Crawford, H.W. Richardson, J.R. Wasson, D.J. Hodgson, W.E. Hatfield, Inorg. Chem. 15, 1976, 2107.
[99] S. Youngme , C. Chailuecha, G.A. v. Albada, C. Pakawatchai, N. Chaichit, J. Reedijk, Inorganica Chimica Acta 357, 2004, 2532–2542.
[100] S. Youngme, G. A. van Albada, H. Kooijman, O. Roubeau, W. Somjitsripunya, A. L. Spek, C. Pakawatchai, and J. Reedijk, Eur. J. Inorg. Chem. 2002, 2367-2374.
[101] H. Astheimer, W. Haase, J. Chem. Phys. 85, 1986, 1427.
[102] E. Ruiz, P. Alemany, S. Alvarez, J. Cano, J. Am. Chem. Soc. 119, 1997, 1297.
[103] E. Ruiz, P. Alemany, S. Alvarez, J. Cano, Inorg.Chem. 36, 1997, 3683.
[104] D.L. Lewis, K.T. McGregor, W.E. Hatfield, D.J. Hodgson, Inorg. Chem. 11, 1972, 2216.
[105] S. Youngme, W. Somjitsripunya, K, Chinnakali, S. Chantrapromma, H-K, Fun, Polyhedron 18, 1999, 857–862.
[106] S. A. Komaei, G. A. v. Albada, J. G. Haasnoot, H. Kooijman, A. L. Spek, J. Reedijk, Inorganica Chimica Acta 286, 1999, 24–29.
[107] M.R. Rosenthal, J. Chem. Educ. 50, 1973, 331.
[108] D. C. Pereira, D. Lúcia A. de Faria and V. R. L. Constantino, J. Braz. Chem. Soc., Vol. 17, No. 8, 1651-1657, 2006.
[109] C. Zafiu, G. Trettenhahn, D. Pum, U. B. Sleytr and W. Kautek, Phys. Chem. Chem. Phys., 2011, 13, 13232–13237.
[110] B. K. Rai, V. Singh, P. Sinha, S. N. Vidyarthi, S. B. Sahi, A.Pandey and Amit, Orient. J. Chem., Vol. 30(3), 1411-1415, 2014.
[111] S. Youngme, C. Pakawatchai, W. Somjitsripunya, K. Chinnakali, H-K. Fun, Inorganica Chimica Acta 303, 2000, 181–189.
[112] Sajila and H. Mohabey, Material Science Research India Vol. 11(1), 63-65, 2014.
[113] K. Helios, R.Wysokinski , A. Pietraszko, D. Michalska, Vibrational Spectroscopy 55, 2011, 207–215.
[114] F. Hasanvand, R. A. Ahmadi, and S. Amani, Journal of Sciences, Islamic Republic of Iran 23(1): 37-43, 2012.
[115] G. De Munno, M. Julve, F. Lloret, J. Faus, M. Verdaguer, and A. Canesch, Inorg. Chem. 1995,34, 157-165.
[116] Hathaway, B. J. In Comprehensive Coordination Chemistry; Wilkinson, G., Gillard, R. D., McCleverty, J. A., Eds.; Pergamon Press: Oxford, U.K., 1985; Vol. 5, pp 601.
[117] R. J. Majeste and E. A. Meyers, The Journal of Physical Chemistry, Vol. 74, No. 19, 1970.
[118] I. Castro, M. JuIve, G. De Munno, G. Bruno, J. A. ReaY F. Lloreta and Juan Fausa, J. CHEM. SOC. DALTON TRANS. 1992.
[119] Y-Q. Zheng and J-L. Lin, Z. Anorg. Allg. Chem. 2003, 629, 1622-1626.
[120] B. Saravanan, A. Jayamani, N. Sengottuvelan, G. Chakkaravarthi and V. Manivannan, Acta Cryst. 2013. E69, m600.

[121] Lu-Lu Han, Su-Na Wang, Zvonko Jagličić, Su-Yuan Zeng, Jun Zheng, Zhong-Hui Li, Jiang-Shan Chen and Di Sun, CrystEngComm, 2015, 17, 1405.
[122] X. Li, D. Cheng, J. Lin, Z. Li, and Y. Zheng, Crystal Growth & Design, Vol. 8, No. 8, 2008.
[123] Thomas Steiner, Angew. Chem. Int. Ed. 2002, 41, 48 - 76.
[124] I. Castro, J. Faus, M. Julve, C. Bois, J.A. Real, F. Lloret, J. Chem. Soc., Dalton Trans. 1992, 47.
[125] Van H. Crawford, H. W. Richardson, J. R. Wasson, D. J. Hodgsonand W. E. Hatfield, Inorg. Chem., 1976, 15,2107.
[126] M. Toofan, A. Boushehri and M. U1-Haque, J. Chem. Soc., Dalton Truns., 1976, 217.
[127] A. T. Casey, B. F. Hoskins and F. D. Whillans, Chem. Commun., 1970, 904; B. F. Hoskins and F. D. Whillans, J. Chem. Soc., Dalton Trans., 1975, 1267; J. A. Barnes, W. E. Hatfield and D. J. Hodgson, 1. Chem. Soc., Chem. Conimun., 1970, 1593; K. T. McGregor, D. J. Hodgson and W. E. Hatfield, tnorg. Chem., 1973, 12, 731; J. A. Barnes, D. J. Hodgson and W. E. Hatfield, Inorg. Chem., 1972,11,144.
[128] I. Castro, J. Faus, M. Julve, M. Verdaguer, A. Monge and E. Gutierrez-Puebla, Inorg. Cliim. Acta, 1990, 170, 25 1.
[129] R. J. Majeste and E. A. Meyers, J. Phys. Chem., 1970,74,3497; K. T. McGregor, N. T. Watkins, D. L. Lewis, R. F. Drake. D. J. Hodgson and W. E. Hatfield, Inorg. Nucl. Chem. Lett., 1973,9,423.
[130] J. E. Johnson, T. A. Beineke, and R. A. Jacobson, J. Chem. SOC. (A), 1971.
[131] M. Du, X-H. Bu, L-H. Weng, X-B. Leng and Y-M. Guo, Acta Cryst. 2001, E57, m25–m27.
[132] C-J. Hsiao, S-H. Lai, I-C. Chen, W-Z. Wang, and S-M. Peng, J. Phys. Chem. A 2008, 112, 13528–13534.
[133] N. Ray, S. Tyagi, B. Hathaway, 1982. J. Chem. Soc. Dalton Trans. pp. 143-146.
[134] O. R. Rodig, T. Brueckner, B. K. Hurlburt, R. K.Schlatzer, T. L.Venable, E.Sinn, (1981). J. Chem. Soc. Dalton Trans. pp. 196-199.
[135] A. N. Chernyshev, D. Morozov, J. Mutanen, V. Yu Kukushkin, G. Groenhof and M. Haukka, J. Mater. Chem. C, 2014, 2, 8285.
[136] Y. Sasada, (1984). Molecular and Crystal Structures in Chemistry Handbook, 3rd ed. Tokyo: The Chemical Society of Japan, Maruzen.
[137] Desiraju, G. R. 1991. Acc. Chem. Res. 24, 290-295.
[138] P. Bombicz, E. Forizs, J. Madarasz, A. Deak, A. Kalman, Inorg. Chim. Acta 315, 2001, 229.
[139] G. Morgant, N. Bouhmaida, L. Balde, N.E. Ghermani, J. d'Angelo, Polyhedron 25, 2006, 2229.
[140] R. Kurtaran, L.T. Yildirim, A.D. Azaz, H. Namli, O. Atakol, J. Inorg. Biochem. 99, 2005, 1937.
[141] W. Luo, X. Meng, X. Sun, F. Xiao, J. Shen, Y. Zhou, G. Cheng, Z. Ji, Inorg.Chem. Commun. 10, 2007, 1351.
[142] Z. Afrasiabi, E. Sinn, W. Lin, Y. Ma, C. Campana, S. Padhye, J. Inorg. Biochem. 99, 2005, 1526.
[143] A. Buschini, S. Pinelli, C. Pellacani, F. Giordani, M.B. Ferrari, F. Bisceglie, M. Giannetto, G. Pelosi, P. Tarasconi, J. Inorg. Biochem. 103, 2009, 666.

[144] N. Chitrapriya, V. Mahalingam, M. Zeller, K. Natarajan, Inorg. Chim. Acta 363, 2010, 3685.
[145] N. Shahabadi, S. Kashanian, F. Darabi, DNA Cell Biol. 28, 2009, 589.
[146] N. Shahabadi, S. Kashanian, F. Darabi, Eur. J. Med. Chem. 45, 2010, 4239.
[147] S. Xiu-min1, W. Hai-yan3, L. Yan-bing, Y. Jing-xiu1, C. Lei1, H. Ge, X. Wei-qing and Z. Bing, CHEM. RES. CHINESE UNIVERSITIES 2010, 26(6), 1011—1015.
[148] H. Hadadzadeh, G. Mansouri, A. Rezvan, H. R. Khavasi, B. W. Skelton, M. Makha, F. R. Charati, Polyhedron 30, 2011, 2535–2543.
[149] C. Ruiz-Pe´rez , P. A. L. Luis, F. Lloret, M Julve, Inorganica Chimica Acta 336, 2002, 131-136.
[150] Lai, H.; Jones, D. S.; Schwind, D. C.; Rillema, D. P. J. Crysrallogr. Spectrosc. Res. 1990, 20, 321.
[151] D. P. Rillema, D. S. Jones, C. Woods and H. A. Levy. Inorg. Chem. 1992, 31, 2935-2938.
[152] F.H. Allen, W.D.S. Motherwell, Acta Crystallogr. B58, 2002, 407.
[153] E. Gonzalez, A. Rodrigue-Witchel, C. Reber, Coord. Chem. Rev. 251, 2007, 351. and references therein.
[154] E. Gonzalez, A. Rodrigue-Witchel, C. Reber, Coord. Chem. Rev. 251, 2007, 351. and references therein.
[155] (a) Zeng, M. H.; Wang, B.; Wang, X. Y.; Zhang, W. X.; Chen, X. M.; Gao, S. Inorg. Chem. 2006, 45, 7069. (b) Houjou, H.; Ito, M.;Araki, K. Inorg. Chem. 2009, 48, 10703. (c) Figgis, B. N. Comprehensive Coordination Chemistry; Wilkinson, G., Ed.; Pergamon: New York, 1987; Vol. 1, p 259. (d) Carlin, R. L. Magnetochemistry; Springer: Berlin, 1986.
[156] B. J. Hathaway, in Comprehensive Coordination Chemistry (Eds.: G. Wilkinson, R. D. Gill, J. A. McCleverty), Pergamon Press, Oxford, 1987, vol. 5.
[157] S. Amani Komaei, G. A. van Albada, I. Mutikainen, U. Turpeinen, J. Reedijk, Polyhedron 1999, 18, 1991-1997.
[158] G. A. van Albada, M. T. Lakin, N. Veldman, A. L. Spek, J. Reedijk, Inorg. Chem. 1995, 34, 4910-4917.
[159] A. Marcu, A. Stanila , D. Rusu , M. Rusu , O. Cozap, L. David, JOURNAL OF OPTOELECTRONICS AND ADVANCED MATERIALS Vol. 9, No. 3, March 2007, p. 741 – 746.
[160] M.Hübner, I. Hauer, C. Muller, D. Rusu, K. Botond, L. David, Analele Universității de Vest din Timişoara Vol. LV, 2011 Seria Fizică.

Appendices:

Appendix A

Table 3.2: Bond length [deg.] of 2,2'-bipyrazine ligand:

N1-C1	1.340	N1A-C4A	1.336
C1-C2	1.408	C3A-C4A	1.396
N2-C2	1.337	N2A-C3A	1.337
N2-C3	1.337	C1A-C2A	1.408
N1-C4	1.336	C3-C4	1.396
C1A-C1	1.484	N2A-C2A	1.337
N1A-C1A	1.340		

Table 3.3: Bond angle [Å] of 2,2'-bipyrazine ligand:

C4-N1-C1	116.618	C1-C1A-N1A	117.507
C2-C1-N1	121.080	C2A-C1A-C1	121.413
C1A-C1-N1	117.507	C2A-C1A-N1A	121.080
C2-C1-C1A	121.413	C4A-N1A-C1A	116.618
C1-C2-N2	122.101	C3A-C4A-N1A	122.110
C3-N2-C2	116.299	C4A-C3A-N2A	121.790
C4-C3-N2	121.790	C3A-N2A-C2A	116.299
C3-C4-N1	122.110	C1A-C2A-N2A	122.101

Table 3.4: Torsions [deg.] 2,2'-bipyrazine ligand:

N1-C1-C1A-N1A	-180.000
C2-C1-C1A-N1A	0.141
C2A-C1A-C1-N1	-0.141
C2-C1-C1A-C2A	-180.000

Appendix B

Table 2.2: Crystal Data and Structure Refinement Parameters of **(1)**:

Molecular formula	$C_{16}H_{22}Cl_2Cu_2N_8O_{14}$
Molecular weight	748.39
Crystal(description, color)	Block, Blue
Temperature (K)	100
Crystal system	Triclinic
Space group	$P\bar{1}$
Fraction N,O Atoms	0.512
Fraction Halogen Atoms	0.049
Unit cell dimensions	
a (Å)	7.9796(5)
b (Å)	8.0290(5)
c (Å)	10.5550(7)
α (°)	77.7120(10)
β (°)	79.9150(10)
γ (°)	84.7840(10)
Volume ($A^{\circ 3}$)	649.526
Z	1
D_{calc} (mg m^{-3})	1.913
μ (mm^{-1}) Absorption coefficient	1.928
Mo *Kα* radiation λ ,(Å)	0.71073
F(000)	378
Theta(Θ) range (deg)	2.000- 26.436
Crystal size (mm^3)	0.250 * 0.200 * 0.200
*T*min, *T*max	0.565, 0.680
Index ranges	9≤ h ≥-9, 10≤ k ≥ -10, 13≥ I ≥ -13
Packing coefficient	0.732
CSD average packing coefficient for organometallic molecules	0.67(5)
R1, wR2 [I ≥ 2σ(I)][a] (final R indices)	0.0355, 0.0901
R1 wR2 (all data)[a] (R indices)	0.0393,0.0925
GOF on F^2 (goodnees-of-fit)	1.069
total no. of data collected	2652
no. of variables	192
no. of obsd data[I ≥ 2σ(I)][a]	2395

Table 3.6: Hydrogen bond interaction of **(1)**:

Donor	Acceptor	D-H (Å)	H...A (Å)	D...A (Å)	D-H...A (°)	Type
O1-H1	O2W	0.96	1.977	2.902	161.1	Intermolecular
O1W-H1W	O2W	0.84	1.919	2.725	161.5	Intermolecular
O2W-H3W	N14	0.88	2.037	2.908	172.0	Intermolecular
O2W-H4W	N24	0.84	2.055	2.885	167.0	Intermolecular
O1W-H2W	O12	0.89	2.574	3.308	139.9	Intramolecular

Table 3.7: Bond angle [deg.] of **(1)**:

O1-Cu1-O1W	92.6(1)	Cu1-O1-H1	112.7
O1-Cu1-N11	97.5(1)	Cu1-O1-Cu1	94.4(1)
O1-Cu1-N21	173.0(1)	H1-O1-Cu1	112.7
O1-Cu1-O11	95.60(8)	Cu1-O1W-H1W	96.6
O1-Cu1-Cu1	43.03(7)	Cu1-O1W-H2W	120.8
O1-Cu1-O1	85.6(1)	H1W-O1W-H2W	106.8
O1W-Cu1-N11	91.0(1)	Cu1-N11-C12	114.4(2)
O1W-Cu1-N21	94.2(1)	Cu1-N1-C16	127.3(2)
O1W-Cu1-O11	162.70(9)	C12-N11-C16	118.2(2)
O1W-Cu1-Cu1	92.61(8)	Cu-N21-C22	115.1(2)
O1W-Cu1-O1	91.2(1)	Cu1-N21-C26	126.3(2)
N11-Cu1-N21	81.10(9)	C22-N21-C26	118.4(2)
N11-Cu1-O11	72.89(8)	N11-C12-C13	120.2(3)
N11-Cu1-Cu1	140.47(7)	N11-C12-C22	114.8(2)
N11-Cu1-O1	176.1(1)	C13-C12-C22	124.9(3)
N21-Cu1-O11	77.46(8)	C12-C13-H13	119.1
N21-Cu1-Cu1	137.70(7)	C12-C13-N14	121.9(3)
N21-Cu1-O1	95.5(1)	H13-C13-N14	119.0
O11-Cu1-Cu1	103.77(5)	C13-N14-C15	117.3(3)
O11-Cu1-O1	104.53(8)	N14-C15-H15	119.2
Cu1-Cu1-O1	42.57(7)	N14-C15-C16	121.7(3)
H15-C15-C16	119.1	N24-C25-C26	121.8(3)
N11-C16-C15	120.7(3)	H25-C25-C26	119.1
N11-C16-H16	119.6	N21-C26-C25	120.3(3)
C15-C16-H16	119.7	N21-C26-H26	119.8
N21-C22-C12	114.5(2)	C25-C26-H26	119.8
N21-C22-C23	120.4(3)	O11-Cl1-O12	106.8(2)
C12-C22-C23	125.0(3)	O11-Cl1-O13	109.8(2)
C22-C23-H23	119.2	O11-Cl1-O14	108.8(1)
C22-C23-N24	121.6(3)	O12-Cl1-O13	110.8(2)
H23-C23-N24	119.2	O12-Cl1-O14	109.4(2)
C23-N24-C25	117.4(3)	O13-Cl1-O14	111.1(2)
N24-C25-H25	119.1	Cu1-O11-Cl1	129.4(1)

Cu1-Cu1-O1	43.03(7)	Cu1-Cu1-O1	42.57(7)
Cu1-Cu1-O1W	92.61(8)	N11-Cu1-O11	72.89(8)
Cu1-Cu1-N11	140.47(7)	N21-Cu1-O11	77.46(8)
Cu1-Cu1-N21	137.70(7)	Cu1-O1-Cu1	94.4(1)
Cu1-Cu1-O11	103.77(5)	Cu1-O1-H1	112.7
O1-Cu1-O1	85.6(1)	Cu1-O1-H1	112.7
O1-Cu1-O1W	91.2(1)	Cu1-O1W-H1W	96.6
O1-Cu1-N11	176.1(1)	Cu1-O1W-H2W	120.8
O1-Cu1-N21	95.5(1)	H1W-O1W-H2W	106.8
O1-Cu1-O11	104.53(8)	Cu1-N11-C12	114.4(2)
O1-Cu1-O1W	92.6(1)	Cu1-N11-C16	127.3(2)
O1-Cu1-N11	97.5(1)	C12-N11-C16	118.2(2)
O1-Cu1-N21	173.0(1)	Cu1-N21-C22	115.1(2)
O1-Cu1-O11	95.60(8)	Cu1-N21-C26	126.3(2)
O1W-Cu1-N11	91.0(1)	C22-N21-C26	118.4(2)
O1W-Cu1-N21	94.2(1)	N11-C12-C13	120.2(3)
O1W-Cu1-O11	162.70(9)	N11-C12-C22	114.8(2)
N11-Cu1-N21	81.10(9)	C13-C12-C22	124.9(3)
H15-C15-C16	119.1	C12-C13-H13	119.1
N11-C16-C15	120.7(3)	C12-C13-N14	121.9(3)
N11-C16-H16	119.6	H13-C13-N14	119.0
C15-C16-H16	119.7	C13-N14-C15	117.3(3)
N21-C22-C12	114.5(2)	N14-C15-H15	119.2
N21-C22-C23	120.4(3)	N14-C15-C16	121.7(3)
C12-C22-C23	125.0(3)	C25-C26-H26	119.8
C22-C23-H23	119.2	O11-Cl1-O12	106.8(2)
C22-C23-N24	121.6(3)	O11-Cl1-O13	109.8(2)
H23-C23-N24	119.2	O11-Cl1-O14	108.8(1)
C23-N24-C25	117.4(3)	O1-Cl1-O13	110.8(2)
N24-C25-H25	119.1	O12-Cl1-O14	109.4(2)
N24-C25-C26	121.8(3)	O13-Cl1-O14	111.1(2)
H25-C25-C26	119.1	Cu1-O11-Cl1	129.4(1)
N21-C26-C25	120.3(3)	H3W-O2W-H4W	107.0
N21-C26-H26	119.8		

Table 3.8: Bond length [Å] of **(1)**:

Cu1-O1	1.917(2)	N21-C22	1.343(4)
Cu1-O1W	2.472(3)	N21-C26	1.332(4)
Cu1-N11	2.009(2)	C12-C13	1.390(5)
Cu1-N21	1.994(2)	C12-C22	1.479(4)
Cu1-O11	2.746(2)	C13-H13	0.95
Cu1-Cu1	2.8258(5)	C13-N14	1.332(4)
Cu1-O1	1.934(2)	N14-C15	1.339(4)

O1-H1	0.96	C15-H15	0.95
O1-Cu1	1.934(2)	C15-C16	1.386(5)
O1W-H1W	0.836	C16-H16	0.95
O1W-H2W	0.894	C22-C23	1.386(4)
N11-C12	1.346(3)	C23-H23	0.95
N11-C16	1.337(4)	C23-N24	1.334(4)
N21-C22	1.343(4)	N24-C25	1.333(4)
N21-C26	1.332(4)	C25-H25	0.95
C12-C13	1.390(5)	C25-C26	1.391(4)
C12-C22	1.479(4)	C26-H26	0.95
C13-H13	0.95	Cl1-O11	1.432(3)
C13-N14	1.332(4)	Cl1-O12	1.440(4)
N14-C15	1.339(4)	Cl1-O13	1.411(3)
C15-H15	0.95	Cl1-O14	1.442(2)
C15-C16	1.386(5)	O2W-H3W	0.877
C16-H16	0.95	O2W-H4W	0.845
C22-C23	1.386(4)	Cl1-O14	1.442(2)
C23-H23	0.95	Cu1-O1	1.917(2)
C23-N24	1.334(4)	Cu1-O1W	2.472(3)
N24-C25	1.333(4)	Cu1-N11	2.009(2)
C25-H25	0.95	Cu1-N21	1.994(2)
C25-C26	1.391(4)	Cu1-O11	2.746(2)
C26-H26	0.95	O1-H1	0.96
Cl1-O11	1.432(3)	O1W-H1W	0.836
Cl1-O12	1.440(4)	O1W-H2W	0.894
Cl1-O13	1.411(3)	N11-C12	1.346(3)
N11-C16	1.337(4)		

Table 3.9: Torsions [deg.] of **(1)**:

O1W-Cu1-O1-H1	152.1	Cu1-Cu1-N21-C26	-3.3(3)
O1W-Cu1-O1-Cu1	-91.1(1)	O1-Cu1-N21-C22	178.2(2)
N11-Cu1-O1-H1	60.7	O1-Cu1-N21-C26	3.6(3)
N11-Cu1-O1-Cu1	177.63(9)	O1-Cu1-O11-Cl1	-131.9(2)
N21-Cu1-O1-H1	-17.1	O1W-Cu1-O11-Cl1	110.2(3)
N21-Cu1-O1-Cu1	99.8(8)	N11-Cu1-O11-Cl1	131.9(2)
O11-Cu1-O1- H1	-12.7	N21-Cu1-O11-Cl1	47.5(2)
O11-Cu1-O1-Cu1	104.20(9)	Cu1-Cu1-O11-Cl1	-89.0(2)
Cu1-Cu1-O1- H1	-116.9	O1-Cu1-O11-Cl1	-45.0(2)
O1-Cu1-O1-H1	-116.9	O1-Cu1-Cu1-O1	180.0(1)
O1-Cu1- O1-Cu1	0.0(1)	O1-Cu1-Cu1-O1W	89.0(1)
O1-Cu1-O1W-H1W	96.4	O1-Cu1-Cu1-N11	-176.3(1)
O1-Cu1-O1W-H2W	-17.6	O1-Cu1-Cu1-N21	-10.2(1)
N11-Cu1-O1W-H1W	-166.0	O1-Cu1-Cu1-O11	-96.6(1)

N11-Cu1-O1W-H2W	79.9	O1W-Cu1-Cu1-O1	91.0(1)
N21-Cu1-O1W-H1W	-84.9	O1W-Cu1-Cu1-O1	-89.0(1)
N21-Cu1-O1W-H2W	161.0	O1W-Cu1-Cu1-O1W	-180.0(1)
O11-Cu1-O1W-H1W	-145.3	O1W-Cu1-Cu1-N11	-85.3(1)
O11-Cu1-O1W-H2W	100.6	O1W-Cu1-Cu1-N21	80.8(1)
Cu1-Cu1-O1W-H1W	53.4	O1W-Cu1-Cu1-O11	-5.62(9)
Cu1-Cu1-O1W-H2W	-60.7	N11-Cu1-Cu1-O1	-3.7(1)
O1-Cu1-O1W-H1W	10.8	N11-Cu1-Cu1-O1	176.3(1)
O1-Cu1-O1W-H2W	-103.3	N11-Cu1-Cu1-O1W	85.3(1)
O1-Cu1-N11-C12	-173.4(2)	N11-Cu1-Cu1-N11	180.0(1)
O1-Cu1-N11-C16	3.6(3)	N11-Cu1-Cu1-N21	-13.9(1)
O1W-Cu1-N11-C12	93.9(2)	N11-Cu1-Cu1-O11	-100.3(1)
O1W-Cu1-N11-C16	-89.1(3)	N21-Cu1-Cu1-O1	-169.8(1)
N21-Cu1-N11-C12	-0.2(2)	N21-Cu1-Cu1-O1	10.2(1)
N21-Cu1-N11-C16	176.7(3)	N21-Cu1-Cu1-O1W	-80.8(1)
O11-Cu1-N11-C12	-79.8(2)	N21-Cu1-Cu1-N11	13.9(1)
O11-Cu1-N11-C16	97.2(3)	N21-Cu1-Cu1-N21	-180.0(1)
Cu1-Cu1-N11-C12	-170.8(1)	N21-Cu1-Cu1-O11	93.6(1)
Cu1-Cu1-N11-C16	6.1(3)	O11-Cu1-Cu1-O1	-83.4(1)
O1-Cu1-N11-C12	-31(2)	O11-Cu1-Cu1-O1	96.6(1)
O1-Cu1-N11-C16	146(1)	O11-Cu1-Cu1-O1W	5.62(9)
O1-Cu1-N21-C22	79.0(8)	O11-Cu1-Cu1-N11	100.3(1)
O1-Cu1-N21-C26	-95.6(8)	O11-Cu1-Cu1-N21	-93.6(1)
O1W-Cu1-N21-C22	-90.2(2)	O11-Cu1-Cu1-O11	180.00(7)
O1W-Cu1-N21-C26	95.3(3)	O1-Cu1-Cu1-O1	-180.0(1)
N11-Cu1-N21-C22	0.2(2)	O1-Cu1-Cu1-O1W	-91.0(1)
N11-Cu1-N21-C26	-174.4(3)	O1-Cu1-Cu1-N11	3.7(1)
O11-Cu1-N21-C22	74.5(2)	O1-Cu1-Cu1-N21	169.8(1)
O11-Cu1-N21-C26	-100.1(2)	O1-Cu1-Cu1-O11	83.4(1)
Cu1-Cu1-N21-C22	171.2(1)	O1-Cu1-O1-Cu1	-0.0(1)
O1-Cu1-O1-H1	-116.9	H13-C13-N14-C15	-179.2
O1W-Cu1-O1-Cu1	92.5(1)	C13-N14-C15-H15	179.9
O1W-Cu1-O1-H1	-24.4	C13-N14-C15-C16	-0.1(4)
N11-Cu1-O1-Cu1	-143(1)	N14-C15-C16-N11	-0.3(5)
N11-Cu1-O1-H1	100	N14-C15-C16-H16	179.6
N21-Cu1-O1-Cu1	-173.1(1)	H15-C15-C16-N11	179.7
N21-Cu1-O1- H1	70.0	H15-C15-C16-H16	-0.4
O11-Cu1-O1-Cu1	-94.66(9)	N21-C22-C23-H23	-178.1
O11-Cu1-O1-H1	148.5	N21-C22-C23-N24	1.9(4)
Cu1-Cu1-O1-H1	-116.9	C12-C22-C23-H23	4.0
Cu1-O1-Cu1-O1	-0.0(1)	C12-C22-C23-N24	-176.0(3)
Cu1-O1-Cu1-O1W	-92.5(1)	C22-C23-N24-C25	0.4(4)
Cu1-O1-Cu1-N11	143(1)	H23-C23-N24-C25	-179.6
Cu1-O1-Cu1-N21	173.1(1)	C23-N24-C25-H25	178.5
Cu1-O1-Cu1-O11	94.66(9)	C23-N24-C25-C26	-1.5(4)

H1-O1-Cu1-Cu1	116.9	N24-C25-C26-N21	0.2(5)
H1-O1-Cu1-O1	116.9	N24-C25-C26-H26	-179.8
H1-O1-Cu1-O1W	24.4	H25-C25-C26-N21	-179.8
H1-O1-Cu1- N11	-100	H25-C25-C26-H26	0.2
H1-O1-Cu1- N21	-70.0	O12-Cl1-O11-Cu1	49.4(2)
H1-O1-Cu1- O11	-148.5	O13-Cl1-O11-Cu1	-70.8(2)
Cu1-N11-C12-C13	178.0(2)	O14-Cl1-O11-Cu1	167.3(1)
Cu1-N11-C12-C22	0.3(3)	Cu1-Cu1-O1 -H1	116.9
C16-N11-C12-C13	0.7(4)	O1-Cu1-O1- Cu1	0.0(1)
C16-N11-C12-C22	-177.0(2)	O1-Cu1-O1-H1	116.9
Cu1-N11-C16-C15	-176.9(2)	O1W-Cu1-O1-Cu1	91.1(1)
Cu1-N11-C16-H16	3.2	O1W-Cu1-O1-H1	-152.1
C12-N11-C16-C15	-0.0(4)	N11-Cu1-O1-Cu1	-177.63(9)
C12-N11-C16-H16	-180.0	N11-Cu1-O1- H1	-60.7
Cu1-N21-C22-C12	-0.1(3)	N21-Cu1-O1-Cu1	-99.8(8)
Cu1-N21-C22-C23	-178.2(2)	N21-Cu1-O1- H1	17.1
C26-N21-C22-C12	175.0(3)	O11-Cu1-O1-Cu1	-104.20(9)
C26-N21-C22-C23	-3.1(4)	O11-Cu1-O1- H1	12.7
Cu1-N21-C26-C25	176.5(2)	Cu1-Cu1-O1W-H1W	-53.4
Cu1-N21-C26-H26	-3.5	Cu1-Cu1-O1W-H2W	60.7
C22-N21-C26-C25	2.1(4)	O1-Cu1-O1W-H1W	-10.8
C22-N21-C26-H26	-177.9	O1-Cu1-O1W-H2W	103.3
N11-C12-C13-H13	178.9	O1-Cu1-O1W-H1W	-96.4
N11-C12-C13-N14	-1.2(4)	O1-Cu1-O1W-H2W	17.6
C22-C12-C13-H13	-3.7	N11-Cu1-O1W-H1W	166.0
C22-C12-C13-N14	176.3(3)	Cu1-N21-C22-C12	0.1(3)
N11-C12-C22-N21	-0.1(3)	Cu1-N21-C22-C23	178.2(2)
N11-C12-C22-C23	177.9(3)	C26-N21-C22-C12	-175.0(3)
C13-C12-C22-N21	-177.7(3)	C26-N21-C22-C23	3.1(4)
C13-C12-C22-C23	0.3(5)	Cu1-N21-C26-C25	-176.5(2)
C12-C13-N14-C15	0.8(4)	Cu1-N21-C26-H26	3.5
Cu1-Cu1-N11-C16	-6.1(3)	C22-N21-C26-C25	-2.1(4)
O1-Cu1-N11-C12	31(2)	C22-N21-C26-H26	177.9
O1-Cu1-N11-C16	-146(1)	N11-C12-C13-H13	-178.9
O1-Cu1-N11-C12	173.4(2)	N11-Cu1-O1W-H2W	-79.9
O1-Cu1-N11-C16	-3.6(3)	N21-Cu1-O1W-H1W	84.9
O1-Cu1-N11-C12	-93.9(2)	N21-Cu1-O1W-H2W	-161.0
O1W-Cu1-N11-C16	89.1(3)	O11-Cu1-O1W-H1W	145.3
N21-Cu1-N11-C12	0.2(2)	O11-Cu1-O1W-H2W	-100.6
N21-Cu1-N11-C16	-176.7(3)	Cu1-Cu1-N11-C12	170.8(1)
O11-Cu1-N11-C12	79.8(2)	N11-C12-C13-N14	1.2(4)
O11-Cu1-N11-C16	-97.2(3)	C22-C12-C13-H13	3.7
Cu1-Cu1-N21-C22	-171.2(1)	C22-C12-C13-N14	-176.3(3)
Cu1-Cu1-N21-C26	3.3(3)	N11-C12-C22-N21	0.1(3)
O1-Cu1-N21-C22	-178.2(2)	N11-C12-C22-C23	-177.9(3)

O1-Cu1-N21-C26	-3.6(3)	C13-C12-C22-N21	177.7(3)
O1-Cu1-N21-C22	-79.0(8)	C13-C12-C22-C23	-0.3(5)
O1-Cu1-N21-C26	95.6(8)	C12-C13-N14-C15	-0.8(4)
O1W-Cu1-N21-C22	90.2(2)	H13-C13-N14-C15	179.2
O1W-Cu1-N21-C26	-95.3(3)	C13-N14-C15-H15	-179.9
N11-Cu1-N21-C22	-0.2(2)	C13-N14-C15-C16	0.1(4)
N11-Cu1-N21-C26	174.4(3)	N14-C15-C16-N11	0.3(5)
O11-Cu1-N21-C22	-74.5(2)	N14-C15-C16-H16	-179.6
O11-Cu1-N21-C26	100.1(2)	H15-C15-C16-N11	-179.7
Cu1-Cu1-O11-Cl1	89.0(2)	H15-C1-C16-H16	0.4
O1-Cu1-O11-Cl1	45.0(2)	N21-C22-C23-H23	178.1
O1-Cu1-O11- Cl1	131.9(2)	N21-C22-C23-N24	-1.9(4)
O1W-Cu1-O11-Cl1	-110.2(3)	C12-C22-C23-H23	-4.0
N11-Cu1-O11-Cl1	-131.9(2)	C12-C22-C23-N24	176.0(3)
N21-Cu1-O11-Cl1	-47.5(2)	C22-C23-N24-C25	-0.4(4)
Cu1-N11-C12-C13	-178.0(2)	H23-C23-N24-C25	179.6
Cu1-N11-C12-C22	-0.3(3)	C23-N24-C25-H25	-178.5
C16-N11-C12-C13	-0.7(4)	C23-N24-C25-C26	1.5(4)
C16-N11-C12-C22	177.0(2)	N24-C25-C26-N21	-0.2(5)
Cu1-N11-C16-C15	176.9(2)	N24-C25-C26-H26	179.8
Cu1-N11-C16-H16	-3.2	H25-C25-C26-N21	179.8
C12-N11-C16-C15	0.0(4)	H25-C25-C26-H26	-0.2
C12-N11-C16-H16	180.0	O12-Cl1-O11-Cu1	-49.4(2)
O13-Cl1-O11-Cu1	70.8(2)		
O14-Cl1-O11-Cu1	-167.3(1)		

Appendix C

Table 2.4: Crystal Data and Structure Refinement Parameters of **(2)**:

Molecular formula	$C_{20}H_{18}N_6O_8CuCl_2$
Molecular weight	604.87
Crystal(description, color)	Prism, blue
Temperature (K)	298
Crystal system	Monoclinic
Space group	C2/c
Fraction N,O Atoms	0.312
Fraction Halogen Atoms	0.031
Unit cell dimensions	
a (Å)	9.416 (3)
b (Å)	12.955 (4)
c (Å)	19.748 (6)
α (°)	90.00
β (°)	103.47
γ (°)	90.00
Volume ($A°^3$)	2339.5 (11)
Z	4
D_{calc} (Mg m^{-3})	2.940
μ (mm^{-1}) Absorption coefficient	1.22
F(000)	2012
Theta(Θ) range (deg)	2.140-28.700
Crystal size (mm)	0.35 × 0.30 × 0.25
*T*min, *T*max	0.674, 0.750
Index ranges	12≤ h ≥-12, 16≤ k ≥ -16, 26≥ I ≥-26
Mo *Kα* radiation, *λ*(Å)	0.71073
Packing coefficient	0.728
CSD average packing coefficient for organometallic molecules	0.67(5)
R1, wR2 [I ≥ 2σ(I)][a] (final R indices)	0.0378, 0.1025
R1 wR2 (all data)[a] (R indices)	0.0400, 0.1033
GOF on F^2 (goodnees-of-fit)	1.152
total no. of data collected	2809
no. of variables	168
no. of obsd data[I ≥ 2σ(I)][a]	2602

Table 3.11: Hydrogen bond interaction of **(2)**:

Donor	Acceptor	D-H (Å)	H...A (Å)	D...A (Å)	D-H...A (°)	Type
N1-H1	O14	0.88	2.044	2.920	173.3	Intermolecular

Table 3.12: Bond angle [deg.] of **(2)**:

N11-Cu1-N21	93.98	C13-C14-C15	119.2(3)
N11-Cu1-N11	139.07	H14-C14-C15	120.4
N11-Cu1-N21	98.62	C14-C15-H15	120.8
N21-Cu1-N11	98.62	C14-C15-C16	118.4(3)
N21-Cu1-N21	143.44	H15-C15-C16	120.8
N11-Cu1-N21	93.98	N11-C16-C15	123.3(2)
H1-N1-C12	114.0	N11-C16-H16	118.3
H1-N1-C22	114.0	C15-C16-H16	118.4
C12-N1-C22	132.0(2)	Cu1-N21-C22	124.5
Cu1-N11-C12	125.4	Cu1-N21-C26	117.6
Cu1-N11-C16	116.5	C22-N21-C26	117.9(2)
C12-N11-C16	118.1(2)	N1-C22-N21	121.8(2)
N1-C12-N11	121.0(2)	N1-C22-C23	117.0(2)
N1-C12-C13	117.6(2)	N21-C22-C23	121.2(2)
N11-C12-C13	121.4(2)	C22-C23-H23	120.1
C12-C13-H13	120.2	C22-C23-C24	119.8(2)
C12-C13-C14	119.6(2)	H23-C23-C24	120.1
H13-C13-C14	120.2	C23--24-H14	120.4
C13-C14-H14	120.4	C23-C24-C25	119.2(3)
H14-C24-C25	120.4	N11-C16-H16	118.3
C24-C25-H25	120.9	C15-C16-H16	118.4
C24-C25-C26	118.3(3)	Cu1-N21-C22	124.5
H25-C25-C26	120.9	Cu1-N21-C26	117.6
N21-C26-C25	123.6(2)	C22-N21-C26	117.9(2)
N21-C26-H26	118.2	N1-C22-N21	121.8(2)
C25-C26-H26	118.2	N1-C22-C23	117.0(2)
H1-N1-C12	114.0	N21-C22-C23	121.2(2)
H1-N1-C22	114.0	C22-C23-H23	120.1
C12-N1-C22	132.0(2)	C22-C23-C24	119.8(2)
Cu1-N11-C12	125.4	H23-C23-C24	120.1
Cu1-N11-C16	116.5	C23-C24-H14	120.4
C12-N11-C16	118.1(2)	C23-C24-C25	119.2(3)
N1-C12-N11	121.0(2)	H14-C24-C25	120.4
N1-C12-C13	117.6(2)	C24-C25-H25	120.9
N11-C12-C13	121.4(2)	C24-C25-C26	118.3(3)
C12-C13-H13	120.2	H25-C25-C26	120.9
C12-C13-C14	119.6(2)	N21-C26-C25	123.6(2)

H13-C13-C14	120.2	N21-C26-H26	118.2
C13-C14-H14	120.4	C25-C26-H26	118.2
C13-C14-C15	119.2(3)	O11-Cl10-O12	109.9(1)
H14-C14-C15	120.4	O11-Cl10-O13	110.2(1)
C14-C15-H15	120.8	O11-Cl10-O14	109.2(1)
C14-C15-C16	118.4(3)	O12-Cl10-O13	109.3(1)
H15-C15-C16	120.8	O12-Cl10-O14	108.2(1)
N11-C16-C15	123.3(2)	O13-Cl10-O14	110.1(1)

Table 3.13: Bond length [Å] of **(2)**:

Cu1-N11	1.962	N1-H1	0.880
Cu1-N21	1.968	N1-C12	1.376(3)
Cu1-N11	1.962	N1-C22	1.371(4)
Cu1-N21	1.968	N11-C12	1.339(3)
N1-H1	0.880	N11-C16	1.368(3)
N1-C12	1.376(3)	C12-C13	1.407(4)
N1-C22	1.371(4)	C13-H13	0.950
N11-C12	1.339(3)	C13-C14	1.367(4)
N11-C16	1.368(3)	C14-H14	0.950
C12-C13	1.407(4)	C14-C15	1.401(4)
C13-H13	0.950	C15-H15	0.951
C13-C14	1.367(4)	C15-C16	1.363(4)
C14-H14	0.950	C16-H16	0.950
C14-C15	1.401(4)	N21-C22	1.341(4)
C15-H15	0.951	N21-C26	1.365(4)
C15-C16	1.363(4)	C22-C23	1.412(3)
C16-H16	0.950	C23-H23	0.951
N21-C22	1.341(4)	C23-C24	1.366(4)
N21-C26	1.365(4)	C24-H14	0.950
C22-C23	1.412(3)	C24-C25	1.398(4)
C23-H23	0.951	C25-H25	0.950
C23-C24	1.366(4)	C25-C26	1.366(4)
C24-H14	0.950	C26-H26	0.950
C24-C25	1.398(4)	Cl10-O11	1.435(2)
C25-H25	0.950	Cl10-O12	1.442(2)
C25-C26	1.366(4)	Cl10-O13	1.434(3)
C26-H26	0.950	Cl10-O14	1.453(2)

Table 3.14: Torsions [deg.] **(2)**:

N21-Cu1-N11-C12	7.3	C22-C23-C24-H14	-178.7
N21-Cu1-N11-C16	-170.4	C22-C23-C24-C25	1.3(4)
N11-Cu1-N11-C12	115.3	H23-C23-C24-H14	1.4
N11-Cu1-N11-C16	-62.3	H23-C23-C24-C25	-178.6
N21-Cu1-N11-C12	-138.3	C23-C24-C25-H25	179.1
N21-Cu1-N11-C16	44.0	C23-C24-C25-C26	-0.9(4)
N11-Cu1-N21-C22	-7.7	H14-C24-C25-H25	-0.9
N11-Cu1-N21-C26	174.4	H14-C24-C25-C26	179.1
N11-Cu1-N21-C22	-148.6	C24-C25-C26-N21	-0.5(4)
N11-Cu1-N21-C26	33.4	C24-C25-C26-H26	179.5
N21-Cu1-N21-C22	102.5	H25-C25-C26-N21	179.5
N21-Cu-N21-C26	-75.4	H25-C25-C26-H26	-0.5
N11-Cu1-N11-C12	115.3	H1-N1-C12-N11	168.5
N11-Cu1-N11-C16	-62.3	H1-N1-C12-C13	-11.3
N21-Cu1-N11-C12	-138.3	C22-N1-C12-N11	-11.4(4)
N21-Cu1-N11-C16	44.0	C22-N1-C12-C13	168.8(3)
N21-Cu1-N11-C12	7.3	H1-N1-C22-N21	-169.0
N21-Cu1-N11-C16	-170.4	H1-N1-C22-C23	10.9
N11-Cu1-N21-C22	-148.6	C12-N1-C22-N21	11.0(4)
N11-Cu1-N21-C26	33.4	C12-N1-C22-C23	-169.2(3)
N21-Cu1-N21-C22	102.5	Cu1-N11-C12-N1	-0.2
N21-Cu1-N21-C26	-75.4	Cu1-N11-C12-C13	179.6
N11-Cu1-N21-C22	-7.7	C16-N11-C12-N1	177.5(2)
N11-Cu1-N21C26	174.4	C16-N11-C12-C13	-2.7(4)
H1-N1-C12-N11	168.5	Cu1-N11-C16-C15	-179.7
H1-N1-C12-C13	-11.3	Cu1-N11-C16-H16	0.3
C22-N1-C12-N11	-11.4(4)	C12-N11-C16-C15	2.5(4)
C22-N1-C12-C13	168.8(3)	C12-N11-C16-H16	-177.5
H1-N1-C22-N21	-169.0	N1-C12-C13-H13	1.2
H1-N1-C22-C23	10.9	N1-C12-C13-C14	-178.9(2)
C12-N1-C22-N21	11.0(4)	N11-C12-C13-H13	-178.6
C12-N1-C22-C23	-169.2(3)	N11-C12-C13-C14	1.3(4)
Cu1-N11-C12-N1	-0.2	C12-C13-C14-H14	-179.7
Cu1-N11-C12-C13	179.6	C12-C13-C14-C15	0.4(4)
C16-N11-C12-N1	177.5(2)	H13-C13-C14-H14	0.2
C16-N11-C12-C13	-2.7(4)	H13-C13-C14-C15	-179.7
Cu1-N11-C16-C15	-179.7	C13-C14-C15-H15	179.4
Cu1-N11-C16-H16	0.3	C13-C14-C15-C16	-0.7(4)
C12-N11-C16-C15	2.5(4)	H14-C14-C15-H15	-0.5
C12-N11-C16-H16	-177.5	H14-C14-C15-C16	179.5
N1-C2-C13-H13	1.2	C14-C15-C16-N11	-0.8(4)
N1-C12-C13-C14	-178.9(2)	C14-C15-C16-H16	179.3
N11-C12-C13-H13	-178.6	H15-C15-C16-N11	179.1

N11-C12-C13-C14	1.3(4)	H15-C15-C16-H16	-0.8
C12-C13-C14-H14	-179.7	Cu1-N21-C22-N1	1.0
C12-C13-C14-C15	0.4(4)	Cu1-N21-C22-C23	-178.8
H13-C13-C14-H14	0.2	C26-N21-C22-N1	179.0(2)
H13-C13-C14-C15	-179.7	C26-N21-C22-C23	-0.9(4)
C13-C14-C15-H15	179.4	Cu1-N21-C26-C25	179.5
C13-C14-C15-C16	-0.7(4)	Cu1-N21-C26-H26	-0.5
H14-C14-C15-H15	-0.5	C22-N21-C26-C25	1.4(4)
H14-C14-C15-C16	179.5	C22-N21-C26-H26	-178.6
C14-C15-C16-N11	-0.8(4)	N1-C22-C23-H23	-0.3
C14-C15-C16-H16	179.3	N1-C22-C23-C24	179.7(2)
H15-C15-C16-N11	179.1	N21-C22-C23-H23	179.5
H15-C15-C16-H16	-0.8	N21-C22-C23-C24	-0.4(4)
Cu1-N21-C22-N1	1.0	C22-C23-C24-H14	-178.7
Cu1-N21-C22-C23	-178.8	C22-C23-C24-C25	1.3(4)
C26-N21-C22-N1	179.0(2)	H23-C23-C24-H14	1.4
C26-N21-C22-C23	-0.9(4)	H23-C23-C24-C25	-178.6
Cu1-N21-C26-C25	179.5	C23-C24-C25-H25	179.1
Cu1-N21-C26-H26	-0.5	C23-C24-C25-C26	-0.9(4)
C22-N21-C26-C25	1.4(4)	H14-C24-C25-H25	-0.9
C22-N21-C26-H26	-178.6	H14-C24-C25-C26	179.1
N1-C2-C23-H23	-0.3	C24-C25-C26-N21	-0.5(4)
N1-C22-C23-C24	179.7(2)	C24-C25-C26-H26	179.5
N21-C22-C23-H23	179.5	H25-C25-C26-N21	179.5
N21-C22-C23-C24	-0.4(4)	H25-C25-C26-H26	-0.5

Appendix D

Table 2.6: Crystal Data and Structure Refinement Parameters of **(3)**:

Molecular formula	$C_{24}H_{20}N_{12}O_9NiCl_2$
Molecular weight	750.13
Crystal (description, color)	Prisms, Brown
Temperature (K)	100(2)
Crystal system	Monoclinic
Space group	P 21/c
Unit cell dimensions	
a (Å)	17.2943(11)
b (Å)	9.8622(6)
c (Å)	17.9612(11)
α (°)	90.00
β (°)	107.7010(10)
γ (°)	90.00
Volume ($A°^3$)	2918.4(3)
Z	4
D_{calc} (Mg m^{-3})	1.707
μ (mm^{-1}) Absorption coefficient	0.924
F(000)	1528
Theta(Θ) range (deg)	2.38-27.39
Crystal size (mm)	0.250 × 0.150 × 0.100
*T*min, *T*max	0.768, 0.912
Index ranges	23≤ h ≥-23, 12≤ k ≥ -12, 23≥ I ≥-23
Mo *Kα* radiation, *λ*(Å)	0.71073
R1, wR2 [I ≥ 2σ(I)][a] (final R indices)	0.0543, 0.1247
R1 wR2 (all data)[a] (R indices)	0.0909, 0.1460
GOF on F^2 (goodnees-of-fit)	1.021
total no. of data collected	7026
no. of variables	461
no. of obsd data[I ≥ 2σ(I)][a]	4799

Table 3.15: Hydrogen bond interaction of **(3)**:

Donor	Acceptor	D-H (Å)	H...A (Å)	D...A (Å)	D-H...A (°)	Type
O1W-H1W	N14	0.915	2.076	2.962	162.52	Intermolecular
O1W-H2W	O22	0.879	2.160	2.992	157.74	Intermolecular
C46-H46	N54	0.949	2.660	3.328	127.85	Intermolecular
C65-H65	N44	0.950	2.705	3.100	105.65	Intermolecular
C25-H25	N34	0.950	2.490	3.435	173.43	Intermolecular
C36-H36	N24	0.950	2.554	3.290	134.50	Intermolecular
C45-H45	N44	0.951	2.688	3.155	110.88	Intermolecular

Table 3.18: Bond length [Å] of **(3)**:

Ni1-N11	2.084(3)	C45-H45	0.951
Ni1-N21	2.071(2)	C45-C46	1.381(5)
Ni1-N31	2.077(3)	C46-H46	0.949
Ni1-N41	2.068(3)	N51-C52	1.342(5)
Ni1-N51	2.104(3)	N51-C56	1.340(5)
Ni1-N61	2.082(3)	C52-C53	1.385(5)
N11-C12	1.348(4)	C52-C62	1.473(6)
N11-C16	1.334(5)	C53-H53	0.950
C12-C13	1.384(5)	C53-N54	1.332(5)
C12-C22	1.475(5)	N54-C55	1.329(6)
C13-H13	0.950	C55-H55	0.950
C13-N14	1.335(5)	C55-C56	1.378(5)
N14-C15	1.334(4)	C56-H56	0.950
C15-H15	0.950	N61-C62	1.359(5)
C15-C16	1.374(5)	N61-C66	1.337(5)
C16-H16	0.950	C62-C63	1.386(6)
N21-C22	1.355(4)	C63-H63	0.951
N21-C26	1.327(5)	C63-N64	1.333(6)
C22-C23	1.376(4)	N64-C65	1.329(7)
C23-H23	0.950	C65-H65	0.950
C23-N24	1.340(5)	N41-C46	1.318(4)
N24-C25	1.325(5)	C42-C43	1.386(4)
C25-H25	0.950	C43-H43	0.950
C25-C26	1.384(4)	C43-N44	1.324(5)
C26-H26	0.950	N44-C45	1.333(6)
N31-C32	1.338(4)	C65-C66	1.375(7)
N31-C36	1.337(4)	C66-H66	0.951
C32-C33	1.390(6)	Cl1-O11	1.443(6)
C32-C42	1.471(5)	Cl1-O12	1.454(8)
C33-H33	0.950	Cl1-O13	1.413(7)
C33-N34	1.330(4)	Cl2-O21	1.429(3)
N34-C35	1.331(5)	Cl2-O22	1.431(3)
C35-H35	0.950	Cl2-O23	1.442(4)
C35-C36	1.383(6)	Cl2-O24	1.408(4)
C36-H36	0.950	O1W-H1W	0.915
N41-C42	1.352(5)	O1W-H2W	0.879

Table 3.19: Bond angle [deg.] of **(3)**:

N11-Ni1-N21	78.9(1)	N41-C46-H46	119.3
N11-Ni1-N31	92.5(1)	C45-C46-H46	119.4
N11-Ni1-N41	97.0(1)	Ni1-N51-C52	114.6(2)
N11-Ni1-N51	175.0(1)	Ni1-N51-C56	127.7(2)
N11-Ni1-N61	97.8(1)	C52-N51-C56	117.1(3)
N21-Ni1-N31	93.9(1)	N51-C52-C53	120.1(3)
N21-Ni1-N41	171.8(1)	N51-C52-C62	116.2(3)
N21-Ni1-N51	97.8(1)	C53-C52-C62	123.7(3)
N21-Ni1-N61	91.3(1)	C52-C53-H53	118.7
N31-Ni1-N41	79.1(1)	C52-C53-N54	122.8(3)
N31-Ni1-N51	91.5(1)	H53-C53-N54	118.6
N31-Ni1-N61	169.3(1)	C53-N54-C55	116.5(3)
N41-Ni1-N51	86.7(1)	N54-C55-H55	119.2
N41-Ni1-N61	96.3(1)	N54-C55-C56	121.7(3)
N51-Ni1-N61	78.5(1)	H55-C55-C56	119.1
Ni1-N11-C12	114.8(2)	N51-C56-C55	121.6(3)
Ni1-N11-C16	128.0(2)	N51-C56-H56	119.2
C12-N11-C16	117.0(3)	C55-C56-H56	119.2
N11-C12-C13	120.7(3)	Ni1-N61-C62	115.1(2)
N11-C12-C22	115.6(3)	Ni1-N61-C66	127.8(2)
C13-C12-C22	123.7(3)	C62-N61-C66	117.0(3)
C12-C13-H13	118.9	C52-C62-N61	115.3(3)
C12-C13-N14	122.3(3)	C52-C62-C63	124.1(3)
H13-C13-N14	118.9	N61-C62-C63	120.6(3)
C13-N14-C15	116.1(3)	C42-N41-C46	117.5(3)
N14-C15-H15	118.8	C32-C42-N41	115.7(3)
N14-C15-C16	122.5(3)	C32-C42-C43	124.0(3)
H15-C15-C16	118.7	N41-C42-C43	120.2(3)
N11-C16-C15	121.3(3)	C42-C43-H43	118.9
N11-C16-H16	119.3	C42-C43-N44	122.1(3)
C15-C16-H16	119.4	H43-C43-N44	119.0
Ni1-N21-C22	115.1(2)	C43-N44-C45	116.6(3)
Ni1-N21-C26	127.6(2)	N44-C45-H45	119.0
C22-N21-C26	117.3(3)	N44-C45-C46	122.1(3)
C12-C22-N21	115.5(3)	H45-C45-C46	119.0
C12-C22-C23	124.3(3)	N41-C46-C45	121.3(3)
N21-C22-C23	120.2(3)	C62-C63-H63	118.9
C22-C23-H23	118.7	C62-C63-N64	122.2(3)
C22-C23-N24	122.7(3)	H63-C63-N64	118.9
H23-C23-N24	118.6	C63-N64-C65	116.2(4)
C23-N24-C25	116.0(3)	N64-C65-H65	118.4
N24-C25-H25	118.8	N64-C65-C66	123.2(4)
N24-C25-C26	122.4(3)	H65-C65-C66	118.5

H25-C25-C26	118.8	N61-C66-C65	120.8(4)
N21-C26-C25	121.3(3)	N61-C66-H66	119.6
N21-C26-H26	119.4	C65-C66-H66	119.6
C25-C26-H26	119.4	O11-Cl1-O12	109.4(3)
Ni1-N31-C32	114.4(2)	O11-Cl1-O13	118.0(4)
Ni1-N31-C36	128.2(2)	O11-Cl1-O14	101.3(4)
C32-N31-C36	117.3(3)	O11-Cl1-O15	95.1(6)
N31-C32-C33	120.4(3)	O12-Cl1-O13	110.1(4)
N31-C32-C42	115.7(3)	O12-Cl1-O14	104.9(4)
C33-C32-C42	123.9(3)	O12-Cl1-O15	56.1(6)
C32-C33-H33	118.7	O13-Cl1-O14	112.0(5)
C32-C33-N34	122.5(3)	O13-Cl1-O15	70.9(6)
H33-C33-N34	118.8	Cl1-O15-O12	65.1(6)
C33-N34-C35	116.6(3)	Cl1-O15-O13	55.7(5)
N34-C35-H35	119.1	O12-O15-O13	105.4(9)
N34-C35-C36	121.8(3)	O21-Cl2-O22	109.4(2)
H35-C35-C36	119.1	O21-Cl2-O23	108.7(2)
N31-C36-C35	121.4(3)	O21-Cl2-O24	110.4(2)
N31-C36-H36	119.4	O22-Cl2-O23	108.9(2)
C35-C36-H36	119.2	O22-Cl2-O24	110.9(2)
Ni1-N41-C42	113.8(2)	O23-Cl2-O24	108.4(2)
Ni1-N41-C46	127.8(2)	H1W-O1W-H2W	107.3

Table 3.20: Torsions [deg.] of **(3)**:

N21-Ni1-N11-C12	3.7(2)	H35-C35-C36-H36	0.3
N21-Ni1-N11-C16	178.2(3)	Ni1-N41-C42-C32	-11.8(4)
N31-Ni1-N11-C12	-89.7(2)	Ni1-N41-C42-C43	165.6(3)
N31-Ni1-N11-C16	84.8(3)	C46-N41-C42-C32	178.6(3)
N41-Ni1-N11-C12	-169.1(2)	C46-N41-C42-C43	-4.1(5)
N41-Ni1-N11-C16	5.4(3)	Ni1-N41-C46-C45	-167.9(3)
N51-Ni1-N11-C12	52(1)	Ni1-N41-C46-H46	12.2
N51-Ni1-N11-C16	-133(1)	C42-N41-C46-C45	0.1(5)
N61-Ni1-N11-C12	93.5(2)	C42-N41-C46-H46	-179.9
N61-Ni1-N11-C16	-92.0(3)	C32-C42-C43-H43	2.2
N11-Ni1-N21-C22	-1.8(2)	C32-C42-C43-N44	-177.8(4)
N11-Ni1-N21-C26	-179.4(3)	N41-C42-C43-H43	-174.8
N31-Ni1-N21-C22	89.9(2)	N41-C42-C43-N44	5.1(6)
N31-Ni1-N21-C26	-87.7(3)	C42-C43-N44-C45	-1.8(6)
N41-Ni1-N21-C22	58.9(9)	H43-C43-N44-C45	178.2
N41-Ni1-N21-C26	-118.7(8)	C43-N44-C45-H45	177.8
N51-Ni1-N21-C22	-178.1(2)	C43-N44-C45-C46	-2.3(6)
N51-Ni1-N21-C26	4.3(3)	N44-C45-C46-N41	3.3(6)
N61-Ni1-N21-C22	-99.5(2)	N44-C45-C46-H46	-176.8

N61-Ni1-N21-C26	82.9(3)	H45-C45-C46-N41	-176.8
N11-Ni1-N31-C32	-103.6(3)	H45-C45-C46-H46	3.1
N11-Ni1-N31-C36	79.2(3)	Ni1-N51-C52-C53	175.5(3)
N21-Ni1-N31-C32	177.3(3)	Ni1-N51-C52-C62	-1.8(4)
N21-Ni1-N31-C36	0.2(3)	C56-N51-C52-C53	2.9(5)
N41-Ni1-N31-C32	-6.9(2)	C56-N51-C52-C62	-174.5(3)
N41-Ni1-N31-C36	175.9(3)	Ni1-N51-C56-C55	-171.1(3)
N51-Ni1-N31-C32	79.5(3)	Ni1-N51-C56-H56	9.0
N51-Ni1-N31-C36	-97.7(3)	C52-N51-C56-C55	0.5(5)
N61-Ni1-N31-C32	58.8(7)	C52-N51-C56-H56	-179.4
N61-Ni1-N31-C36	-118.4(6)	N51-C52-C53-H53	175.3
N11-Ni1-N41-C42	101.3(3)	N51-C52-C53-N54	-4.5(6)
N11-Ni1-N41-C46	-90.3(3)	C62-C52-C53-H53	-7.5
N21-Ni1-N41-C42	41.8(9)	C62-C52-C53-N54	172.6(4)
N21-Ni1-N41-C46	-149.9(7)	N51-C52-C62-N61	5.4(5)
N31-Ni1-N41-C42	10.2(2)	N51-C52-C62-C63	-176.5(3)
N31-Ni1-N41-C46	178.5(3)	C53-C52-C62-N61	-171.8(3)
N51-Ni1-N41-C42	-82.0(3)	C53-C52-C62-C63	6.2(6)
N51-Ni1-N41-C46	86.4(3)	C52-C53-N54-C55	2.4(5)
N61-Ni1-N41-C42	-160.0(2)	H53-C53-N54-C55	-177.5
N61-Ni1-N41-C46	8.3(3)	C53-N54-C55-H55	-178.9
N11-Ni1-N51-C52	41(1)	C53-N54-C55-C56	1.1(5)
N11-Ni1-N51-C56	-147(1)	Ni1-N21-C22-C12	-0.2(4)
N21-Ni1-N51-C52	88.6(3)	Ni1-N21-C22-C23	-179.0(3)
N21-Ni1-N51-C56	-99.7(3)	C26-N21-C22-C12	177.7(3)
N31-Ni1-N51-C52	-177.3(3)	C26-N21-C22-C23	-1.2(5)
N31-Ni1-N51-C56	-5.6(3)	Ni1-N21-C26-C25	175.8(3)
N41-Ni1-N51-C52	-98.3(3)	Ni1-N21-C26-H26	-4.3
N41-Ni1-N51-C56	73.5(3)	C22-N21-C26-C25	-1.8(5)
N61-Ni1-N51-C52	-1.1(2)	C22-N21-C26-H26	178.2
N61-Ni1-N51-C56	170.6(3)	C12-C22-C23-H23	4.8
N11-Ni1-N61-C62	-172.5(2)	C12-C22-C23-N24	-175.3(3)
N11-Ni1-N61-C66	3.9(3)	N21-C22-C23-H23	-176.5
N21-Ni1-N61-C62	-93.5(3)	N21-C22-C23-N24	3.4(5)
N21-Ni1-N61-C66	82.9(3)	C22-C23-N24-C25	-2.4(5)
N31-Ni1-N61-C62	25.2(8)	H23-C23-N24-C25	177.5
N31-Ni1-N61-C66	-158.4(5)	C23-N24-C25-H25	179.3
N41-Ni1-N61-C62	89.5(3)	C23-N24-C25-C26	-0.6(5)
N41-Ni1-N61-C66	-94.1(3)	N24-C25-C26-N21	2.8(6)
N51-Ni1-N61-C62	4.1(2)	N24-C25-C26-H26	-177.1
N51-Ni1-N61-C66	-179.5(3)	H25-C25-C26-N21	-177.2
Ni1-N11-C12-C13	173.1(3)	H25-C25-C26-H26	2.9
Ni1-N11-C12-C22	-5.0(4)	Ni1-N31-C32-C33	-176.5(3)
C16-N11-C12-C13	-2.0(5)	Ni1-N31-C32-C42	2.9(4)
C16-N11-C12-C22	179.9(3)	C36-N31-C32-C33	1.0(5)

Ni1-N11-C16-C15	-174.0(3)	C36-N31-C32-C42	-179.6(3)
Ni1-N11-C16-H16	6.0	Ni1-N31-C36-C35	176.5(3)
C12-N11-C16-C15	0.4(5)	Ni1-N31-C36-H36	-3.7
C12-N11-C16-H16	-179.6	C32-N31-C36-C35	-0.6(5)
N11-C12-C13-H13	-178.2	C32-N31-C36-H36	179.2
N11-C12-C13-N14	1.9(5)	N31-C32-C33-H33	179.2
C22-C12-C13-H13	-0.3	N31-C32-C33-N34	-0.8(6)
C22-C12-C13-N14	179.8(3)	C42-C32-C33-H33	-0.1
N11-C12-C22-N21	3.5(4)	C42-C32-C33-N34	179.9(3)
N11-C12-C22-C23	-177.7(3)	N31-C32-C42-N41	6.0(5)
C13-C12-C22-N21	-174.5(3)	N31-C32-C42-C43	-171.2(3)
C13-C12-C22-C23	4.2(5)	C33-C32-C42-N41	-174.7(3)
C12-C13-N14-C15	0.1(5)	C33-C32-C42-C43	8.1(6)
H13-C13-N14-C15	-179.9	C32-C33-N34-C35	0.2(5)
C13-N14-C15-H15	178.1	H33-C33-N34-C35	-179.9
C13-N14-C15-C16	-1.8(5)	C33-N34-C35-H35	-179.9
N14-C15-C16-N11	1.6(6)	C33-N34-C35-C36	0.3(5)
N14-C15-C16-H16	-178.4	N34-C35-C36-N31	-0.0(6)
H15-C15-C16-N11	-178.3	N34-C35-C36-H36	-179.8
H15-C15-C16-H16	1.7	H35-C35-C36-N31	-179.9
N54-C55-C56-N51	-2.6(6)	N64-C65-C66-N61	1.0(7)
N54-C55-C56-H56	177.3	N64-C65-C66-H66	-179.0
H55-C55-C56-N51	177.4	H65-C65-C66-N61	-178.8
H55-C55-C56-H56	-2.7	H65-C65-C66-H66	1.2
Ni1-N61-C62-C52	-6.3(4)	O11-Cl1-O12-O15	-83.0(7)
Ni1-N61-C62-C63	175.5(3)	O13-Cl1-O12-O15	48.3(7)
C66-N61-C62-C52	176.9(3)	O14-Cl1-O12-O15	169.0(7)
C66-N61-C62-C63	-1.2(5)	O11-Cl1-O13-O15	85.6(6)
Ni1-N61-C66-C65	-176.6(3)	O12-Cl1-O13-O15	-41.0(6)
Ni1-N61-C66-H66	3.3	O14-Cl1-O13-O15	-157.3(6)
C62-N61-C66-C65	-0.3(5)	O11-Cl1-O15-O12	109.9(5)
C62-N61-C66-H66	179.6	O11-Cl1-O15-O13	-117.9(4)
C52-C62-C63-H63	4.3	O12-Cl1-O15-O13	132.2(7)
C52-C62-C63-N64	-175.6(4)	O13-Cl1-O15-O12	-132.2(7)
N61-C62-C63-H63	-177.7	O14-Cl1-O15-O12	-30(2)
N61-C62-C63-N64	2.3(6)	O14-Cl1-O15-O13	102(2)
C62-C63-N64-C65	-1.6(6)	Cl1-O12-O15-O13	-39.5(5)
H63-C63-N64-C65	178.4	Cl1-O13-O15-O12	44.2(6)
C63-N64-C65-H65	179.8		
C63-N64-C65-C66	0.0(6)		

تحضير وتشخيص مركبات تناسقية احادية وثنائية النواة من النيكل (II), النحاس(II) مع 2,2'- bipyrazine ligand و 2,2′−Dipyridylamine

اعداد: خالد عادل نايل أبوشرخ

المشرف الرئيسي: د. حسين علقم

شملت هذه الدراسة تحضير ثلاثة مركبات معقدة وهي $[Cu(bpz)(OH)(ClO_4)(H_2O)]_2.H_2O$, $[Cu(dipyam)]_2(ClO_4)_2$ and $[Ni(bpz)_3](ClO_4)_2.H_2O$, وتم تشخيصها باستخدام تحليل حيود الاشعة السينية (SCXRD), تحليل مطياف الاشعة تحت الحمراء (FTIR), تحليل مطياف الاشعة المرئية وفوق البنفسجية (UV-Vis) ودراسة الخواص الحرارية (DSC). وتم تحضير مركب 2,2'- bipyrazine وتشخيصه بتفصيل باستخدام مطياف الاشعة تحت الحمراء, مطياف الاشعة المرئية وفوق البنفسجية, وتم دراسة تحليل حيود الاشعة السينية.

المركب الجديد ثنائي النواة $[Cu(bpz)(OH)(ClO_4)(H_2O)]_2.H_2O$ حيث ان نظام الكرستل ثلاثي الميلان و ابعاد الخلية الواحدة كتالي :

$a = 7.9796(5)$, $b = 8.0290(5)$, $c = 10.5550(7)$ Å, $\alpha = 77.7120(1)°$, $\beta = 79.9150(1)°$,

$\gamma = 84.7840(1)°$, $Z=1$ and $V= 649.526$ $A°^3$

ويتكون الهيكل لهذا المركب من مركز تماثل مكون ثنائي هيدروكسو النحاس(II) مع 2,2'- bipyrazine من الخارج ومرتبط مع ايون ClO_4^- وجزيئات المذيب (H_2O) ,وتبين من تحليل هذا المركب ان المسافة بين ذرتين النحاس 2.824 Å, والزاوية بين ذرتين النحاس والاكسجين 94.40° وتبين من خلال البحث ان هذه المسافه والزاوية هي اقل مسافة تم التوصل اليها حتي الان لمثل هذا النوع من المركبات , ومن خلال الدراسة تبين ان هذا المركب لديه تجاذب مغاطيسي قوي . الشكل الهندسي حول كل ذرة نحاس هو مشوه ممدود رباعي ثماني السطوح مع مجموعات هيدروكسو واثنين من ذرات النيتروجين 2,2'- bipyrazin، والموقع القمي المرتبطة من قبل اثنين من ذرة الأكسجين من مجموعات ClO_4^- و H_2O. ويظهر ترابط بين كل جزي وجزي اخر ترابط من نوع π ---- π بين حلقات 2,2'- bipyrazine . يظهر مسعر المسح التبايني (DSC) قمتين واحدة طارده للحرارة عند 130.74 درجة مئوية ناتجة من التحلل والثانية ماصة للحراره عند 272.45 درجة مئوية بسبب نقطة الانصهار.

تم تحضير المركب $[Cu(dipyam)]_2(ClO_4)_2$ والبنية البلورية التي تحددها دراسة حيود الأشعة السينية ،FTIR، مطياف الأشعة المرئية وفوق البنفسجية ، والتحليل الحراري (DSC). النحاس (II) في المركز مرتبط بأربعة ذرات نيتروجين من حلقات 2,2′-Dipyridylamine ، عن طريق

trans-trans. والشكل الهندسي حول ايون النحاس هو مشوه رباعي السطوح. والبلورة أحادية الميلان، مع مجموعة الفضاء C2 / c وأبعاد خلية الوحدة (3) a = 9.416، (4) b = 12.955، c = 19.748 (6) Å ، α = 90.00 °، β = 103.47 °، = 90.00 °، Z = 4 و V = 2339.5 $A^{\circ 3}$ (11) . أيونات البيركلورات تربط مع اليونات الموجة للمعقدة لتشكيل سلسلة من خلال ارتباطات وثيقة C-H ••• O و N-H ••• O. يظهر مسعر المسح التبايني (DSC) قمتين واحدة طارده للحرارة عند 262.79 درجة مئوية ناتجة من التحلل والثانية ماصة للحراره عند 308.65 درجة مئوية بسبب نقطة الانصهار.

المركب المعقد نيكيل (II) الاول من نوع ، $[Ni(bpz)_3](ClO_4)_2 . H_2O$. تظهر التحاليل الهيكلية للأشعة السينية أن الشكل الهندسي حول مركز نيكيل (II) هو ثماني السطوح المشوهة الثلاثية، والبلورة أحادية الميلان، مع مجموعة الفضاء P 21 / c وأبعاد خلية الوحدة (11) a = 17.2943، b = (6) Å، c = 17.9612 (11) ، α = 90.00 °، β = 107.7010 (1) °، γ = 90.00 °، Z = 4 و V = 2918.4 (3) (11) $A^{\circ 3}$. وتم دراسة الارتباطات بين الجزيئات في هذا المعقد بشكل دقيق حيث اظهرت ارتباطات مهمة من نوع π ---- C-H، C-H •••N-C, وتجاذب بين حلقات 2,2'- bipyrazine من نوع π ---- π. ويظهر مسعر المسح التبايني (DSC) قمتين واحدة طارده للحرارة عند 183.60 درجة مئوية ناتجة من التحلل والثانية ماصة للحراره عند 334.15 درجة مئوية بسبب نقطة الانصهار.